Final Technical Report

LEAD TELLURIDE BONDING AND SEGMENTATION STUDY

F. Wald
S. J. Michalik
S. Mermelstein
H. Bates

Contract No.: NAS5-9149

February 26, 1965 – October 15, 1970

Prepared by

Tyco Laboratories, Inc.
Bear Hill
Waltham, Massachusetts 02154

for

National Aeronautics and Space Administration
Goddard Space Flight Center
Greenbelt, Maryland 20771

STANDARD TITLE PAGE FOR TECHNICAL REPORTS	1. Report No. Interim Report	3. Recipient's Catalog No.
4. Title and Subtitle LEAD TELLURIDE BONDING AND SEGMENTATION STUDY		5. Report Date 2/26/65 - 10/15/70 6. Performing Organization Code
7. Author(s) F. Wald, S. J. Michalik, S. Mermelstein, H. Bates		8. Performing Organization Rept. No.
9. Performing Organization Name and Address Tyco Laboratories, Inc. 16 Hickory Drive Waltham, Massachusetts 02154		10. Project/Task/Work Unit No. 11. Contract/Grant No. NAS5-9149
12. Sponsoring Agency Name and Address National Aeronautics and Space Administration Goddard Space Flight Center Greenbelt, Maryland 20771 Monitor: Joseph Epstein		13. Type of Report & Period Covered Final Technical 14. Sponsoring Agency Code

15. Supplementary Notes

16. Abstracts

This is the final report on contract no. NAS5-9149 which started on February 26, 1965. In Section I, it presents an introduction to the philosophy on which the whole effort was based and describes highlights in summary form in Section II. Further sections cover in detail the investigations on commercial PbTe-based thermoelectric materials, the engineering of PbTe-SiGe segmented submodules, as well as the constitution of the ternary Co-Ge-Si system and the binary Pd-Ge system. The report concludes with appendices which give all abstracts of previous reports written under the contract as well as summaries of papers and patents which resulted from the effort.

17. Key Words and Document Analysis. 17a. Descriptors

Thermoelectric Generators
Segmented Elements
Lead Telluride
Silicon-Germanium Solid Solutions

17b. Identifiers/Open-Ended Terms

Metallurgy, Phase Diagrams

17c. COSATI Field/Group

18. Distribution Statement	19. Security Class (This Report) UNCLASSIFIED	21. No. of Pages 102
	20. Security Class (This Page UNCLASSIFIED	22. Price

ABSTRACT

This is the final report on contract no. NAS5-9149 which started on February 26, 1965. In Section I, it presents an introduction to the philosophy on which the whole effort was based and describes highlights in summary form in Section II. Further sections cover in detail the investigations on commercial PbTe-based thermoelectric materials, the engineering of PbTe-SiGe segmented submodules, as well as the constitution of the ternary Co-Ge-Si system and the binary Pd-Ge system. The report concludes with appendices which give all abstracts of previous reports written under the contract as well as summaries of papers and patents which resulted from the effort.

Table of Contents

Table of Contents (Cont.)

List of Illustrations

List of Illustrations (Cont.)

List of Illustrations (Cont.)

List of Tables

I. INTRODUCTION*

The widespread use of thermoelectric power generation as the solution to a number of specialized power supply problems has been anticipated for some years. However, the application of thermoelectrics has been hindered by a number of major materials problems. These problems can be divided into those associated with (1) the physical characteristics, (2) the chemical behavior, or (3) the low conversion efficiency of thermoelectric materials.

The predominantly covalent nature of most thermoelectric alloys results in materials which are generally weak and brittle. In addition, PbTe alloys have a high thermal expansion coefficient which leads to susceptibility to thermal shock and thermal stress cracking. The mismatch in expansion coefficient between PbTe and metals also causes a fundamental physical incompatibility which must be dealt with in contacting these materials at the hot side. The vapor pressure of PbTe alloys precludes operation in vacuum or requires encapsulation. Porosity in sintered PbTe not only contributes to its mechanical instability, but may also pose a substantial long term hazard to the integrity of metallurgical bonds by migration of the pores in the temperature gradient. The high temperature mechanical properties of PbTe alloys are very poorly defined, and there is an almost complete lack of understanding as to what role they may have in generator design.

The reactive nature of one or more elements in all thermoelectric materials places severe limitations on the materials for use as hot side contacts. Reaction between the metal contact and the thermoelectric material can produce electrically active or mechanically destructive phases at the interface. Interactions between the dopants and contacts, which can drastically affect the electrical properties, are also possible. In fact, the consequences of reaction between the thermoelectric material and any of the several materials which constitute its environment are such that extreme care must be exercised in the choice of all such materials. However, without a basic knowledge of the interactions of the thermoelectric material with metals, potential brazes, insulations, etc., selection of these materials can only be by a trial and error process.

---

*H. E. Bates and F. Wald

The low efficiency of thermoelectric generating materials has been the main impediment to their wider application as power sources. The search for new materials has been largely abandoned; however, the need for higher efficiencies still exists. The most feasible means for achieving higher efficiencies appears to be the combination of existing materials over extended temperature ranges. The best known thermoelectric power generation materials, PbTe and Si-Ge, have optimum temperature ranges which complement each other for operation over a temperature interval of 800 to 1000 °C to 200 to 50 °C. Devices utilizing these materials over such a temperature interval should exhibit higher conversion efficiency than either material alone.

This program comprised a study of: (1) the bonding of PbTe thermoelements to non-magnetic electrodes, (2) the behavior of the elements and contacts at operational temperatures, (3) the compatibility of PbTe and SnTe with metals and the interactions of Si-Ge thermoelectric materials with potential hot contact meterials and brazes, and (4) the physical and chemical characteristics of the PbTe thermoelements. Other aspects of the program included a study of the segmenting of Si-Ge thermoelements with PbTe for higher efficiency, life testing of PbTe thermoelements and couples, design and construction of a prototype test device for Si-Ge-PbTe thermocouples, and the design of modules incorporating tungsten bonded PbTe and segmented SiGe-PbTe.

The general aims of the program were to define the most appropriate system and process for the preparation of low resistance, high strength bonds of nonmagnetic electrodes to PbTe alloys and to study the factors and processes involved in the degradation of thermoelements and contacts during extended service.

II. GENERAL SUMMARY REVIEW*

The contract originated from an earlier short investigation on non-magnetic bonds to commercial lead telluride based thermoelectric materials.[1] It was originally conceived as a continuation to that effort. However, as became apparent very soon, iron hot shoes on lead telluride were not easily replaced by another material without seriously compromising the long term reliability of the thermoelectric component. But at the same time, questions arose whether iron itself was indeed the ideal shoe material for high efficiency thermocouples. Various detrimental observations relative to iron bonds in certain specific circumstances were reported throughout the thermoelectric community. It became clear that more basic metallurgical work was needed to specify all sources of degradation in the material and in the bond in order to get a clear idea about the details of the interactions in the material itself, and in the bond in order to correlate the various observations arising from engineering testing of the thermoelectric components and devices.

From this time on, our perception of the work we had to do changed significantly. We perceived our contract now as being a service to the thermoelectric community. The service would consist of specifying various possible modes of degradation of the material and the bond and of providing data to prove our contentions as well as guiding component development into fruitful directions which were sound from a materials standpoint. A strong concentration of this effort on the hot junction region of PbTe based components remained, but was supplemented with studies on commercial p- and n-type PbTe based material, segmented couples and modules; and finally certain questions relating to Si-Ge based devices were addressed.

The most outstanding and obvious development during the contract period was the suggestion for using tungsten as a hot shoe material to PbTe based thermoelectric components. This suggestion was based on metallurgical investigations and long duration testing of bonded couples under operational conditions. The metallurgical investigations demonstrated that tungsten would be completely compatible with PbTe, SnTe and MnTe. Also, it could be shown that it would be compatible even with materials containing excess tellurium, since WTe_2 apparently forms a passivitating, diffusion blocking, thin layer on tungsten. This metallurgical information was supported by life testing of elements and couples and has in the meantime been verified throughout the thermoelectric community by operational results because tungsten is now generally accepted as a hot shoe material for stringent service conditions.

A more incidental observation which is so far not practically utilized in operational generators was also made. This observation showed that, by some up-till-now unidentified diffusion mechanisms, PbTe based commercial thermoelements could be metallurgically bonded to tungsten, leading to extremely low thermal and electrical impedances in the junction.

---

*F. Wald

This development has been thoroughly reviewed in the Fourth Semiannual Phase Report on this contract (covering the period from February 1, 1969 to July 31, 1969) and will therefore not be elaborated here. In and of itself, it might lead to integrally bonded PbTe couples which would be much easier to handle in assembly and also would have somewhat higher efficiencies due to the observed low thermal and electrical impedances in the junction. Besides this, the development opened the door to the design and preparation of segmented GeSi - PbTe couples which was subsequently undertaken in the contract and carried through to the building of prototype modules. In these modules, certain design principles are pointed out which are important in coping with the low strength of PbTe coupled with the various thermal expansion problems and the fact that good heat transfer and electrical insulation must be provided at the cold shoe area. These developments again enlivened the somewhat subdued debate of cascading versus segmenting for higher efficiency. From our results, we believe that the two methods are just about equal in mechanical and design complexity as well as efficiency. Ultimately we would expect segmenting, however, to be able to provide slightly more power dense modules.

Less obviously, a large number of investigations were started on this program which for the first time definitively and explicitly demonstrated various modes of behavior which commercial PbTe based alloys exhibited in operation. Some of these modes were further demonstrated by basic studies on model systems. These various investigations will be reviewed in detail in another section of this report. Thus, only some listing will be provided here. The first definitive studies on evaporation, room temperature and elevated temperature strength and pore migration were conducted under this contract. Also, studies on the intentional and unintentional impurities in p-type PbSnTe and n-type PbTe were made. It was tried to demonstrate the presence, distribution and concentration of oxygen in the material and its bearing on junction properties. Also, the precipitation of MnTe in p-type PbSnTe was studied and the suggestion was made that this was a degradation mode, but could also provide an advantage by a "metallurgical segmentation" effect. This effect was demonstrated to exist in the PbTe - Ag_2Te system. This system also showed the dependence of the Ag doping action in PbTe on the Ag/Te ratio introduced.

Finally, metal silicon germanium systems were studied to shed some light on the degradation modes of Ge-Si hot junctions. From a literature study, it could be shown that due to the nature of the W-Si-Ge system a degradation of W-GeSi bonds at rather low temperatures is to be expected. Various platinum group metals have been suggested as bonding agents for GeSi in several patents. It can be shown from the literature and our own supplementary phase diagram investigations that not much hope lies here, since Ge-Si - Platinum Metal Systems generally show some very low melting eutectics of the order of 700 to 800°C.

If the present Air Vac bond^{TM} needs improvement (it is not clear to us whether it does), our suggestion is to use stoichiometric disilicides as hot shoes. Tungstendisilicide (WSi_2) would be the best candidate since it has excellent electrical and thermal conductivity comparable to metals. It is, however, not commerically available. $MoSi_2$, which has thermal and electrical properties of only a slightly inferior nature, is an excellent second choice because it is commercially available under the trade name "Super-Kanthal," and its properties are thus extremely well documented and its availability is guaranteed.

In these latter cases, however, a braze will have to be sought. Our thinking here went in the direction of Co-Si-Ge alloys for that purpose. They, however, may have their

difficulties as is explained in another section of this report. We feel, in general, that it will be difficult to develop a truly optimized contact system which allows GeSi to be operated effectively at temperatures over 1050°C.

REFERENCES TO SECTION II

1. M. Weinstein and H.E. Bates, Thermoelectric Bonding Study, NASA Contractor Report - NASA-CR-290, Sept 1965.

III. PHYSICAL-CHEMICAL CHARACTERISTICS OF COMMERCIAL PbTe MATERIALS*

While a great deal of emphasis in this program has been put on the chemical interactions of PbTe materials, it is also obvious that their physical characteristics are of equal importance to their performance in a generator. Early in the program we began an effort to characterize physically and chemically the thermoelectric materials produced by Minnesotta Mining and Manufacturing. We have summarized this work here, with some discussion of the implications of our findings and recommendations for areas of further exploration.

It should be clearly understood that the subsequent discussion is of a commercial material. The thermoelements referred to throughout were made by crushing a cast ingot of the desired composition and then cold-pressing and sintering the powered material. The discussion which follows is concerned with three thermoelement types designated 3N, 3P, and 2P by 3M's. These are n-type PbTe, p-type SnTe-PbTe, and p-type PbTe, respectively.

A. Thermoelement Chemistry

1. Composition and impurities

Thermoelements were analyzed by semiquantitative spectrographic and wet chemical techniques. Table 1 lists the results of the spectrographic analyses. Sodium is present as a major impurity in 2P since it is the p-type dopant. The presence of substantial amounts of Ni and Fe in the n-type elements cannot be readily explained, for while both should behave as n-type dopants, major doping action is supposed to be achieved by the addition of iodine. (Iodine may be introduced as NiI_2, however.) Similarly, the large amount of Mn found in 3P elements is somewhat puzzling. The overall composition of the 3P material leads to considerable complexity which will be discussed further below.

Chemical analysis of 3N and 2P materials showed them to be substantially PbTe. Analyses of 3P elements from four purchase lots are shown in Table 2. The interesting points here are the substantial amounts of excess Te and of MnTe. It should also be noted that the ratio of SnTe to PbTe is about 60:40. Three earlier analyses for Mn showed amounts of 1.10, 0.82, and 1.26%, indicating that the amounts in the Table are extreme, as far as our observations went.

*H. E. Bates

Table 1. Semiquantitative Spectrographic Analysis of Thermoelements*

Concentration Range	3N	3P	2P
A	Pb, Te		Pb, Te
3 B		Pb, Sn, Te	
B		Mn	
c	Ni		
3 d	Fe		Na
3 e		Na	Sn, Fe, Si, Al
e	Sn, Cu, Si	Fe, Ag, Si	Cu
3 f		Ni	Mg
f	Mn, Ag, Ca	Cu, Ca, Sb, Cd	Cd, Ca, Mn
3 g	Cr, Cd	Cr	Ag, Bi, Ni

*Semiquantitative Code:

A = 10 - 100%, B = 1 - 10%, c = 0.1%, d = 0.01 - 0.1%, e = 0.001 - 0.01%, f = 0.0001 - 0.001%, g = 0.00001 - 0.0001%. A number before the letter multiplies the range. Thus, 3B = 3 - 30%, 3e = 0.003 - 0.03%.

Table 2. Composition of 3P Thermoelements

	Pb	Sn	Te	Mn
	29.2	23.0	46.5	0.52
	28.0	24.9	45.0	0.72
	23.8	22.9	51.9	1.40
	28.1	22.7	47.8	1.40
Ave wt %	27.5	23.4	47.8	1.01
Ave at. %	18.4	27.3	51.9	2.33

Compounds	Mole %
SnTe	52.6
PbTe	35.5
MnTe	5.0
Te (excess)	7.0

2. Manganese in 3P materials

The presence of Mn in the 3P materials first provoked our interest when it appeared in chemical analyses and when inclusions of MnO were identified with the electron microprobe. This eventually led us to start an investigation of PbTe-MnTe-SnTe system, which unfortunately was curtailed before getting into the SnTe portion of the system. This work is reported in detail in the Semiannual Phase Report No. 2. It is reviewed here with some observations on life-tested 3P elements which showed some unusual precipitates and electrical behavior.

The pseudobinary PbTe-MnTe phase diagram was constructed. This diagram is shown in Fig. 1. Later results indicated that this diagram may not represent the equilibrium situation. Alloys annealed for several hundred hours at 400 and 500 °C showed $MnTe_2$ and thus some of the phase fields in this diagram must contain $MnTe_2$.

Given the assumption that the SnTe-MnTe system shows a similar complexity (which is more than likely), it may still be concluded that the precipitation phenomena in 3P material arise from the fact that a metallurgically very complex system has to be used to produce desirable thermoelectric properties.

In Fig. 2, the high PbTe side is of interest in that the boundary between a two-(or three-) phase and a single-phase field runs through the temperature and MnTe ranges which would be encountered in thermoelements. We never observed any precipitates in new or as-bonded elements (3P) and this seems reasonable in view of the large solid solution field which probably extends along the PbTe-SnTe side of the pseudoternary diagram. A number of 3P elements which had run in a 510 to 60 °C gradient for 3850 hr showed substantial decreases in resistivity and Seebeck coefficient over their hot portions in post-test analysis. (See Semiannual Phase Report No. 1 for details.) Metallographic examination of these elements revealed the interesting and theretofore unseen precipitates shown in Fig. 3

Elements from one purchase lot showed an unusually large amount of manganese oxide (Fig. 3). Examination of untested elements from the same lot showed similarly frequent occurrence of this phase. Each element showed (on a diametric cross section) five or six clusters of MnO particles of the size of those shown in Fig. 3. Previously, only isolated particles or single clusters of about a dozen particles had been observed (see, for example, p. 95 of the First Interim Summary Report).

Generally, in association with the clustered MnO particles, particles of another phase were found. These can be seen in Fig. 3. It was also found that in all of the elements examined (ten out of fifteen) a band of precipitated particles had formed roughly 0.090 in. away from the hot junction. The transition into this band of precipitation is shown in Fig. 3-a. The hot side is toward the left of the photomicrograph and the precipitation zone can be best distinguished by the wide grain boundaries. Higher magnification shows that the grain boundaries are sites for precipitation and growth of these second phase particles, as are the interfaces of the matrix and MnO particles (Fig. 3-b). Fig. 3-b occurred in the bulk of the grains.

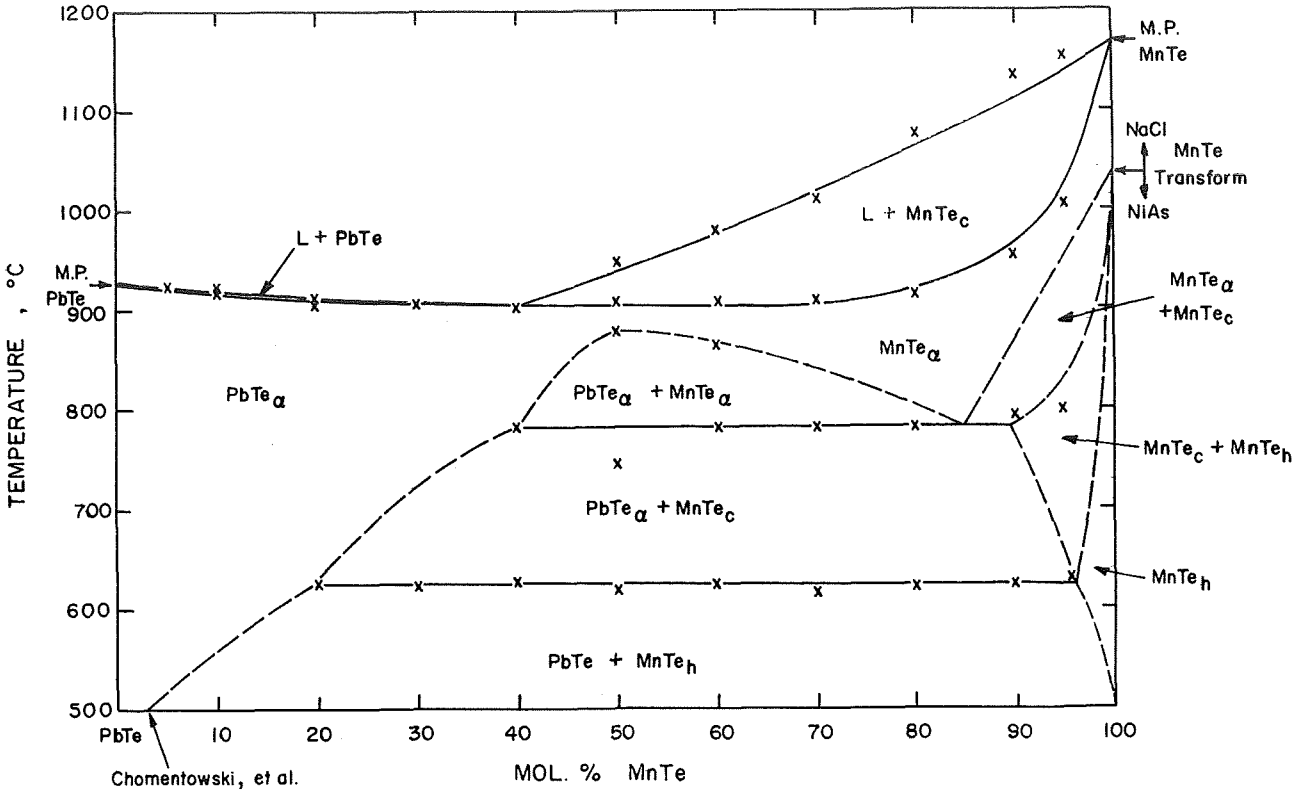

Fig. 1. Preliminary phase diagram of the pseudobinary system lead telluride-manganese telluride, based on thermal analysis results and microscopic observations on as-cast specimens

Phase Designations:

$PbTe_\alpha$ = Sodium chloride structure type solid solution of PbTe-MnTe with high PbTe content and variable composition

$MnTe_\alpha$ = Sodium chloride structure type solid solution of MnTe-PbTe with high MnTe content and variable composition

PbTe = Terminal solid solution of sodium chloride structure type PbTe

$MnTe_c$ = Terminal solid solution of sodium chloride structure type (high temperature form) MnTe

$MnTe_h$ = Terminal solid solution of hexagonal NiAs type (low temperature form) MnTe

(All thermal arrests were averaged from at least two heating and cooling points.)

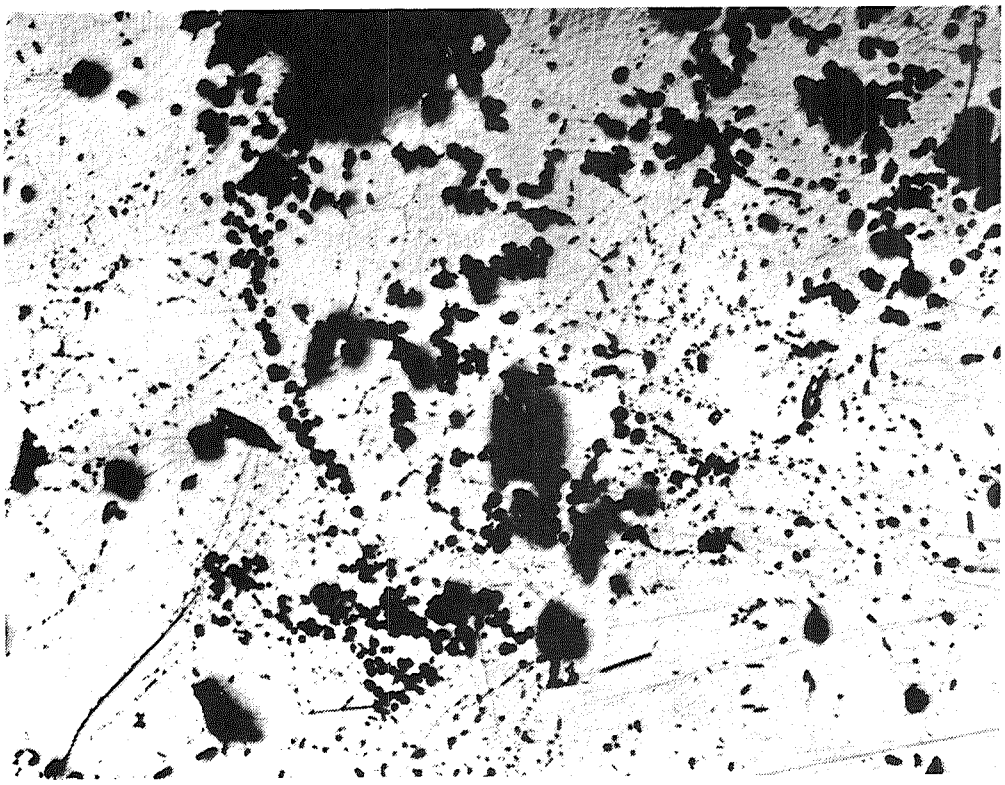

Fig. 2. (a) Manganese oxide particles near hot junction of gradient-tested 3P element, plus unknown second phase-medium gray (150X)

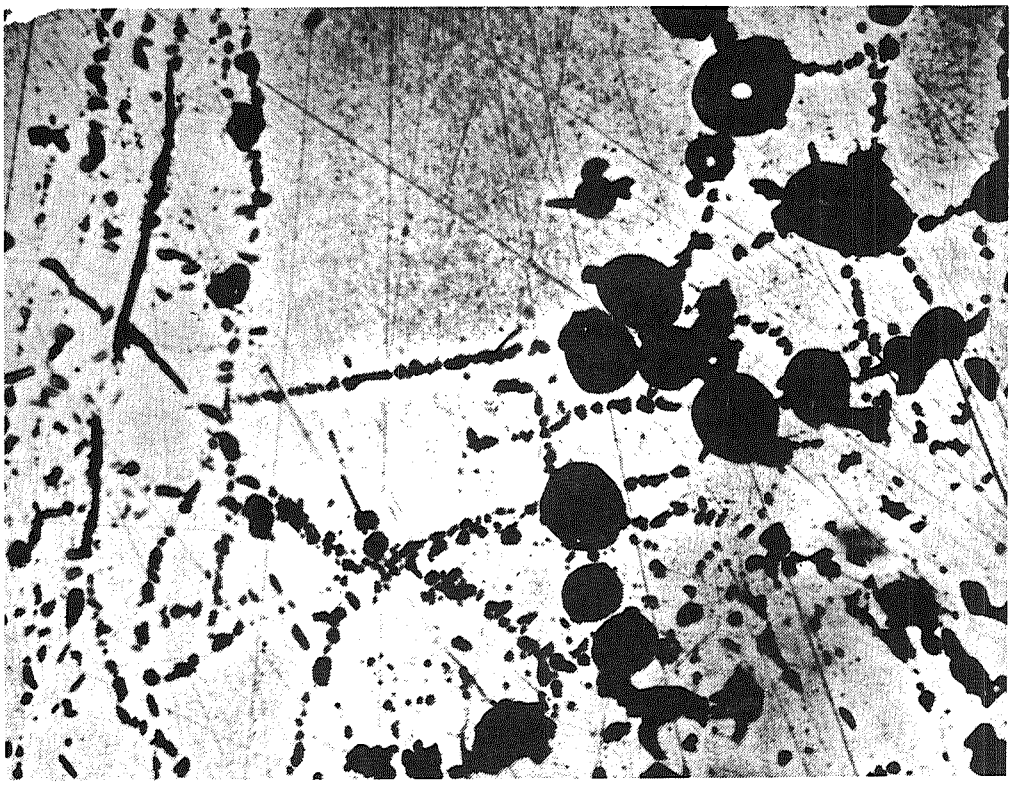

Fig. 2. (b) Manganese oxide particles and unknown phase-same as above (750X)

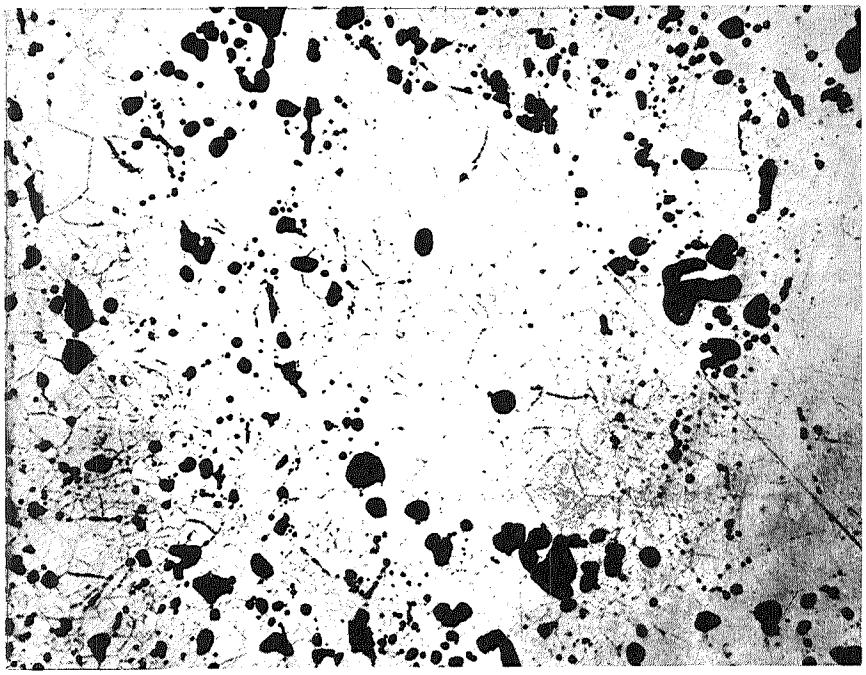

Fig. 3. (a) Transition area into band of precipitation of unknown phase in gradient-tested elements (70X)

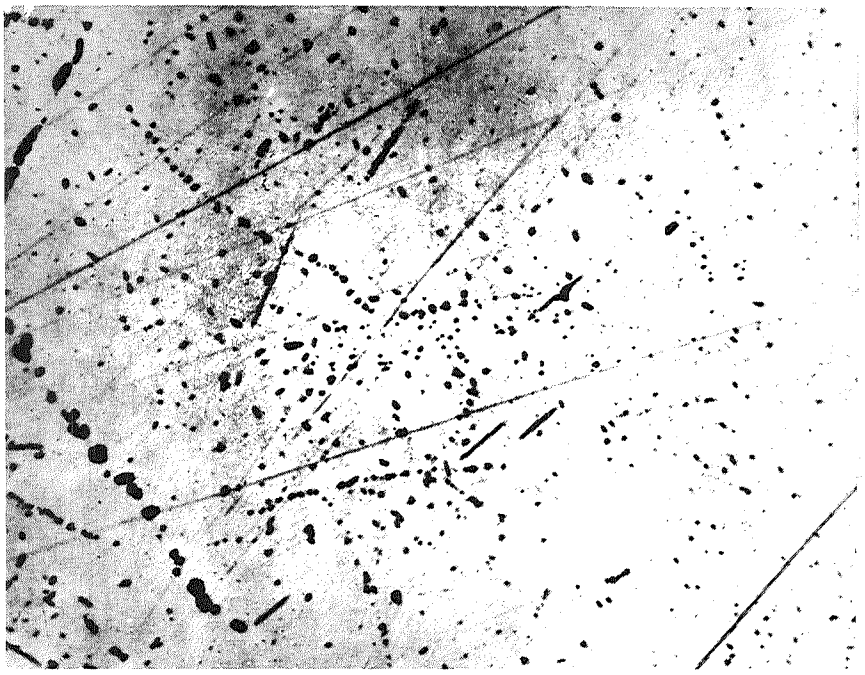

Fig. 3. (b) Particles of unknown phase precipitated in gradient tested in 3P elements (750X)

The effect was found in bonded and unbonded elements, and elements from three different purchase lots, the first and last of which were separated by a year in purchase date.

An element from the oldest lot showed a lesser tendency toward clustering of the MnO particles and an apparently smaller amount of MnO. The precipitation zone was further down the element, that is, at a lower temperature, and the morphology of the fine precipitates was less distinct than in the other elements. This is shown in Fig. 4, which also shows clearly, by the depletion of fine precipitates around the central area, that the large particles, nucleated on what is probably a graphite particle, are the same material as the fine bulk precipitates.

The general appearance indicates that this phase has precipitated in the solid state from the PbTe-SnTe matrix. The existence of what appears to be the same phase at both high (~500°) and intermediate temperatures (~300°) would seem to indicate that this is more than a simple temperature dependent solubility effect. All of which is not surprising as the emerging complexity of the MnTe-PbTe-SnTe system indicates. This might be of largely academic interest, if it were not extremely probable that this gradual redistribution of MnTe apparently can substantially reduce the Seebeck coefficient of the 3P elements. Lowered Seebeck voltage was found in these elements and was also observed to be an important degradation factor in other gradient life tests. It would seem in the case of 3P material that a basically unstable system has been chosen, and whatever benefits may be initially realized, it appears that they are lost in the long term.

3. Oxygen content of thermoelements

Oxygen in and around bonded PbTe thermoelements has been a major concern during this program. It has been implicated in both the formation and degradation of the bond to tungsten (see Section III, Semiannual Phase Report No. 4). Whether it is truly responsible in either, both, or neither case has not been definitely determined.

Vacuum fusion analyses on a number of elements of the various types are summarized in Table 3.

Table 3. Oxygen Content of 3M's Thermoelements

Material	Range, ppm	Average, ppm
3N	40 - 90	70
3P	320 - 540	420
2P	40 - 60	70

It is difficult to determine what part of the oxygen content may represent adsorbed water vapor and where or how the remainder of the oxygen resides, whether in solution as oxides or as adsorbed or trapped gas in the pores of the elements.

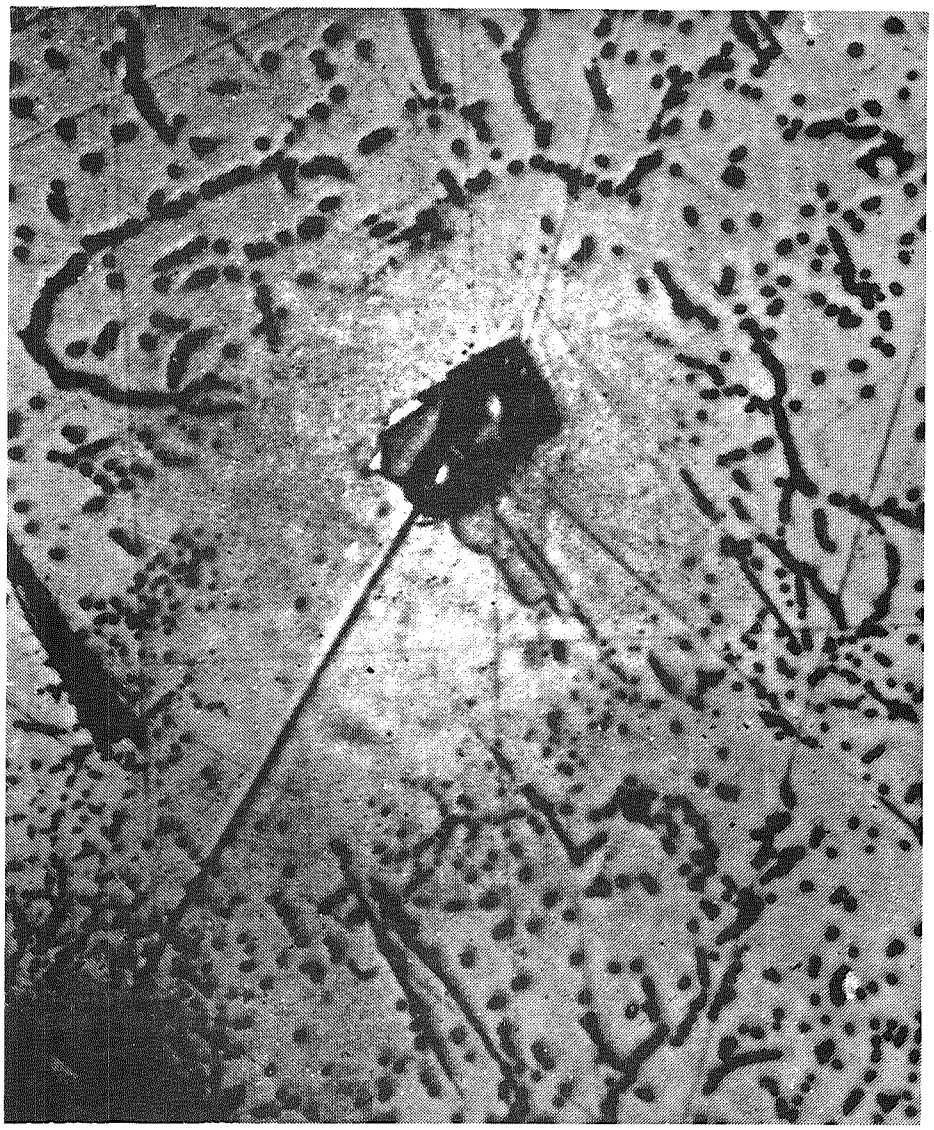

Fig. 4. Area within unknown precipitate zone showing poorly defined morphology or particles (750X)

In one experiment, we measured the oxygen content at all stages of pressing and sintering high-purity n-type PbTe and 3N powder. The high purity PbTe contained less than 10 ppm O_2 initially; after crushing, ball-milling, and pressing, the green pellets contained 500 ppm. The green pellets pressed from 3N powder contained 170 ppm. The sintering treatment was in hydrogen up to 500 °C, then under argon for 30 min at 600 °C and 15 min at 700 °C. The sintered 3N pellets showed 60 ppm O_2 and the high purity PbTe showed 195 ppm. The percent reduction in O_2 is about the same for both materials at 60%. These results are of some interest in relation to the oxygen contents of the various 3M materials. There is no obvious reason why the 3P material should contain six times as much oxygen as the n-type. However, it is obvious from our experiments that different processing can drastically alter the oxygen level found in the final element. The high-purity PbTe was ball-milled to a finer particle size than the 3N powder, thus incorporating a much greater amount of oxygen in one form or another. Thus one could speculate that the 3P material because of its higher hardness requires addition of a certain fraction of more finely ground powder with a higher oxygen level in order to achieve a reasonable density in the sintered element. A somewhat lower sintering temperature (because of the lower melting temperature of the PbTe-SnTe solid solution) may result in a smaller reduction in oxygen content which in combination gives the high final levels in 3P.

Whatever the source, it seems in general desirable to reduce the high level of oxygen in 3P elements, particularly in tungsten-contacted systems. We have some indications that hydrogen annealing at temperatures above 700 °C can lower the oxygen level, but a thorough study is needed.

B. Evaporation Rate and Vapor Pressure

Measurements were made of the evaporation rates of 3N and 3P thermoelements in a dynamic vacuum.[1] These results were published[2] and the calculated vapor pressures confirmed by another investigator using a different technique.[3] The temperature dependence of the evaporation rate and vapor pressures are shown in Figs. 5 and 6.

The effect of inert gas atmospheres at varying pressures has been studied by a group of Russian investigators.[4] Their results show a reduction in evaporation rate of PbTe at 575 °C of approximately 1400 times in a 150-mm Hg argon atmosphere compared to a dynamic vacuum. Further increases in argon pressure to 8 atm did not further reduce the evaporation rate.

The sublimation of PbTe materials, even when inhibited by an atmosphere, remains a problem when long-life generators are considered. Techniques to limit sublimation effects such as those described by Killian must be considered.[5]

C. Microstructure

The major consequence of powder metallurgical fabrication, particularly for a brittle material, is one thing – porosity.

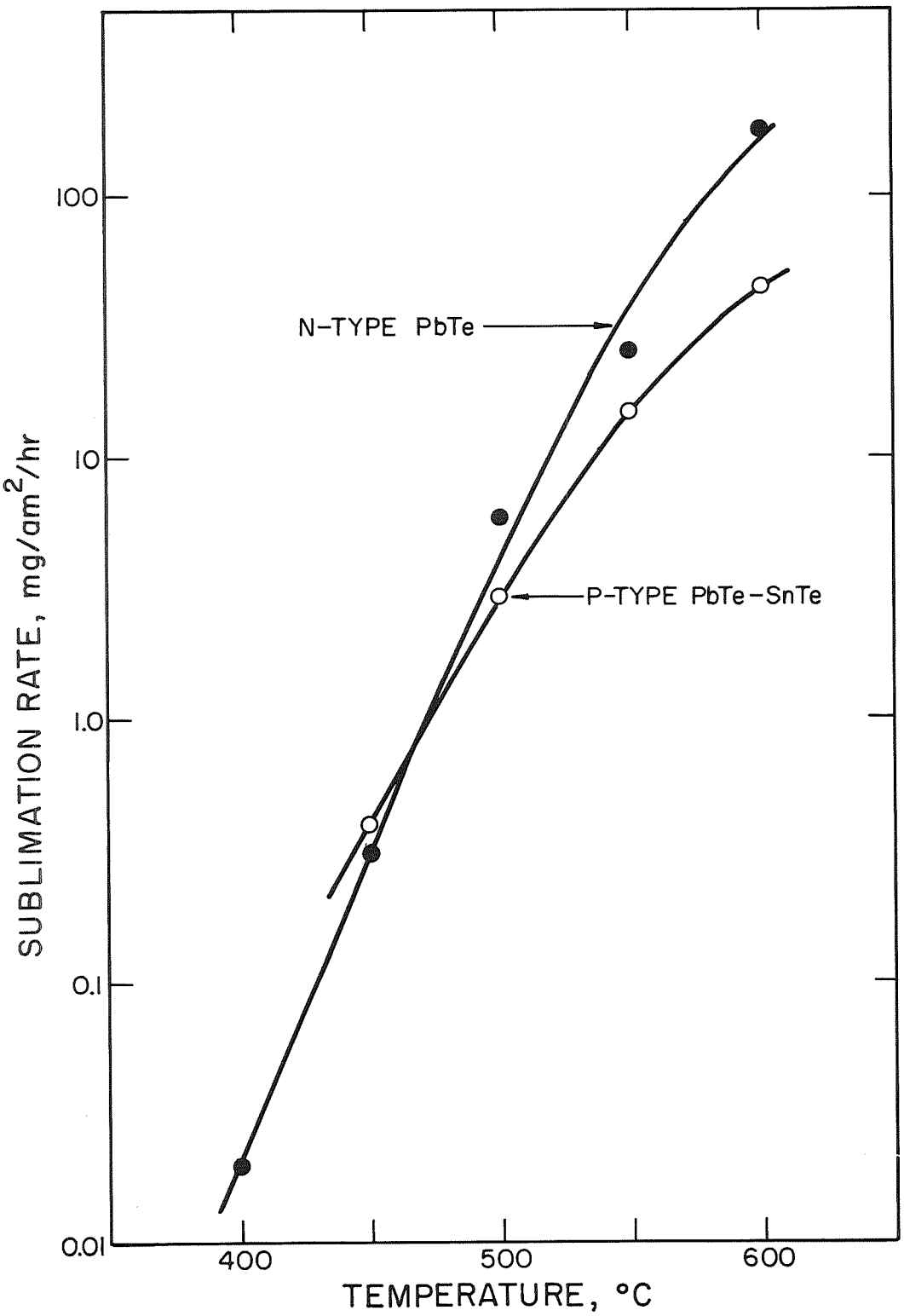

Fig. 5. Sublimation rate as a function of temperature for cold-pressed and sintered N-type PbTe and P-type PbTe-SnTe elements

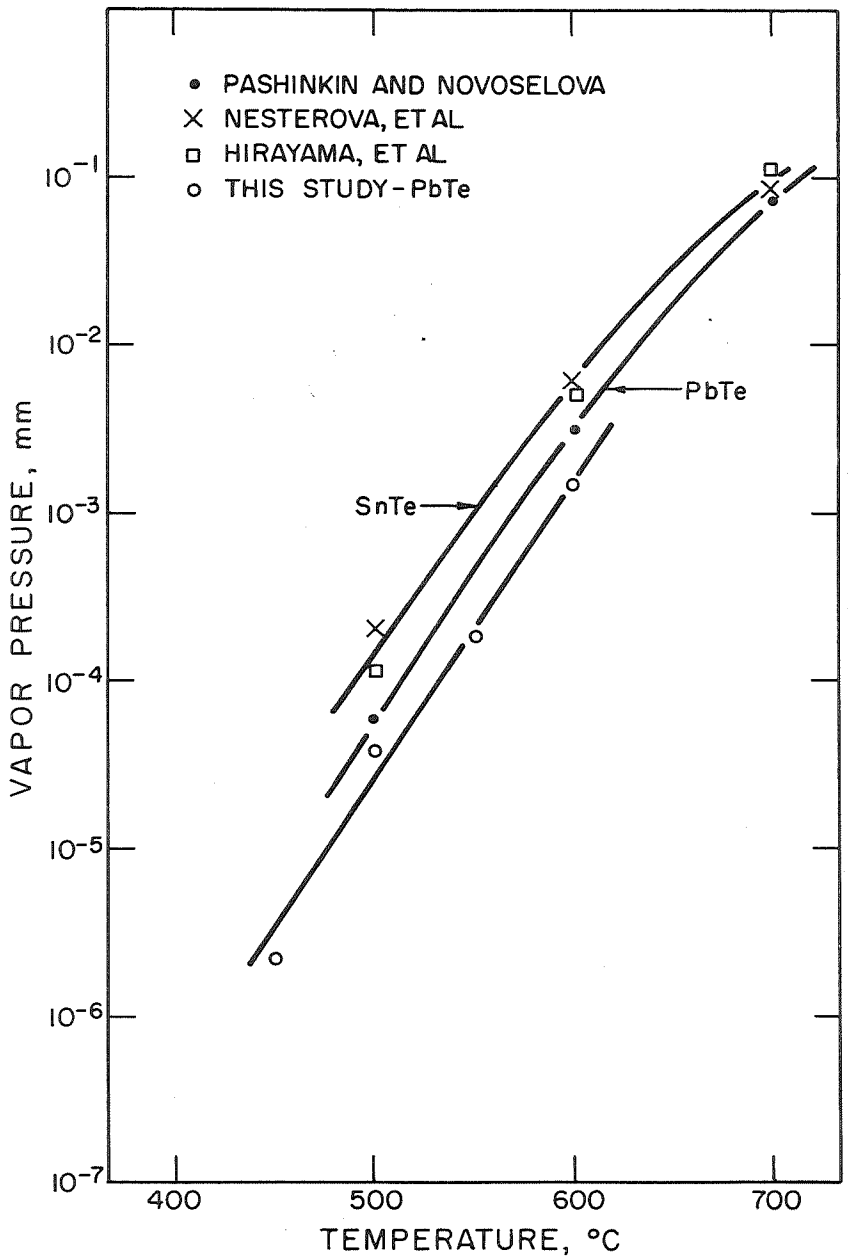

Fig. 6. Vapor pressure as a function of temperature of PbTe and SnTe

Figs. 7, 8, and 9 show the macro- and microstructures of 3N, 3P, and 2P, respectively. In the macrophotographs, the pores appear as white specks outlining large areas of dense material. The n-type element shows a rather regular layered arrangement of the large grains, which we term "pseudo-grains" since they are actually composed of many small, real grains. This can be seen in the microphotographs. The p-type materials show a much more irregular structuring of the porous and dense areas. This is probably a result of their higher hardness and almost complete absence of plastic deformation which inhibits high compact densities before sintering. If a reasonably high density is not achieved initially, the sintering process is not as effective in producing a densified structure. The 3N and 3P structures appear to be the equilibrium structures as far as grain growth at any probable service temperature is concerned. (These structures are, after all, the result of sintering at a fairly high temperature.) It should also be noted that the pore structure has tied up virtually all the grain boundaries. No significant grain growth was found on annealing n-type elements 1500 hr at 540 °C and 855 hr at 650 °C in a 1961 study at Atomics International.[6] We found no change in structure after 100 hr at 700 °C.

P-type PbTe (2P) appears to have been sintered at either a lower temperature or for a shorter time, since anumber of grains within the large "pseudo-grains" show curved boundaries, a situation which is obtained during the process of grain growth. It is not unexpected that this material might have a less complete sintering treatment in order to minimize loss of the Na dopant. Whatever further grain growth might occur in operation should have negligible consequences for the performance of the elements.

In general, it is to be expected that grain growth will not contribute significantly to any degradation process. The pore structure is of greater importance. While it substantially prevents grain growth and probably reduces the over-all thermal expansion coefficient and thermal conductivity, it also is significantly harmful to the mechanical properties of the p-type alloys as will be shown and probably contributes to the degradation of contacts to the materials.

D. Porosity

1. Characterization of pores

The average pore size and the distribution of pore sizes were determined for 3N, 3P, and 2P elements. In n-type elements, the average pore size was found to be 6 μ with 60% of the pores lying within $\pm$ 0.9 μ of this average. ($\pm$ 0.9 μ represents the range of the categories; thus within a total range of about 3 μ, about 60% of the pores will be found.) The average pore size of 3P elements was 27 μ with 77% of the pores falling within the three categories nearest the average. The 2P material is rather similar with an average pore size of 24 μ and 75% of the pores falling near the average. This means that the p-type materials have a rather uniform pore size, while the n-type elements have a somewhat greater range of (smaller) sizes.

It was also found that the pores are not likely to be the repository of the oxygen present in the elements. As an adsorbed double layer, the typical amount of oxygen would occupy several thousand times the surface area available from pores.

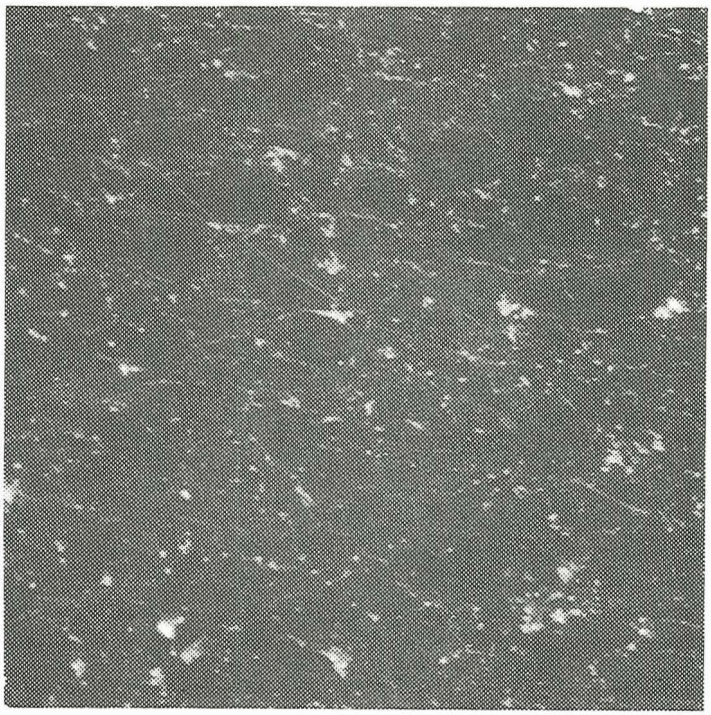

(a) 9X

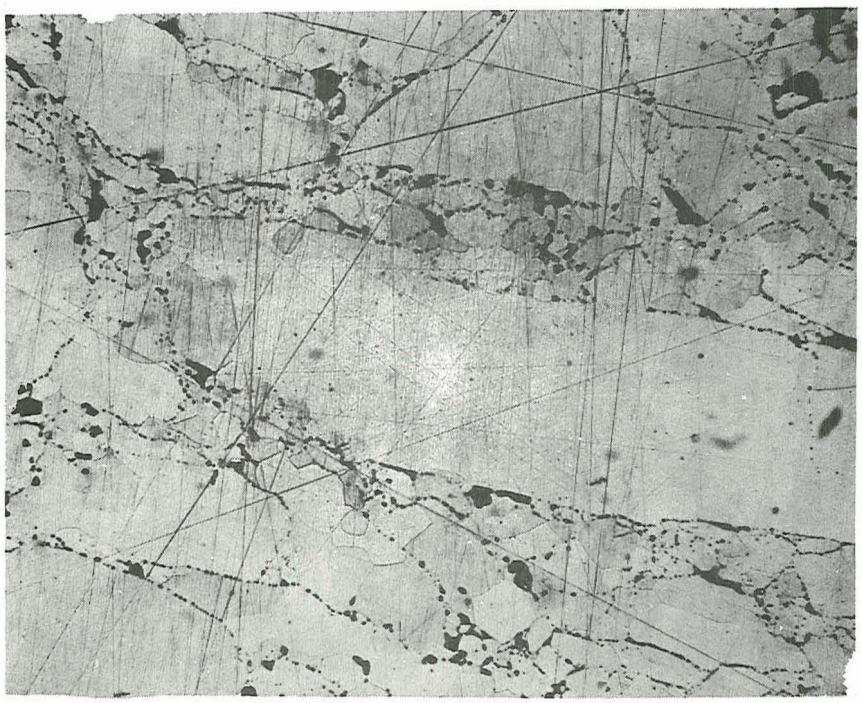

(b) 100X

Fig. 7. Sections of N-type PbTe (3N) thermoelements

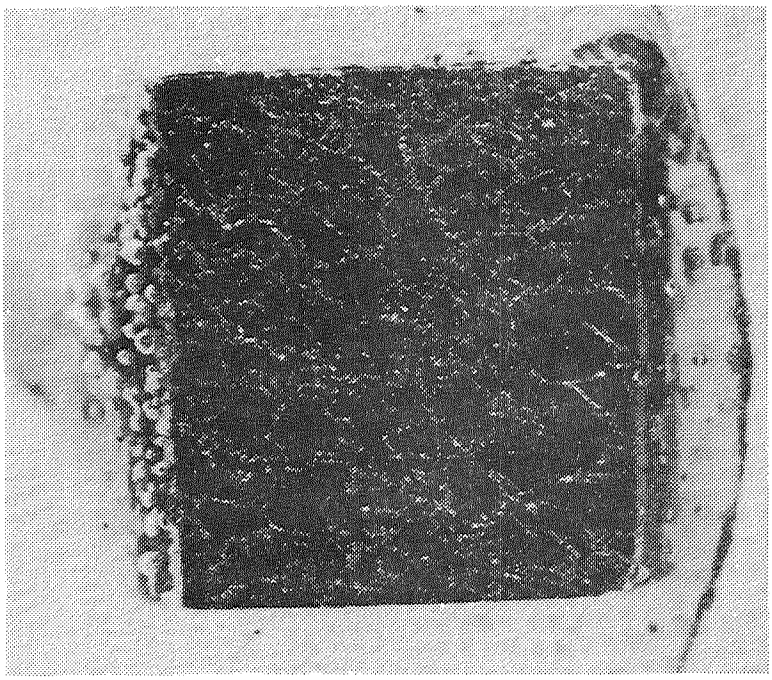

(a) 9X

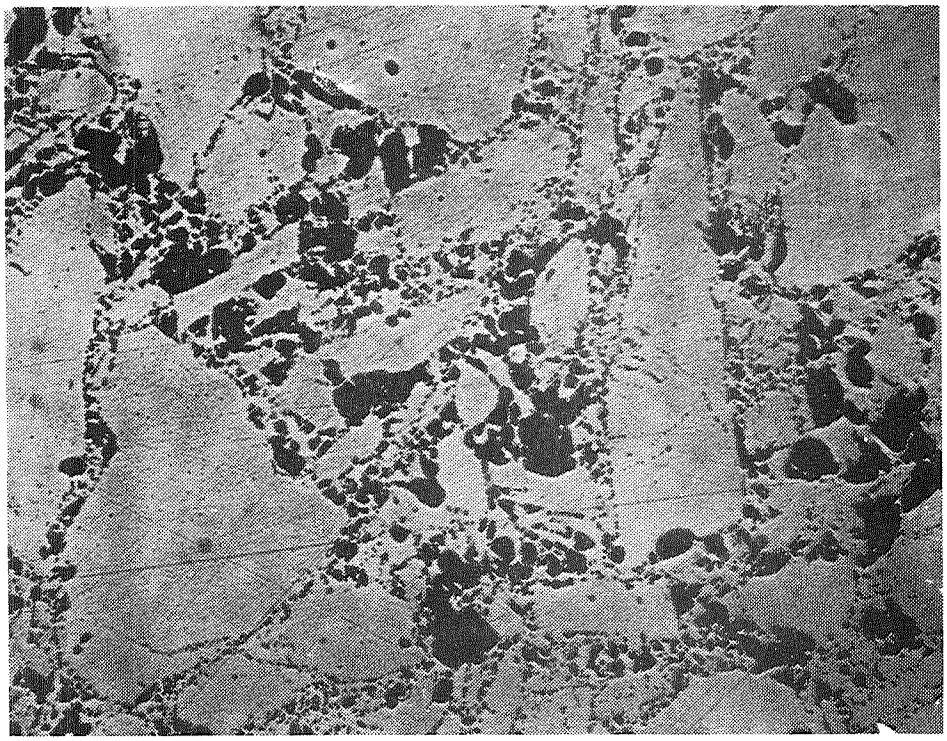

(b) 100X

Fig. 8. Sections of P-type SbSnTe (3 P) thermoelements

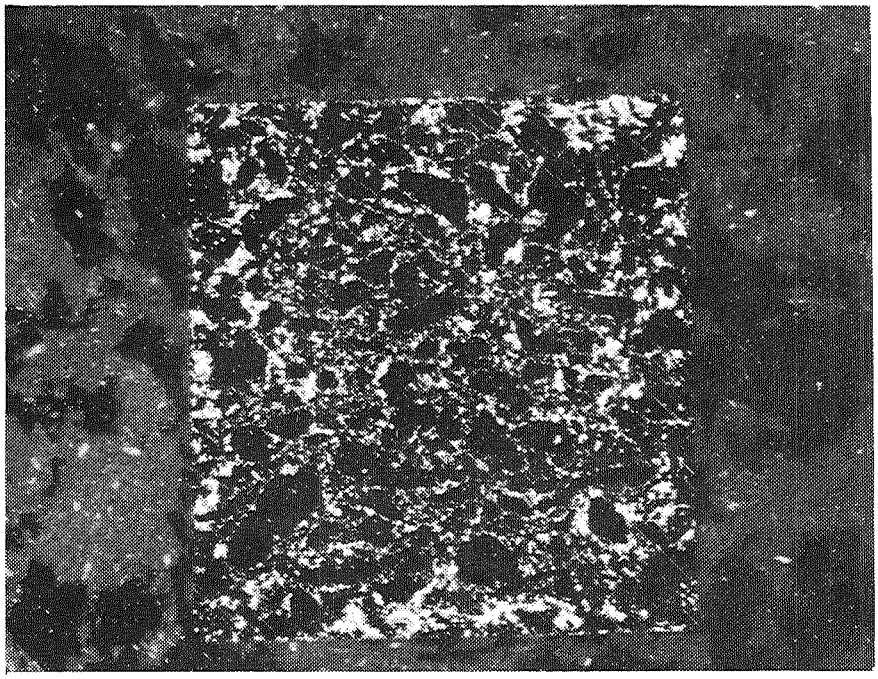

(a) 9X

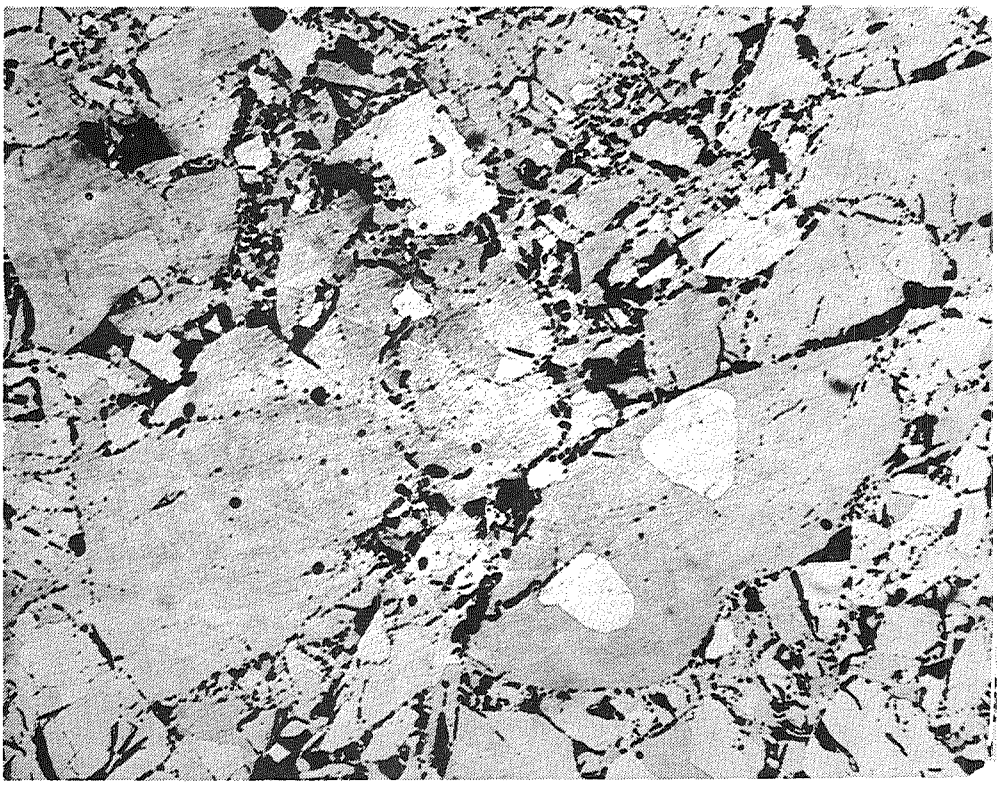

(b) 100X

Fig. 9. Sections of P-type PbTe (2 P) thermoelements

2. Pore migration

Midway through the program, in speculating on long-term degradation mechanisms in PbTe materials, it was hypothesized that, given the fairly high vapor pressure of PbTe, pores might migrate in a temperature gradient by vapor transport.

An equation for the velocity of migrating pores was derived, which may properly describe the motion of the pores in a gradient.[7, 8, 9]

Rough calculations based on our knowledge of the volume fraction of pores and average pore diameter in 3P materials and on calculated migration velocities indicated that migrating pores could destroy a significant fraction (such as one third) of the area of a contact at 525 °C within times of the order of 10,000 hr. These predictions would be modified considerably for real materials, however. Instead of every pore being able to move freely for the entire length of the element, in real materials many pores are already pinned at grain boundaries and the availability of grain boundaries and second phase particles and foreign inclusions should serve to trap many more which might be free to migrate initially.

The distribution of pores in gradient-tested 3P elements (3850 hr at T_H = 510 °C, T_C = 60 °C) were compared to similar elements with no gradient history. A significant difference was found in the distribution curves showing an increase in the number of pores at the hot end of the gradient-tested elements. No differences were apparent in comparing the frequency distributions of pore sizes between the ends of the tested and control elements indicating that coalescence had not occurred to any great extent and also, possibly but not necessarily, that there is not a strong radius dependence of migration velocity infact. (See Semiannual Phase Report No. 1 for details.)

While our sample size was small in this experiment, we do feel that a real effect was detected. Given the possible effects of statistical fluctuations, that is all we feel safe in saying. However, we do believe that, if there is any possibility of sintered PbTe being used in long term generators, this subject must be studied more carefully, using both real and simulated materials.

E. Mechanical Properties

Lead and tin telluride are substantially covalently bonded compounds. When made into thermoelements by cold-pressing and sintering, the resulting elements, not unexpectedly, are weak and brittle. They are also neither necessarily homogeneous nor isotropic. In addition to low tensile and shear strengths, their low thermal conductivity and high thermal expansion combine to give materials with poor resistance to thermal stress and shock. Yet, these materials must operate in steep temperature gradients.

A number of physical/mechanical properties were measured on 3M's thermoelements early in the program. These are summarized in Table 4. Clearly, these are not structural materials. Only the n-type elements possess any reasonable capacity to deform "plastically" before failure. In actual testing, the differences are more apparent than the figures might indicate. The p-type elements fail very abruptly and simply turn into powder, while the n-types are rather more gradual and break into chunks. Obviously, the large amounts of porosity in the

Table 4. Summary of Mechanical Properties of PbTe Thermoelements

Type	Density, gm/cm^3	Theoretical, %	Vickers Hardness	Tensile Strength, psi	Compressive Strength, psi	Reduction in length, %	Shear Strength, psi	
							New	Bonded
3N	8.06	97.5	40	1370	12,700	12	1755	1715
3P	6.65	92	110	660	12,550	2.5	1040	1080
2P	7.6	92	70	625	12,500	2.3	1090	830

p-type elements contribute to this, since their structure consists largely of grains held together by thin webs of porous material.

One area of mechanical behavior of these materials which is very important to the design of generators but has not been investigated is the high temperature properties, both short and long term. The creep strengths (and rates) determine, after all, the maximum compressive loadings which can be employed. These should be measured.

F. Discussion

While much of the preceeding material might seem to cast a very unfavorable light on PbTe alloys, such is not our intention. Even though PbTe is a difficult material to apply in power generation, it is neither useless nor hopeless. The materials have many limitations, and it is vital that designers of generators recognize them. At the same time, these materials are presently the best available to satisfy the requirements for intermediate temperature thermoelectric power generation. Thus, most of the physical deficiencies of the PbTe alloys must be viewed as constraints on any potential design. The vagaries of the composition of 3P material, however, would seem to be an area where basic changes might yield definite improvement over the present performance.

REFERENCES TO SECTION III

1. H. E. Bates and Martin Weinstein, NASA Contractor Report CR-290 under Contract NAS5-3986 (1965).
2. H. E. Bates and Martin Weinstein, Adv. Energy Conversion, 6, 177 (1966).
3. P. Winchell, Energy Conv., 8, 81 (1968).
4. B. G. Arabei, M. B. Bronfin, G. B. Kurganov, and V. A. Timojeev, Geliotekhnika (Applied Solar Energy-USSR), 2, (1) 25 (1966).
5. J. Killian, Inter. Soc. Energy Conv. Eng. Conf. Proc., 1968, p. 272.
6. P. Elkins (Atomics Int'l., Division of North American Aviation), Mechanical Properties, Thermal Expansion, Compatability and Heat Treatment of PbTe, U.S. Atomic Energy Comm. NAA-SR-Memo-7172 (1962).
7. P. G. Shewmon, Trans. AIME, 230, 1134 (1964).
8. W. Oldfield and A. J. Markwood, Mater. Sci. Eng., 4, 353 (1969).
9 F. A. Nichols, J. Metals, January 1969, p. 19.

IV. DESIGN AND TESTING* OF SEGMENTED COUPLE MODULES

A. Preparation of Couples

Bonding of couples was continued and essentially completed with some material attrition. All couples were bonded except for two that had been returned to Germany because of high "N" type leg resistivity. This resistivity had not been in evidence for the leaded sample we originally received with the shipment of couples.

These couples were returned to us with the explanation that the material was perfectly satisfactory, and we should see much lower resistivities at the proper hot shoe temperature. While we tended to remain dubious, there was little to be done since the drawing from which the parts were ordered does not directly specify a room temperature resistivity value.

We continued working with the couples as they were, since the higher resistivities could be taken into account when calculating efficiencies and since the couples were acceptable in all other respects.

For couple shoe soldering, a silver/tin solder with a melting point of 221 °C and good plastic flow characteristics was selected. This is a 96.5 Sn-3.2 Ag alloy commercially available as Eutectic welding alloy no. 157 which is typically used for stainless steel. A companion flux Eutectic no. 157 is being used which works well on the nickel plated PbTe.

The shoe tinning fixture was proven to be impractical and a preform was employed instead. This required solder ribbon which was prepared in-house by casting the 20 gauge no. 157 alloy into a 0.25- by 4-in. rod and rolling down. Disks were cut from this ribbon to match the size and shape of the "N" and "P" shoes.

The shoes were cleaned, fluxed, and placed on a hot plate with the preform in place and the solder allowed to reflow and tin the shoe to bring the conical surface into a flat condition (some slight sphericity due to surface tension was evident).

Certain improvements were also made in the shoe sweating fixture. Previously, steel bolts were used to hold the fixture together and differential expansion between the bolts and aluminum fixture components caused yielding of threads in the aluminum as evidenced by the loosening up of the fixture after each run.

Such loosening is a real factor in loss of shoe to strap parallelism. This problem was overcome by using spring loaded tie rods in place of the bolts (Fig. 10). Since shoe sweating is

*Sy Mermelstein

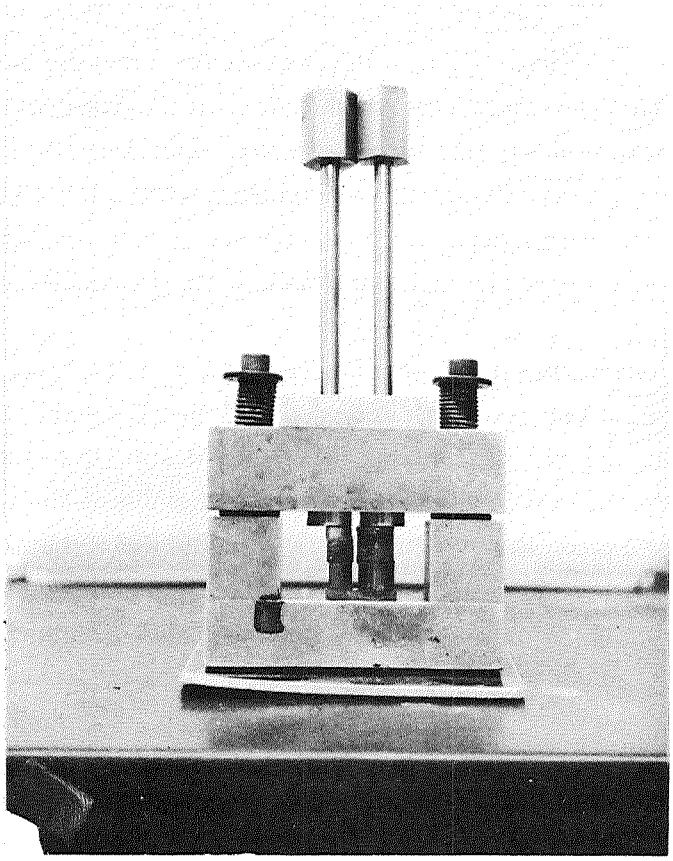

Fig. 10. Modified couple shoe sweating fixture

being done on a roomy hot plate rather than a confined muffle furnace, dead weights ot tungsten can be used in place of inconel springs for more uniform soldering.

The results of sweating shoes in the reworked fixture were checked in the CEJ Microkator Comparator and all shoes were coplanar to the hot strap within 0.0004 in.

B. Twelve-Couple Module Consistency Check Model

The design and fabrication of the 12-couple module consistency check model (Fig. 11) is based upon the submodular concept which has been developed under this contract.

The 12-couple module is geometrically and dimensionally consistent* with the print of the 12-couple Astro Module supplied by NASA. The dimensions of the Astro Module exclusing the heat sink studs are as follows: length – 5.960 in.; width – 1.960 in.; height – 0.965 in.

Our 12-couple module uses 12 submodules grouped as follows: 8 units whose long side is common, along the 5.960-in. dimension and adding up to nominal total of 8 × 0.750 in. or 6 in. which is only 0.040 in. over dimension but does include self-insulation.

The remaining four submodules share a common short side and abut the eight previously mentioned units so that the total width is a unit of submodule length plus a unit of submodule width or 1.264 in. plus 0.750 in. or 2.014 in. which is only 0.054 in. over dimension and again includes self-insulation. Since the last four units mentioned add up to less than 5.960-in. length, filler insulation would be used to make up the difference.

The height of the 12-couple module is the base thickness of 0.250 in. plus the module height of 1.750 in.

The heat sinks studs have been made dimensionally similar to those of the Astro-Module and they are located on the same centers for geometrical harmony with the Astro-Module.

In the model, the submodule packages are represented by blocks of plexiglas except for the end units which are complete models of the submodular packages one of which is fully sectioned (Fig. 12).

Certain design changes would be required to meet the increased temperatures at the hot and cold shoes of the 12-couple module. At the cold end, the 350 °C maximum requirement would limit the thickness of hardcoat to 0.001 or less to prevent crazing due to thermal stresses generated by the expansion of the aluminum base metal. Some form of piston lubrication would also be desirable and a sputtered coat of molybdenum disulfide would appear to be the ideal material since it is an excellent high temperature solid lubricant and nonorganic. The coating of course would not extend beyond the skirt of the piston since molybdenum disulfide is a relatively good electrical conductor.

*Minor dimensional differences are neglected and height is not considered critical since head room exists in NASA fixturing.

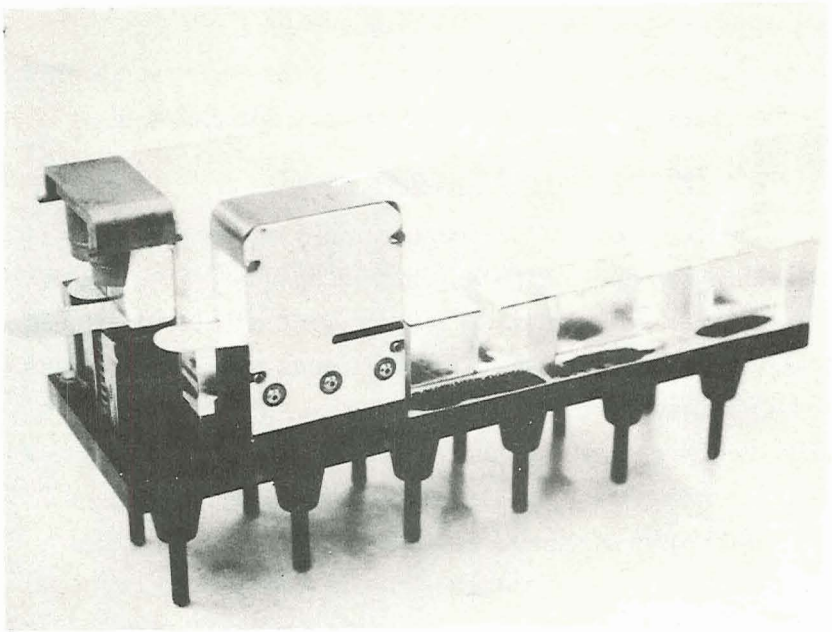

Fig. 11. View of 12-couple module consistency check model

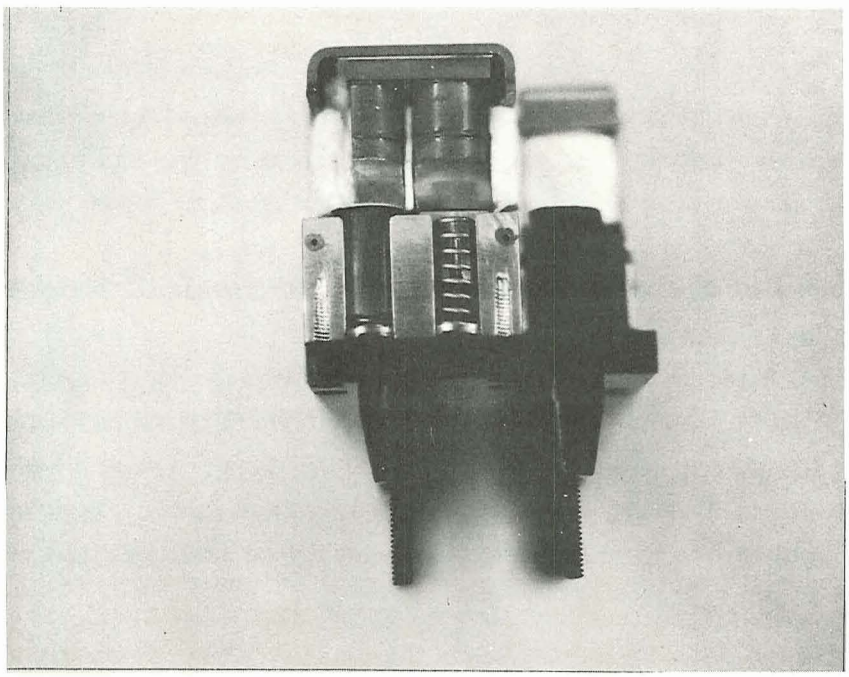

Fig. 12. View of fully sectioned submodule of 12-couple module consistency check model

Experience has indicated the ceramic side plates of the submodules are the weak link in the design and should be replaced by a slender metal strut of minimal cross section appropriately notched to receive the hot and cold shoe lugs. Naturally a metal having good hot strength at 900 °C and low thermal conductivity should be used. This suggests a metal in the chromium-nickel austenitic group such as type 310, rated at about 1150 °C continuous service temperature in air.

C. Testing of Modules

1. Phase I

The test equipment was extensively modified and a preliminary run was made on a partially assembled package (Fig. 13). The purpose of this run was to generally check equipment functioning and determine whether an unloaded module assembly of cold shoe side plates and hot shoe could successfully weather an 880 °C/50 °C gradient.

The heater was set about 0.25 in. from the hot shoe and a chromel/alumel couple was cemented to the hot shoe using Sauereisen cement. The hot shoe was brought to 850 °C over a 2-hr period in a vacuum of about 200 μ. No damage was in evidence upon disassembly, although some oxidation of the molybdenum strap had taken place. The tiny chromel/constantan couples in the copper heat flux rod did not read properly, and it was later discovered that one feedthrough lead was defective being partially shorted to the ground.

The next test consisted of making up a new package with pistons installed with 1.5-lb load springs and dummy steel rods in place of the couple. No insulation was employed in order to eliminate it from consideration as a variable in causing side plate breakage.

This setup was run at 800 °C/50 °C with all Min-K insulation rings in place (no sight holes) and the heater 1/16 in. from the hot shoe. When the insulation rings were removed, one side plate was found to have failed at the deep notch (Fig. 14).

In reviewing possible causes for this failure, a small but important dimensional error was discovered in the module design. If a maximum tolerance length couple (0.883) is used, the pistons are virtually flush with the top of the cold shoe at assembly, and couple expansion (dummy rod expansion is larger) could conceivably cause the ends of the couple to bear against the hot and cold shoes directly (no springing) which would of course generate large forces and break the ceramics.

In line with our discovery of this dimensional error in the module, which could cause side plate breakage, height expansion room was created for the couple by reducing the molybdenum hot shoe tab from 0.065 to 0.040 in. The strength of the tab was still adequate and 0.015 in. extra free height was gained this way.

The same module was reassembled using the cold shoe, pistons, and springs (1.5-lb load, 10-psi and 16-psi leg loading, respectively) used on the previous run and new side plates and the modified hot shoe as explained above. The couple was wrapped in a Micro-Quartz blanket but this time the blanket was not precompressed but rather sized and trimmed to the proper finish dimensions that would allow free insertion between the side plates.

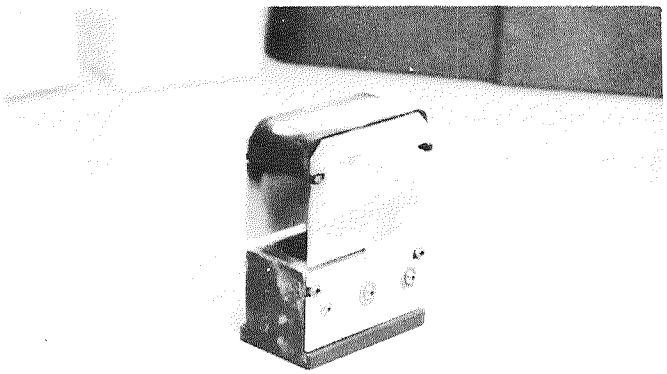

Fig. 13. Partially assembled module runs at 800 °C/50 °C gradient for 3 hr

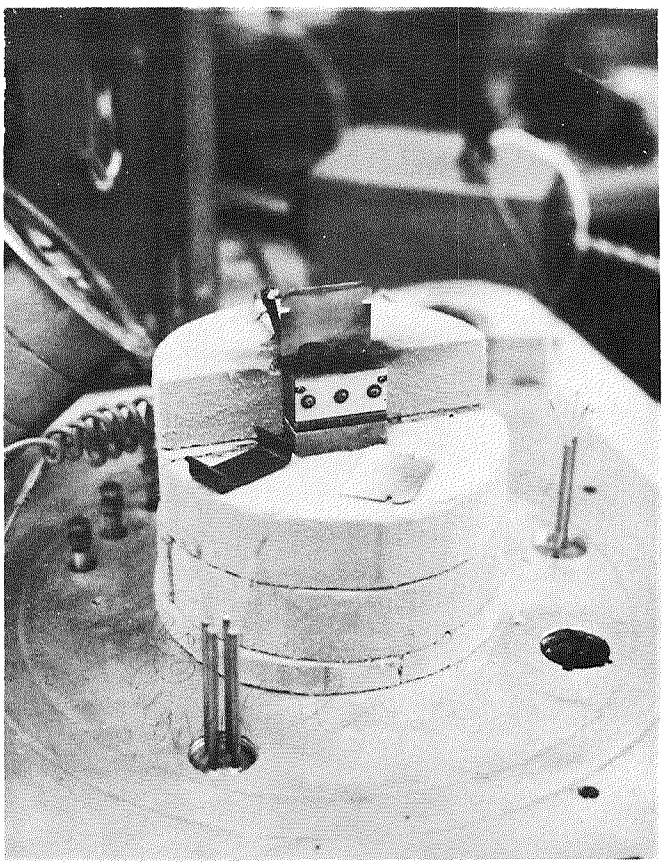

Fig. 14. Module with "dummy" couple (removed) showing side plate failure after run

Since instrumenting the module involves considerable extra time, we chose to make this run a basic test of mechanical and electrical feasibility rather than one in which actual efficiencies and thermal drops could be measured. Therefore, the only leads external to the package were output leads of 10-mil-diameter fine silver wire about 7 in. long, soldered to the module strap.

This lead material was chosen to limit thermal losses from the module without placing unduly high resistivities in series with the module. Actually, the resistivity of the silver wire is 0.1 ohm/ft and the two 7-in. leads used had a combined resistivity of 0.116 ohms or 116 mohm which was far too high. However, this was not realized at the time.

The resistivity of the total open circuit was as follows.

1)	Module	– 40 mohm (couple 39 to 40 mohm)
2)	Silver leads	– 116 mohm
3)	Feedthroughs	– 8 mohm
4)	Cables	– 3 mohm
	Total circuit	– 167 mohm
	Circuit less module	– 127 mohm

Based on previous segmented couple testing programs, the correct average total load resistance is about 15 mohm. Therefore, a loading of 125/15 or 8-1/2 times would be expected to severely reduce the output which is in fact what happened.

The module was insulated as before with only the top of the hot shoe exposed and run in 95 Ar/5 H after evacuation in the 60-μ range. Heatup time was rather rapid, 150 to 300 °C/hr, with the couple output building steadily and smoothly.

At ≈ 800 °C/≈ 50 °C, the output was 165 mW at 1.1 amperes and 15 mV (load switch position no. 9) while the open circuit voltage was 225 mV.

Cool down was conducted at a slow rate of about 100 °C/hr per recommendations of other testers on the couple program. Fig. 15 shows the unit in place on the test with some insulation rings removed. Careful inspection prior to and after assembly revealed no damage to any component and only slight oxidation of the molybdenum hot shoe. The contact surfaces were in very good condition (Fig. 16a and b).

2. Phase II

The next phase of testing was to try a module which was instrumented using thermocouples.

A module was thermocouple instrumented and numbered as follows (reading up from the heat flux leg to the furnace):

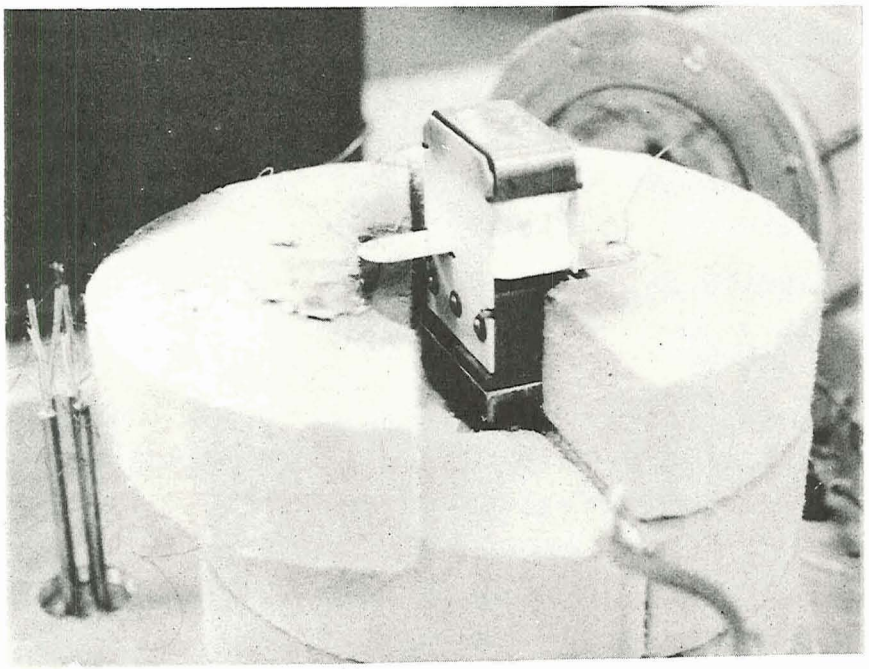

Fig. 15. Complete module after being cycled at 800 °C/50 °C gradient

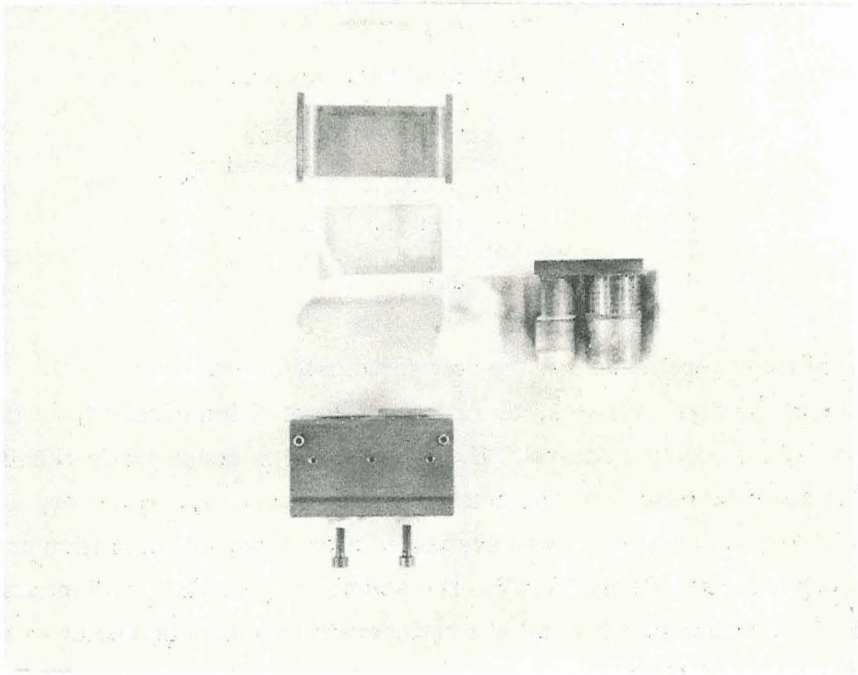

Fig. 16(a). Module disassembled after run at 800 °C/50 °C

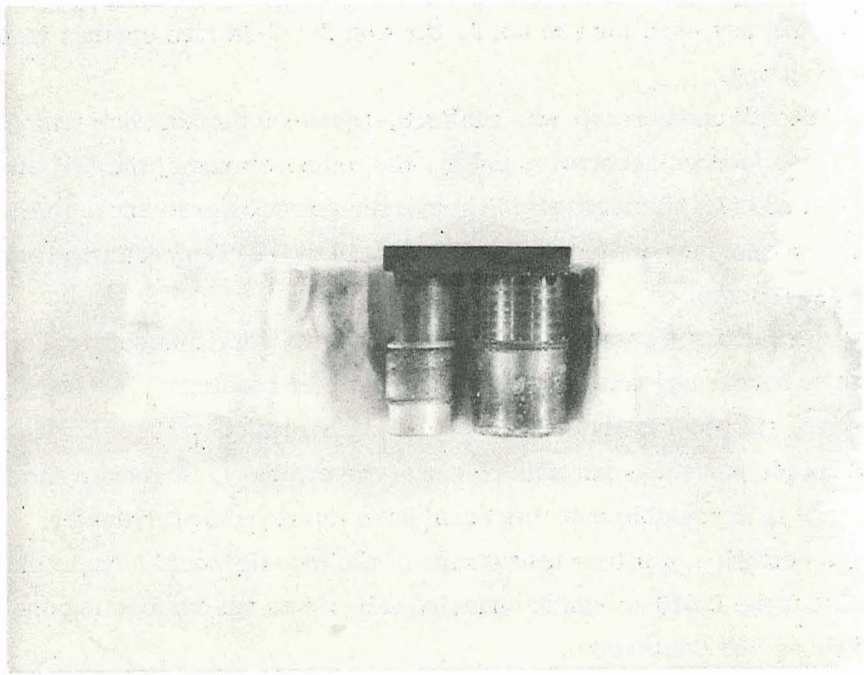

Fig. 16(b). Couple and insulation blanket after run in module at 800 °C/50 °C

Couple No.	Location
1	Bottom of heat flux leg
2	Top of heat flux leg
3	Copper mounting base
4	Base of cold shoe (outside)
5	Silver output lead "N"
6	Silver output lead "P"
7	Top of hot shoe
8	Furnace

Actually two separate runs were made and the data for these follow.

As inspection of the data indicates, there is high thermal impedance from the couple cold shoe to the base of the copper pedestal. The silver strap is consistently running at 267 to 395 °C (measured at about 0.50 in. from the center of couple contact). However, a temperature of around 50 °C is ideal. Test run no. 1 was suspended after 2 days of operation at temperature because of a poor couple output of only 15 mV. The actual temperature gradient across the couple was only 132 °C because of a low hot shoe temperature caused by heater problems and a high cold shoe temperature of 395 °C.

When the module was disassembled, everything seemed normal and it was felt that a combination of tolerances or low spring pressure resulted in a particularly poor interface condition for good heat transfer and low resistivity.

The same module was used for run no. 2, but with 2-1/2-lb load springs installed in place of the 1-1/4-lb spring.

An output of 268 mV open circuit was realized, but since the hot shoe temperature stabilized at about 878 °C (no feedback control is used), the temperatures of the "N" and "P" package leads were 267 °C and 330 °C, respectively. The net temperature gradient in this case averaged 578 °C. The module was run under these conditions for 14 days. Temperatures stabilized at those shown on the data sheets.

Some of the thermocouple data were suspect, since the very fine chromel/constantan couples are difficult to handle and sometimes produce strange readings.

When examined, the module showed some heat deterioration of the microquartz insulation, especially near the couple surfaces, but nothing out of the ordinary. A rocker shoe "burn-in" was not attempted, and it is possible that this could have improved heat transfer.

It was felt the condition of silver lead straps of the module would have to be investigated, because it appeared that the 0.010-in.-thick annealed silver was not conforming under pressure between the couple shoes and the pistons.

3. Phase III

Four modules were run during this phase with the runs numbered 3, 4, 5, and 6 as a continuation of the previously started sequence.

Run No. 1

Date
4/8/70

Description:

Standard module package using 1 1/4-lb load springs; couple instrumented nos. 1 through 8

Purpose of Test:

To check for thermal drops and couple output

Start Heat-Up
Date 4/6/70 Time 10 A.M.

Shut Down Furnace
Date 4/8/70 Time 11 A.M.

Couple No.	Couple Location	Mounting	Insulation	Couple Output, Steady State, °C
1	Bottom heat flux leg	Hole/RTV	RTV	73
2	Top heat flux leg	Hole/RTV	RTV	69.5
3	Copper mounting base	Surface/sauereisen	Sauereisen/NP†	455
4	Base of cold shoe	Surface/sauereisen	Hard coat	51.0
5	"N" output lead	Surface/solder	None	395
6	"Γ" output lead	Surface/solder	None	395
7	Top of hot shoe	Surface/sauereisen	Sauereisen/NP†	527
8	Furnace‡	Surface/sauereisen	Sauereisen/NP†	649

Spare

---

* After rocker shoe "burn-in."

† Not planned for insulation.

‡ Furnace data (steady state); heater voltage = ——
heater current = ——

Run No. 1

Room Temperature Resistivity, m-ohms

Cable "N"	Cable "P"	Feedthrough "N"	Feedthrough "P"	Lead "N"	Lead "P"	Segmented Couple	Module
1.1	1.1	0.4	0.4	5.4	5.4	70	70

Segmented Couple Output (Steady State)

Load Tap:	Open	No. 1	No. 2	No. 3	No. 4	No. 5	No. 6	No. 7	No. 8	No. 9
Amperes										
Millivolts	15									
Milliwatts (calculated)										

Run No. 2

Date
4/23/70

Description:

Standard module package using 2 1/2-lb load springs for better interface contact; couple instrumented nos. 1 through 8 (same module as run no. 1)

Purpose of Test:

To lower thermal drop at strap interface by using heavier load springs

Start Heat-Up
Date Time
4/9/70 ——

Shut Down Furnace
Date Time
4/23/70 ——

Couple No.	Couple Location	Mounting	Insulation	Couple Output, Steady State *, °C
1	Bottom heat flux leg	Hole/RTV	RTV	40
2	Top heat flux leg	Hole/RTV	RTV	Open
3	Copper mounting base	Surface/sauereisen	Sauereisen/NP†	53.5
4	Base of cold shoe	Surface/sauereisen	Hard coat	41.5
5	"N" output lead	Surface/solder	None	267
6	"P" output lead	Surface/solder	None	330
7	Top of hot shoe	Surface/sauereisen	Sauereisen/NP†	878
8	Furnace‡	Surface/sauereisen	Sauereisen/NP†	896
Spare				

* After rocker shoe "burn-in."

† Not planned for insulation.

‡ Furnace data (steady state); heater voltage = ——
heater current = ——

Run No. 2

Room Temperature Resistivity, m-ohms

Cable "N"	Cable "P"	Feedthrough "N"	Feedthrough "P"	Lead "N"	Lead "P"	Segmented Couple	Module
1.1	1.1	0.4	0.4	5.4	5.5	70.0	70.0

Segmented Couple Output (Steady State)

Load Tap:	Open	No. 1	No. 2	No. 3	No. 4	No. 5	No. 6	No. 7	No. 8	No. 9
Amperes										
Millivolts	268									
Milliwatts (calculated)										

Run No. 3

Date 5/5/70

Description:

Standard module package using 2 1/2-lb load springs for better interface contact; couple instrumented nos. 1-8 (same module as run no. 2 with new straps installed)

Purpose of Test:

To lower thermal drop at strap interface by using annealed strap.

Start Heat-Up
Date Time
5/1/70 —
Shut Down Furnace
Date Time
5/4/70 —

Couple No.	Couple Location	Mounting	Insulation	Steady State Temperature, °C
1	Bottom heat flux leg	Hole/RTV	RTV	35
2	Top heat flux leg	Hole/RTV	RTV	45.3
3	Copper mounting base	Surface/sauereisen	Sauereisen/NP†	63.2
4	Base of cold shoe	Surface/sauereisen	Hard coat	67.7
5	"N" output lead	Surface/solder	None	146
6	"P" output lead	Surface/solder	None	125
7	Top of hot shoe	Surface/sauereisen	Sauereisen/NP†	795
8	Furnace‡	Surface/sauereisen	Sauereisen/NP†	789

Spare

† Not planned for insulation.

‡ Furnace data (steady state); heater voltage = 48
heater current = 2

Run no. 3

Room Temperature Resistivity, m-ohms

Cable "N"	Cable "P"	Feedthrough "N"	Feedthrough "P"	Lead "N"	Lead "P"	Segmented Couple	Module
1.1	1.1	0.4	0.4	5.4	5.4	70	91

Segmented Couple Output (Steady State)

Load Tap:	Open	No. 1	No. 2	No. 3	No. 4	No. 5	No. 6	No. 7	No. 8	No. 9
Amperes										
Millivolts	269									
Milliwatts (calculated)										

Run No. 4

Date 5/5/70

Description:

Indium disks on both sides of silver strap

Purpose of Test:

To lower thermal drop of strap interface by using malleable filler material.

Start Heat-Up
Date Time
5/5/70 —
Shut Down Furnace
Date Time
5/5/70 —

Couple No.	Couple Location	Mounting	Insulation	Steady State Temperature, °C
1	Bottom heat flux leg	Hole/RTV	RTV	34
2	Top heat flux leg	Hole/RTV	RTV	43.5
3	Copper mounting base	Surface/sauereisen	Sauereisen/NP†	55
4	Base of cold shoe	Surface/sauereisen	Hard coat	63
5	"N" output lead	Surface/solder	None	118.7
6	"P" output lead	Surface/solder	None	104
7	Top of hot shoe	Surface/sauereisen	Sauereisen/NP†	124
8	Furnace‡	Surface/sauereisen	Sauereisen/NP†	582

Spare

† Not planned for insulation.

‡ Furnace data (steady state); heater voltage = 36
heater current = 1.6

Note: Run stopped because hot shoe couple opened at 582 °C. Restored after hot shoe couple was repaired. Package side plate broke shortly thereafter.

Run No. 5

Date 5/8/70

Description:

Same as no. 4 but with indium plating 0.001 to 0.002 in. thick

Purpose of Test:

Same as no. 4

Start Heat-Up
Date Time
5/8/70 —

Shut Down Furnace
Date Time
5/8/70 —

Couple No.	Couple Location	Mounting	Insulation	Steady State Temperature, °C
1	Bottom heat flux leg	Hole/RTV	RTV	—
2	Top heat flux leg	Hole/RTV	RTV	—
3	Copper mounting base	Surface/sauereisen	Sauereisen/NP†	—
4	Base of cold shoe	Surface/sauereisen	Hard coat	—
5	"N" output lead	Surface/solder	None	—
6	"P" output lead	Surface/solder	None	—
7	Top of hot shoe	Surface/sauereisen	Sauereisen/NP†	—
8	Furnace‡	Surface/sauereisen	Sauereisen/NP†	—

Spare

† Not planned for insulation.

‡ Furnace data (steady state); heater voltage =
heater current =

Note: Package came apart before testing and before furnace was put on top of package. Second sheet not included due to suspension of testing.

Run No. 6

Date 5/22/70

Description:

Same as run no. 5

Purpose of Test:

Same as run no. 5

Start Heat-Up
Date Time
5/22/70 —

Shut Down Furnace
Date Time
5/26/70 —

Couple No.	Couple Location	Mounting	Insulation	Couple Output, Steady State *
1	Bottom heat flux leg	Hole/RTV	RTV	45.2°
2	Top heat flux leg	Hole/RTV	RTV	52.7°
3	Copper mounting base	Surface/sauereisen	Sauereisen/NP†	61.5°
4	Base of cold shoe	Surface/sauereisen	Hard coat	72°
5	"N" output lead	Surface/solder	None	138°
6	"P" output lead	Surface/solder	None	128.5°
7	Top of hot shoe	Surface/sauereisen	Sauereisen/NP†	open
8	Furnace‡	Surface/sauereisen	Sauereisen/NP†	657°

Spare

† Not planned for insulation.

‡ Furnace data (steady state); heater voltage = 51
heater current = 2

Note: Run suspended due to heater deterioration. Second sheet not included due to suspension of testing.

The silver interconnection straps were inspected for any condition that might inhibit good contact prior to run no. 3. The material used for fabricating these straps was ordered as fully annealed and yet the strap seemed overly rigid for 10-mil-thick material. We suspected that the reason for this was peripheral work hardening due to the shear-break phenomenon that naturally occurs during a stamping operation. All of the stamped straps were given a post-anneal treatment and were noticeably easier to flex afterwards.

Run no. 3 was conducted to determine the changes in thermal drop (strap temperature) due to the switch to a postannealed, stamped, interconnection strap, using the module of run no. 2.

An inspection of the data shows an average strap temperature (couples 5 and 6) of 135 °C contrasted with a 298 °C average for run no. 2.

Run no. 3 lasted for 4 days with no change in data of any significance. It is interesting to note that the couple output (open circuit) remains the same for run nos. 2 and 3 despite what appears to be better heat transfer. The difference in hot shoe temperatures for runs 2 and 3 is probably the cause. Run no. 3 hot shoe temperature was 100° less than run no. 2 due to heater deterioration which limited the maximum temperature obtainable. This situation made the effect of the strap change unclear at the time.

Some of the annealed straps were sent out for indium plating and in the interim some indium foil was prepared and disks (5 mil thick) punched from this foil were applied to annealed straps to check heat transfer with the use of a malleable void filler material (run no. 4).

This run was prematurely halted when the hot shoe thermocouple failed at 582 °C. The run was restarted after repairs were effected but was terminated after the module side plate failed (probably due to excessive handling during couple repair, after heat cycling had already taken place).

A new set of side plates was installed for run no. 5 which was to be a repeat of run no. 4 but a side plate failed before the run could be started.

Run no. 6 was a rerun of no. 5 with care taken in installing new side plates, making sure no dirt was lodged under the plates when the screws were tightened and backing off the piston jack screws very slowly. Run no. 6 data show no significant change in trend for the strap temperature (133 °C) average despite the indium separator. The heater seriously deteriorated during this run and a maximum furnace temperature of only 357 °C was obtained.

During this phase, most of our efforts were frustrated by equipment failings and some unaccounted for module breakage.

4. Phase IV

After making repairs to the heater, etc., testing was resumed with a view toward obtaining a complete set of reliable data concerning thermal impedances on the cold end of the module and finally to determining the efficiency of the unit.

Before the final run, some peripheral investigations were made into trying to improve the thermal impedance at the strap interface by using silicone grease on the pistons (vacuum rather than heat sink type which tends to jam pistons). While data were collected that seem to confirm some improvement (5 to 8 °C) by lowering the thermal impedance between piston and shoe, it is not presented here because its value is questionable since a proper control module or basis of comparison was not operated as part of the test.

The finale to testing came with run no. 7 in which a module was operated for 288 hr at a hot shoe temperature of about 367 °C (742 °F) and an estimated cold shoe temperature of about 158 °F (70 °C).

Actually, due to a shortage of feethrough terminals for couples (some were shorted, some broken) and a change in couple layout, there was no couple available to mount directly to the cold shoe. However, the thermal drop from module cold shoe to copper mounting base has been fairly well established to be about 4 to 8 °C depending on heat flux. For a copper base temperature of 64 °C, 70 °C is then a good average for the cold shoe temperature obtained for the run.

It was found that because of shunt heat loss, etc., the heat sink was unable to dissipate quite enough heat to lower the cold shoe to about 50 °C and it was replaced by a liquid cooler in which the copper heat flux leg is immersed in a mixture of dry ice and n-propyl alcohol. Occasionally some dry ice had to be added but not often enough to be bothersome.

In run no. 7 using this cooling system, equilibrium was achieved at a cold shoe temperature of 64 °C. Thus the gradient or differential across the modulus was 1367-64 °C or 1303 °C.

The temperature gradient in the heat flux calibration leg was 47-32 °C or 15 °C between two couples 1 in. apart on the 0.3753-in.-diameter OHFC-101 copper rod.

For this run, the module cold shoe was modified by notching into the upper side walls exposing an area on the N piston which was very close to the silver interconnection strap.

In this way, thermocouples (redundantly paired) could easily be bonded close to the strap/piston interface. A pair of thermocouples was also bonded to the N shoe of the segmented couple. At equilibrium, the gradient across the strap interface averaged about 62 °C which of course is far higher than the original pretest estimate of about 2 °C which was predicated upon much higher piston spring loadings.

A rocker "burn in" was tried by removing the immersion bath and heating the copper rod with a hot air gun until the couple shoe temperature reached about 190 °C. Once equilibrium was obtained along with the original gradient a recheck of couple reading showed no improvement in thermal impedance at the strap interface.

Since the particular module available for this run had an unusually high installed contact resistance (22-70 or 48 milliohms), there is a good chance that an unusual problem existed prior to testing and it could not be overcome during test or "burn in."

Run No. 7	Description:	Purpose of Test:	Duration of Test:
Date 7/20/70	Standard module package using 1 1/4 lb load springs	To check thermal drop at silver strap, piston, and cold shoe interface	288 hr

Couple No.	Couple Location	Mounting	Insulation	Couple Output, Steady State, °F*
1	Bottom heat flux leg	Hole/RTV	RTV	32 - 89.5
2	Top heat flux leg	Hole/RTV	RTV	47 - 116.5
9	Copper mounting base	Surface/sauereisen	Sauereisen/NP	64 - 147.0
3	"N" Piston	Surface/sauereisen	Hard coat	95 - 203.0
4	"N" Piston	Surface/solder	None	102 - 215.5
5	"N" cold shoe	Surface/solder	None	162 - 324.0
6	"N" cold shoe	Surface/sauereisen	Sauereisen/NP†	159 - 318.0
8	Furnace†	Surface/sauereisen	Sauereisen/NP†	847 - 1557.0
Spare 7	Hot Shoe			742 - 1367.0

---

* After rocker shoe "burn-in."

+ Not planned for insullation.

‡ Furnace data (steady state) ; heater voltage = 48
heater current =0.85

Room Temperature Resistivity, m-ohms

Cable "N"	Cable "P"	Feedthrough "N"	Feedthrough "P"	Lead "N"	Lead "P"	Segmented Couple	Module
1.1	1.1	0.4	0.4	5.4	5.4	22	70

Segmented Couple Output (Steady State)

Load Tap:	Open	No. 1	No. 2	No. 3	No. 4	No. 5	No. 6	No. 7	No. 8	No. 9
Amperes		3.44	3.2	3.1	3.05	3.0	2.9	2.85	281	2.8
Millivolts	220	5	17	20	25	29	30	35	40	41
Milliwatts (calculated)		17.2	54.4	62.0	7625	870	87.0	99.75	112.4	114.80

The problem may have been one of an out-of-flat N shoe, or a nonparallel N shoe which was out of "spec" enough to inhibit correction, dirt, or an interconnection strap of poor quality.

It is unfortunate that the test was run with this particular module but the shortage of segmented couples and the pressure of time made it a necessity.

The maximum power output achieved was 114.80 mV or 2.8 amps at 41 mV with an open circuit voltage of 220 mV.

Fig. 17 shows the module after 288 hr under test.*

D. Module Internal Resistance

The series resistance of the module (couple, pressure contacted interface and silver straps) generally averaged 8.5 milliohms higher than the couple alone. This is roughly equal to the resistivity of a good segmented couple whose room temperature resistance would be about 7 to 10 milliohms and is higher than what was expected.

Since the resistivity of the silver strap is expressed in microohms, virtually all of the module package resistivity is contact resistance which could be reduced by using spring loadings greater than 1.25 lb (previously arrived at for safe loading).

There is no strong evidence to indicate that the rocker shoe "burn-in" technique will definitely lower contact resistance by creating additional parallel avenues of material impingement. However, the contact pressures that were generally employed were not great enough to really totally flatten the silver interconnection strap which would initiate better contact once parallelism had been achieved in the "burn-in."

Measurements of couple and module resistances for a group of nine assembled but untested units are given in Table 5 and can probably be considered more realistic than units assembled and then tested (usually to destruction) since they were assembled as a group rather than individually using a 1.25-lb load spring.

Table 5. Measurements of Couple and Module Resistances for a Group of Six Units (Assembled but Untested)

Module No.	Segmented Couple Resistance, milliohms	Total Module Resistance, milliohms	Module Internal Contact Resistance
4	78	88	10
5	75	88	13
7	19	23	4
9	50	63	13
10	12	23	11
11	48	55	7

*This unit was shipped to NASA with thermocouples in place.

† Shipped to NASA.

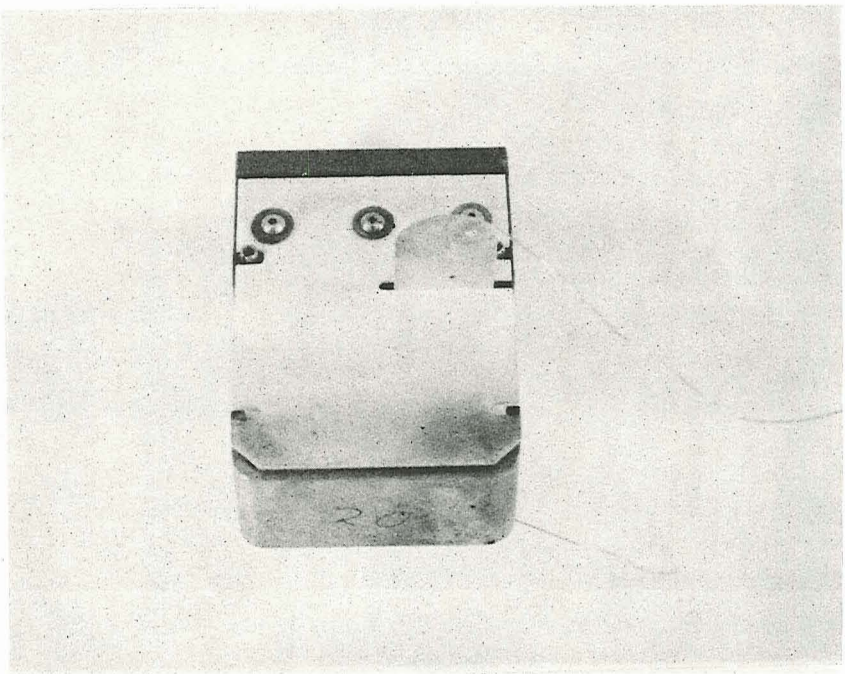

Fig. 17. Run no. 7 module after 280-hr test

E. Module Efficiency

The power output of the modules was determined as in previous segmented couple measurements by allowing equilibrium to be established and then load matching for the best EI output using a load tap selector switch. The open circuit voltage E_o was then read by moving the switch to an open tap.

The power output is the power dissipated in the load plus the power dissipated in interconnection cabling, etc., external to the module. The current of course is the same for both since series connection is used.

$$\text{Module Power Output - } P_M = E_{load}(I) + I^2 (Rc)$$

where Rc is the summation of all external resistivities or cabling (switch contacts read in micro-ohms and are being neglected).

$$\Sigma Rc = R_{n\ cable} + R_{p\ cable} + R_{n\ feedthrough} + R_{p\ feedthrough} + R_{n\ lead} + R_{p\ lead} + R_{switch\ contacts}$$

$$\Sigma Rc = 1.1 + 1.1 + 0.4 + 0.4 + 5.4 + 5.4 + 0 = 13.8 \text{ mohms}$$

Using the data of run no. 7 taken on load tap no. 9, we find:

$I = 2.8$ amps — $R = 22$ mohms

$E_{load} = 41$ mV — R module = 70 mohms

Vo = 220 mV — R pressure contacts = 70-22 = 48 mohms

Then:

$$Pm = 41\ (2.8) + 2.8^2\ (13.8)$$
$$= 115 + 1.08.1$$
$$Pm = 223.1 \text{ mW or } 0.2231 \text{ W}$$

The internal resistance of the module may be determined from:

$$Ri = \frac{Vo.c. - V\ load}{I} - Rc$$

$$Ri = \frac{220-41}{2.8} - 13.8$$

$$Ri = 64 - 13.8 = 49.20 \text{ mohms}$$

It is interesting to note that this value of internal resistance correlates closely with room temperature values of segmented couple resistance and module resistance.

If the couple resistance drastically dropped at working temperatures as the supplier claimed it would and measured only a few milliohms, this would equate with the room temperature resistance of the pressure contacts above, which is 48 milliohms. More simply stated,

the couple resistance could have dropped to 1.20 milliohms while the pressure contact resistance remained at 48 milliohms for a total of 49.20 milliohms.

If we pursue this line of thinking for the moment and recompute Pm with 48 milliohms lumped into the Rc factor, we have:

$$Pm_{corrected} = 41\ (2.8) + 2.8^2\ (13.8 + 48)$$
$$= 115 + 485$$
$$Pm_{corrected} = 600\ mV$$

which perhaps is the actual power output of the couple although it cannot be positively verified.

In calculating the efficiency of the module, the portion of total power generated by the module on Pm is taken as a fraction of the total power input which can be expressed by the summation of heat flux or Q + Pm

$$\text{Efficiency, } E = \frac{Pm}{Q + Pm}$$

The heat flux Q is measured in the lagged (insulated) copper rod (0.3743 diameter) by measuring the temperature at two points 1.000-in. apart. Thus:

$$Q = \frac{Ak_m\ (t_1 - t_2)}{X}$$

where

$$A\ rod = \frac{\pi\ (0.3743^2)}{4} \times \frac{ft^2}{144\ in.^2} = 0.000764\ ft^2$$

$$k_m = 228\ Btu/ft^2/ft/hr/°F \text{ at } 68\ °F \text{ for OFHC Copper 101 material}$$

$$t_1 - t_2 = 116.5\ °F - 89.5\ °F = 27\ °F$$

$$X = 1.000\ in. \times \frac{ft}{12\ in.} = 0.0834\ ft$$

$$Q = \frac{0.000764\ (228)\ (27)}{0.0834}$$

$$\text{Heat flux, } Q = 56.5\ \frac{Btu}{hr} \text{ or } \frac{56.5}{3.412} = 16.57\ W$$

Thus:

$$E = \frac{Pm}{Q + Pm}$$

$$= \frac{0.2231}{16.57 + 0.2231}$$

$$= 0.0133$$

Therefore, overall module efficiency, E = 0.0133 or 1.33% for run no. 7.

If the module used in run no. 7 did not have the unfortunately high contact resistance of 48 milliohms but rather a typical 8 milliohms resistance the efficiency would have been much higher of course.

These computations do not take shunt heat flow through insulation, ceramic side plates and through voids into account. If they did, Q would be lower and the calculated efficiency higher but since shunt heat was not measured we can only conjecture about this.

The desired temperature gradient of 800 °C/50° was not obtained exactly but rather 742 °C/72 °C which would effectively decrease power output and efficiency in the calculations.

F. Summarization and Conclusions

The measured performance of segmented Si-Ge-PbTe thermoelectric couples has been previously reported at 8.7% for a 800 °C/50 °C temperature gradient, and it was expected that module efficiency or performance might approach this figure.

However, an efficiency of 1.3% was realized, drawing upon only limited data and being unfavorably influenced by unknowns such as shunt heat flow and the necessity of working with an above average resistivity module at a lower than desired temperature gradient.

The modules had several failings. One of these was purely structural and related to the steatite ceramic side plates being weaker than calculations indicated they would be. These calculations took note of the fact that only limited high temperature data were available, but a large enough safety factor was not used as it turned out.

The weakness of the ceramics which occassionally made for handling difficulties was not really the limiting factor because failures of the couple legs became persistent at loadings as low as 2.5 lb. The most common type of failure was at the bonded SiGe/PbTe interface although several PbTe elements failed in the body of the material and even a few SiGe elements failed at the hot joint and in the body of the material.

This breakage necessitated working at a safe low spring load on the pistons of 1.25 lb/piston and as so often happens in design work, one small change cascades, because at 1.25 lb/load an interconnection strap of fine silver which has a low modulus cannot be brought into a flat or total area contact condition.

The first modules that were assembled had measured restivities that were only 1 or 2 milliohms higher than the couples because a 2 1/2 lb-load spring was used. The final assembly of a group of modules showed resistivities 6-13 milliohms higher and the final test module of run no. 7 read 48 milliohms higher for some unexplained reason.

Attempts to improve contact resistivities and heat flow within the module by the use of "rocker" shoes met with little success. The low contact pressure and the possibility of high breakout friction may have both combined significantly here.

It is possible that during the "burn-in" operation the application of vibration through the copper rod might have helped the shoes settle into position but this was not thought of at the time.

The ceramic side plates were used to keep packed insulation in place in the design of module as originally conceived. It later turned out that a blanket of Micro-Quartz could be used rather than loose packing and the side plate configuration became redundant. Four slender metals struts notched to receive the hot shoe tab and drilled to pick up a screw in the base would have sufficed nicely if made of a stainless steel having poor thermal conductivity, since the blanket wrapped insulation tended to maintain its integrity with little or no side enclosure required.

Somewhat greater attention should have been given to simple ways of attaching thermocouples to various points of interest on the module. Toward the end of the testing phase, a method was evolved that made such attachment (at least on the cold side of the module where most of the couples are) a relatively simple task.

The beads of the thermocouples were quickly fitted in place with a cyanoacrylate adhesive such as Eastman 910, an operation which only took seconds. Encapsulation was then accomplished with an epoxy.

The use of very small gage thermocouples which were primarily (0.005-in. diameter to limit heat flow out of the package and provide extreme flexibility also hampered much of the test setup work. These couples and their matched emf feedthroughs were a constant source of trouble and led to many erroneous temperature readings, often after a run was well under way. Although great care was taken to avoid ground loop between couples, heater, feedthroughs, module, etc., obviously some weak points existed in the system that could not be entirely debugged.

The modules despite the shortcomings elaborated upon were dependable and easy to assemble and came up to almost all mechanical expectations under the applied thermal gradient.

G. Acknowledgements

Gratitude is expressed to Louis Bellomo for mechanical design of the modules and to Charles Lamport for technical assistance in the area of assembling and testing.

V. THE COBALT-SILICON-GERMANIUM SYSTEM*

A. Introduction

Work on this system was originally started to find whether the failures of high temperature bonds which were found in Ge-Si - $MoSi_2$ Si eutectic couples from a German supplier (known in the U.S. generally as Air Vac couples) at 830°C were due to the Co content found in the braze in the German but not in the American couples. It was felt that there might be certain compositional areas in the Co-Si-Ge system which would exhibit melting below 800°C, a fact which could indeed by confirmed. As the investigations proceeded, it was nevertheless felt that other well chosen compositions in that system might exhibit no melting below 1100°C and thus might form a braze for the bonding of hot shoes to GeSi elements for high temperature service. We still feel that it would be more desirable to use stoichiometric $MoSi_2$ for a hot shoe material. This material, commercially available under the tradename "Super-Kanthal" seems still a better choice for a hot shoe than the present Air Vac $MoSi_2$ - Si eutectic composition. Super-Kanthal is more stable and has a better thermal and electrical conductivity in comparison with that eutectic. It also requires no doping of any kind to ensure its conductivity. What it requires is a braze to bond it to Ge-Si. This braze must have a precisely defined melting point in between the potential operating temperature of the element at 1000 - 1100°C and the solidus temperatures of the Ge-Si compositions of interest, which lie around 1200°C. Such a precisely fitting melting range is hard to find if simultaneously the stringent requirements of compatibility both with Ge-Si and $MoSi_2$ at temperatures over 1000°C are considered. Time intervals for deep space missions which exceed 5 years are also to be considered here and any aging of the junction region should thus go in a predictable direction and in particular not produce phases with such undesirable properties as low melting points, high electrical or thermal impedances, and drastic changes in volumes which cause stresses in the junction leading to cracking. Also, a braze should not react with dopants in the Ge-Si thermoelements or provide a ready diffusion path for such dopants to react with, or dissolve in the shoe material. We feel that all these conditions are reasonably satisfied by a Co-Si-Ge braze composition of approximately 75 at.% Co, 10 at.% Si, and 15 at.% Ge. Such a composition melts at 1113°C, and its melting interval is so small as not to be visible in regular thermal analysis. The Co-Si-Ge phase diagram to be presented later shows also that further reactions on the Ge-Si interface will not lead to any phase melting below 1025°C. Reactivity

---

* F.Wald and S.J. Michalik.

with boron and phosphorous is slight and might be further reduced by small boron and phosphorus additions to the braze. A drawback to the use of the braze with $MoSi_2$ hot shoe materials would however be the necessity of using fluoride based fluxes during the brazing process, since SiO_2 formation on both the Super-Kanthal and the braze prevents wetting totally. This happens even in a moderately clean vacuum, since the SiO_2 films formed are very thin. All in all, we feel that using Super-Kanthal hot shoes brazed with Co 75%, Si 10%, Ge 15% onto GeSi might be beneficial to long term stability of thermoelectric elements at temperatures up to 1025 °C. Whether this assumption is true can only be decided by building such elements and testing them for long times to compare their hot junction stability with that of presently available Air Vac couples for which long term test data are already available.

B. Literature on Co-Si and Co-Ge Systems and Other Pertinent Data

Both of these systems are fairly well covered in "Constitution of Binary Alloys" by Hansen[1] and the two recent supplements to it by Elliot[2] and Shunk.[3] A very good survey of data on the silicides can also be found in a recent book by Goldschmidt, entitled "Interstitial Alloys."[4] Information of a similar nature on germanides has recently been summarized by Samsonov and Bondarev.[5] Goldschmidt[4] also mentions a number of ternary systems but ternary systems containing Ge, Si and a metal have so far not been extensively investigated. However, the systems W-Si-Ge,[6] Th-Si-Ge,[7] and V-Si-Ge[8] have been investigated by Nowotnry and his coworkers. Also, Brixner has investigated some systems of solid solutions between silicides and germanides,[9, 10] but has not given any general phase information.

The binary systems Co-Si, Co-Ge and Si-Ge have in our case been taken directly from Hansen[1] and its supplements. In the course of our investigations, no major discrepancies with these data seemed to manifest themselves, except in the Co_2Ge region. We found the composition Co_2Ge not to lie in the single phase field at all either after casting or after annealing as evidenced by Fig. 18, which clearly demonstrates the two phase nature of that composition after annealing. The composition $Co_{64}Ge_{36}$ was, however, found to be single phase, in the as-melted state as well as after annealing. X-ray investigations showed that $Co_{64}Ge_{36}$ was isomorphous with the hexagonal close packed β-phase in the Fe-Ge system and could be indexed with: $c = 5.018$ Å, $a = 3.940$ Å, $c/a = 1.274$. X-ray diffraction data for the Co_2Ge composition both in the as-cast state and after annealing were very similar and both totally different from the $Co_{64}Ge_{36}$ composition. The Debye Scherrer spectra were exceedingly complex and have not been indexed. To us it appears at present that the "Co_2Ge" phase does undergo a phase transformation in the temperature range considered here only at its cobalt rich compositions, but the phase field does not seem to include the actual Co_2Ge composition at least not below 1000 °C. Thus, it behaves rather more similar to the β-phase in the Fe-Ge system than the literature presently suggests. As will be seen further below, solid solutions with Si are based only on the hcp structure. Thus, the still existing puzzle involving the high Co-end of the β-phase range was not further pursued.

C. Experimental Methods

The raw materials used in the experiments came from the following sources: Co from A.D. Mackay Co. (rod, 0.4-in. diameter) 99.5% Co.

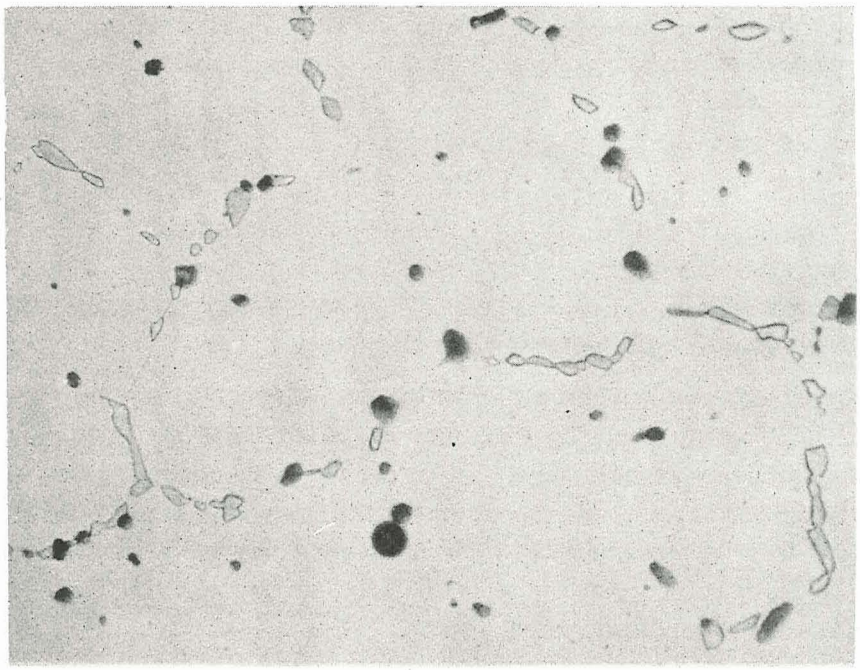

Fig. 18. Co_2Ge, 950 °C in vacuum, 24 hr, quenched; 225X (under regular light, a grain boundary precipitate is seen in the heat-treated compound of a stoichiometric compound)

Ge and Si both were of semiconductor grade purity. Ge was from Sylvania Electric Products, Tonawanda Penna, (zone refined ingot, minimum resistivity at 27 °C = 40 Ω cm). The Si was in the form of single crystalline wafers of 1-in. diameter, float zone grown by Texas Instruments, Inc., Dallas, Texas.

The cobalt rod was cut with a metallurgical cutoff wheel and was thoroughly cleaned afterwards. Ge and Si were broken by impact.

Charges of ~ 5 g total were weighed on an analytical balance to 0.1 mg, and argon arc melted with a tungsten tip on a water cooled copper hearth. All alloys were turned over several times and remelted for thorough homogenization. After melting, weight losses were established which were never significant enough to require correction of the weighed alloy compositions.

The alloys were all viewed under the microscope in the arc melted and thus rapidly quenched state after polishing in a regular fashion with diamond and alumina preparations on rotating wheels. Etches composed of slightly varying concentrations around 4 parts concentrated HCl, 1 part concentrated HNO_3, and 1 part concentrated HF (sometimes adding 2-4 parts glycerine)gave the best results. Polarized light was used extensively in distinguishing optically very active phases such as most of the germanides.

X-ray photographs were taken with a Philips Debye Scherrer powder camera of 114.6-mm diameter. The readings were converted into d-spacings with the aid of a computer. Intensities were established visually on a very strong to weak six-step scale. Lattice constants too were electronically computed, extrapolating all applicable reflexes to 90° Θ via the Nelson Riley function by a least squares method. The computer program also provided a tabulation of the deviation of every reflex from the least squares line and an error limit based on that tabulation. This is the error limit stated.

Annealing was performed in evacuated quartz ampoules. Times at the various temperatures ranged from 1000 to 2600 hr and were frequently established by checking for homogeneity at various intervals, either using microscopy or X-ray line broadening indications.

There were scattered DTA investigations in various parts of the system generally only to provide guidelines for annealing temperatures. These were not sufficient to establish crystallization paths in the system.

D. Results

A general description of all results obtained from annealed alloys is given in Table 6.

These results lead to the general assignment of phases as depicted in Fig. 19. The lower half of the diagram (below 50 at.% Co) constitutes an isothermal section at 760°C, the upper half (above 50 at.%) is isothermal at 960°C. This somewhat anomalous presentation was necessitated by various low melting phases existing in alloys below 50 at.% Co and the desire to minimize annealing times for the alloys above 50 at.% Co. Despite the rather long annealing times, some alloys did not come fully into equilibrium, notably those in the germanium corner of the diagram. Nevertheless, to the extent of the accuracy of the presentation made here, this is of no particular significance. Also, a number of alloys not shown in

Table 6. Experimental Results on Annealed Co-Si-Ge Alloys in the Area of the CoSi-CoGe Section and Below 50 at. % Co

Composition	Microscopy	a_0 Co(Si, Ge) Å	a_0 $CoSi_2$ (Å)	a_0 GeSi (Å)	Remarks
864 hr, 900 °C					
$(CoSi)_{.9}(CoGe)_{.1}$	Single phase	4.467 ± 0.005	–	–	Single phase X-ray
$(CoSi)_{.7}(CoGe)_{.3}$	Single phase	4.504 ± 0.006	–	–	Single phase X-ray
$(CoSi)_{.5}(CoGe)_{.5}$	Single phase	4.549 ± 0.005	–	–	Single phase X-ray
2000 hr, 760 °C					
$(CoSi)_{.9}(CoGe)_{.1}$	Single phase	4.466 ± 0.002	–	–	Single phase X-ray
$(CoSi)_{.7}(CoGe)_{.3}$	Single phase	4.504 ± 0.007	–	–	Single phase X-ray
$(CoSi)_{.5}(CoGe)_{.5}$	Single phase	4.553 ± 0.004	–	–	Single phase X-ray
$(CoSi)_{.3}(CoGe)_{.7}$*	Two phase	4.583 ± 0.003	–	–	Two phase X-ray
$(CoSi_{.1}(CoGe)_{.9}$*	Two (three?) phase	?	–	–	CoGe present? Co(Si, Ge) s.s. not present
1300 hr, 700 °C + 1500 hr, 760 °C					
$(CoSi_2)_{.75}(2Ge)_{.25}$	Three phase	4.449 ± 0.007	5.371 ± 0.005	5.59 ± 0.01	–
$(CoSi_2)_{.5}(2Ge)_{.5}$	Three phase	4.445 ± 0.007	5.374 ± 0.005	5.594 ± 0.008	–
$(CoSi_2)_{.25}(2Ge)_{.75}$	Two (three?) phase	4.432 ± 0.005	–	5.65 ± 0.02	X-ray ($CoGe_2$ present ?)
$(CoSi_2)_{.1}(2Ge)_{.9}$	Three phase	4.45 ± 0.01	–	5.656 ± 0.003	X-ray ($CoGe_2$ present ?)
1090 hr, 760 °C					
$(CoSi)_{.75}(2Ge)_{.25}$	Two phase	4.451 ± 0.004	–	5.654 ± 0.004	–
$(CoSi)_{.66}(2Ge)_{.33}$	↓	4.455 ± 0.004	–	5.652 ± 0.004	–
$(CoSi)_{.5}(2Ge)_{.5}$	↓	4.454 ± 0.004	–	5.649 ± 0.005	–
$(CoSi)_{.25}(2Ge)_{.75}$	↓	4.471 ± 0.006	–	5.654 ± 0.001	X-ray ($CoGe_2$ present ?)

*Heat treatment: 2586 hr, 750 °C

Table 6. (Cont.)

Composition	Microscopy	a_0 Co(Si, Ge) (Å)	a_0 $CoSi_2$ (Å)	a_0 GeSi (Å)	Remarks
$(CoSi)_{.2}(2Ge)_{.8}$ †	Three phase	?	–	5.652 + 0.001	X-ray, $CoGe_2$ definitely present
$(CoSi)_{.1}(2Ge)_{.9}$	Three phase	4.48 ± 0.01	–	5.654 ± 0.002	X-ray, $CoGe_2$ present?
2000 hr, 760 °C					
$Co_{.1}Ge_{.45}Si_{.45}$	Two phase	–	5.388 ± 0.018	–	X-ray, GeSi (inhomogeneous)
$Co_{.1}Ge_{.2}Si_{.7}$	Two phase	–	5.373 ± 0.003	5.449 ± 0.001	
$(CoSi_2)_{.75}$ $(CoGe_2)_{.25}$	Three phase	4.457 ± 0.007	5.371 ± 0.003	5.585 ± 0.004	
$(CoSi_2)_{.25}$ $(CoGe_2)_{.75}$	Three phase	–	–	5.656 ± 0.003	X-ray, a $CoGe_2$ is a second phase
$Co_{.40}Ge_{.55}Si_{.05}$	Three phase	4.563 ± 0.009	–	–	$CoGe_2$ is the primary phase
$Co_{.45}Ge_{.46}Si_{.09}$	Three phase	4.550 ± 0.003	–	–	Probably contains Co_2Ge_3 or a related compound

† Heat treatment: 2000 hr, 760 °C

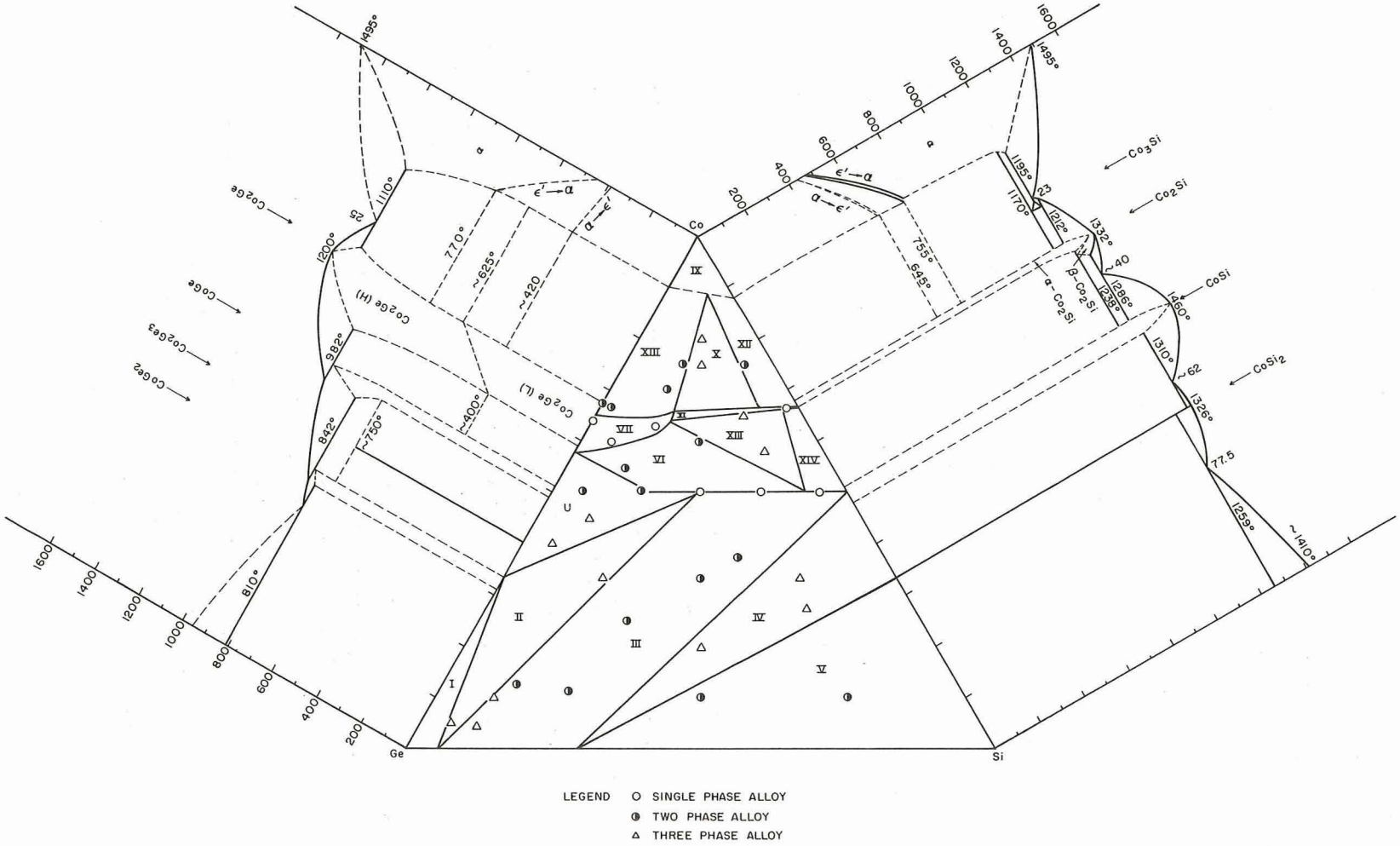

Fig. 19. Phase distribution in the ternary system Co-Si-Ge

Fig. 19 were investigated only in the as-cast condition. There was in no case any reason to indicate changes in the phase areas as they were deduced from annealed alloys. The phase areas which are identified by roman numerals will now be further discussed.

E. Discussion of Diagram

The most outstanding feature of the diagram is the large solid solution range based on CoSi which reaches to 67% CoGe in CoSi as determined from the linear extrapolation of the lattice parameter changes of the cubic CoSi phase at 760°C and 900°C shown in Fig. 20. The lattice parameter of 4.583 ± 0.003 Å was measured on an alloy containing 70 mol% CoGe which is two phase (Fig. 21). However, the extension of this section to higher CoGe concentrations seems to cross rather complex phase spaces which could not be delineated, as will be discussed below.

There is one other solid solution range of significance extending from the hexagonal close packed Co deficient "Co_2Ge" β-phase range. An alloy of the composition $Co_{63}Si_{11}Ge_{26}$ is completely single phase in the as-cast and annealed state (Fig. 22) as is an alloy of the composition $Co_{60}Si_5Ge_{35}$. Table 7 shows a and c parameters on all alloys, single and two phase which contain this solid solution and from it some more information on the size of the solid solution region may be deduced. The remainder of the system at the temperatures under discussion here is constituted of single and two phase regions, which is not too surprising since the boundary compounds have in general rather different structures. Thus, these phase ranges will be discussed in order.

Range I consists of a two phase region between Ge-Si solid solutions of up to 6% Si and $CoGe_2$. No alloys were situated in this area and the extent of the solid solution is somewhat uncertain due to the aforementioned difficulties in equilibrating the alloys. Range II is a three phase region constituted of $CoGe_2$ with rather unchanged d-spacings from pure $CoGe_2$, a Co(Si, Ge) solid solution containing 50 mol% CoGe and the aforementioned Ge-Si solid solution of 6% Si. Fig. 23 is a typical example of an annealed three phase structure found in this region. Range III is a large area in which various solid solutions of Co(Si, Ge) from 50 to virtually 0% CoGe are in equilibrium with Ge-Si solid solutions of 6 to 29 at.% Si (Fig. 24). Range IV is a three phase region constituted of pure CoSi, pure $CoSi_2$, and the Ge-Si solid solution at 29 at.% Si (Fig. 25). Range V is a two phase region where different solid solution concentrations of Ge-Si (29 to virtually 100% Si) are in equilibrium with pure $CoSi_2$ (Fig. 26). Range VI is constituted of equilibria between solid solutions based on the defect Co_2Ge, and Co(Si, Ge) from the phase limit of that solid solution at ~ 67 mol % CoGe, down to ~ 15 mol % CoGe (Fig. 27). Here the previous discussion of range VII (Co_2Ge solid solutions) and Table 7 mentioned there are pertinent. Range VIII is a two phase region based on the Co_2Ge solid solutions being in equilibrium with solid solutions of Ge and Si in cobalt (Fig. 28). The latter phase range IX has simply been linearly extrapolated from the binary systems as reported in the literature; its extent is therefore quite uncertain. Also, the actual connecting points of our Co, Si, Ge solid solutions could not be accurately measured due to difficulties in the comminution of these alloys and attendant line broadening due to deformation.

Range X is a three phase area constituted of a Co_2(Ge, Si) solid solution, a solid solution of Si and Ge in Co and Co_2Si with a small amount (not much more than 5 mol%)Co_2Ge

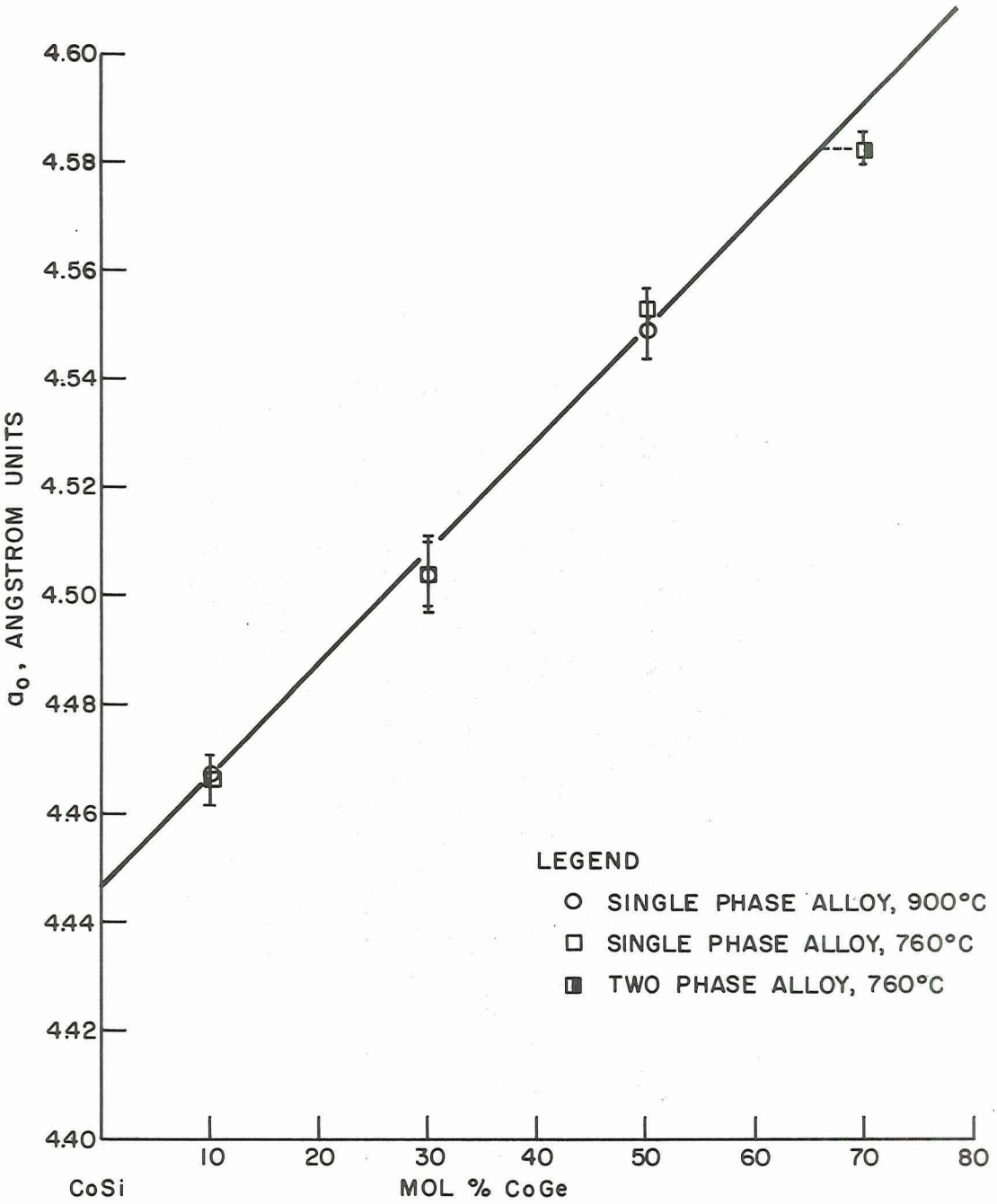

Fig. 20. Lattice parameters of Co-Si s. s. phase versus mol % CoGe

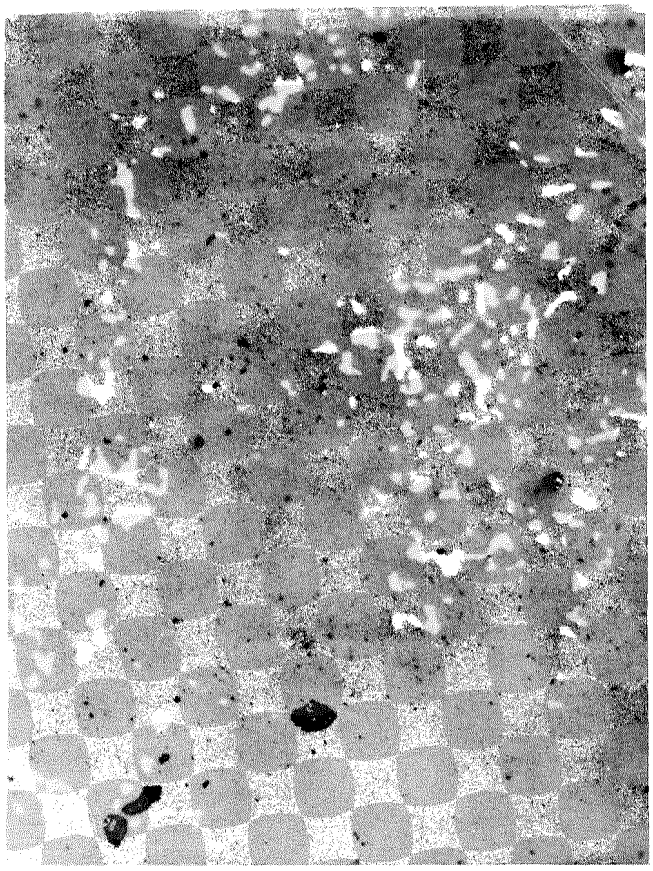

Fig. 21. $(CoSi)_3(CoGe)_7$, 750 °C, 2586 hr (CoGe precipitate in CoSi s. s. matrix; polarized light; 150X)

Fig. 22. $Co_{63}Si_{11}Ge_{26}$, as-melted (single-phase alloy based upon Co_2Ge; 115X, polarized light)

Table 7. Experimental Results on Annealed CoSiGe Alloys in the Area Over 50 at. % Co

Composition	Microscopy	hcp $Co_{2-x}(Ge, Si)$* a_0, Å	hcp $Co_{2-x}(Ge, Si)$* C_0, Å	a_0 Co(Si, Ge), Å	Remarks on X-Ray Results
24 hr, 950 °C					
$Co_{.64}Ge_{.36}$	Single phase	3.940	5.018	–	
				–	
360 hr, 950 °C					
$Co_{.60}Ge_{.35}Si_{.05}$	Single phase	3.872	4.981	–	
$Co_{.63}Ge_{.26}Si_{.11}$	Single phase	3.887	4.989	–	
$Co_{.55}Ge_{.35}Si_{.10}$	Two phase	3.871	4.980	4.571 ± 0.003	
$Co_{.60}Ge_{.20}Si_{.20}$	Two phase	3.868	4.978	4.479 ± 0.006	
$Co_{.58}Ge_{.11}Si_{.32}$	Three phase	–	–	4.472 ± 0.002	Definitely Co_2Si, probably Co_2Ge s.s.
$Co_{.65}Ge_{.11}Si_{.25}$	Three phase	–	–	–	Definitely Co_2Si, probably Co_2Ge s.s.
$Co_{.70}Ge_{.20}Si_{.10}$	Two phase	–	–	–	ϵ'-Co present + Co_2Ge
$(Co_2Si)_{.95}(Co_2Ge)_{.05}$	Complex single phase	–	–	–	α-Co_2Si solid solution [$Co_2Si(Ge)$]
$(Co_2Si)_{.05}(Co_2Ge)_{.95}$	Two phase	–	–	–	Complex Co_2Ge phase (not hcp)
$Co_{.75}Ge_{.12}Si_{.13}$	Three phase	–	–	–	ϵ'-Co present + ?
$Co_{.75}Ge_{.15}Si_{.10}$	Two phase	–	–	–	ϵ'-Co present + ?
$Co_{.75}Ge_{.05}Si_{.20}$	Two phase	–	–	–	ϵ'-Co + Co_2Si
$Co_{.80}Ge_{.10}Si_{.10}$	Three phase	–	–	–	ϵ'-Co a_0 = 2.5 Å, c_0 = 4.1 Å c/a = 1.64;-

*Error less than ±0.005 Å.

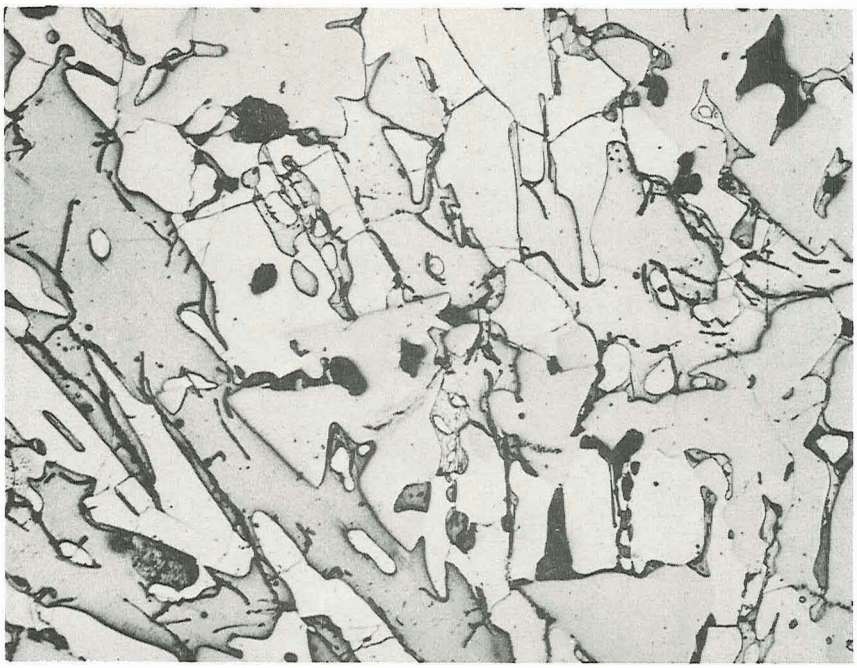

Fig. 23. 75($CoGe_2$) 25($CoSi_2$); 760 °C; 2000 hr

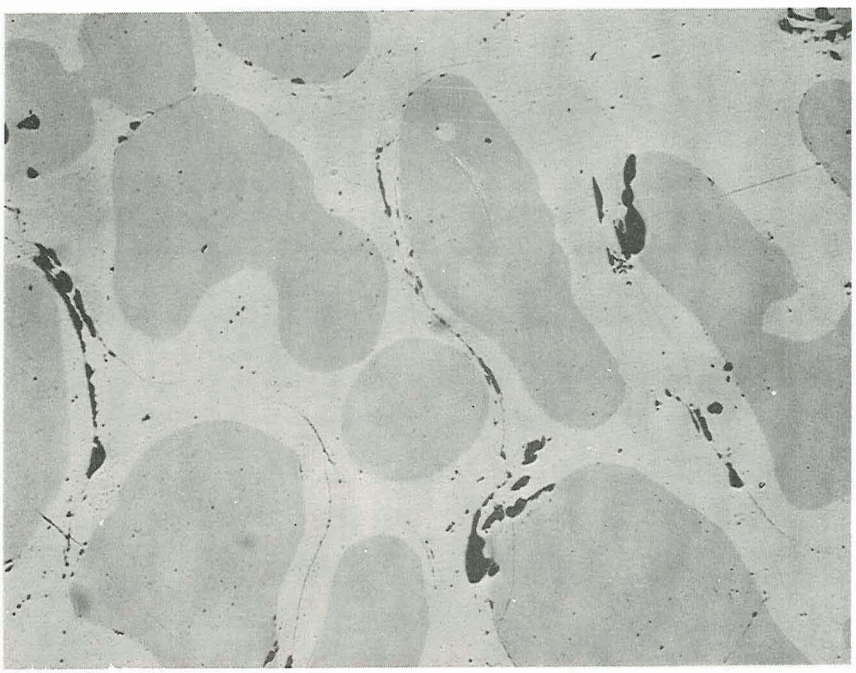

Fig. 24. $(CoSi_2)_{0.5}$ $(CoGe)_{0.5}$; 760 °C; 1090 hr; 150X

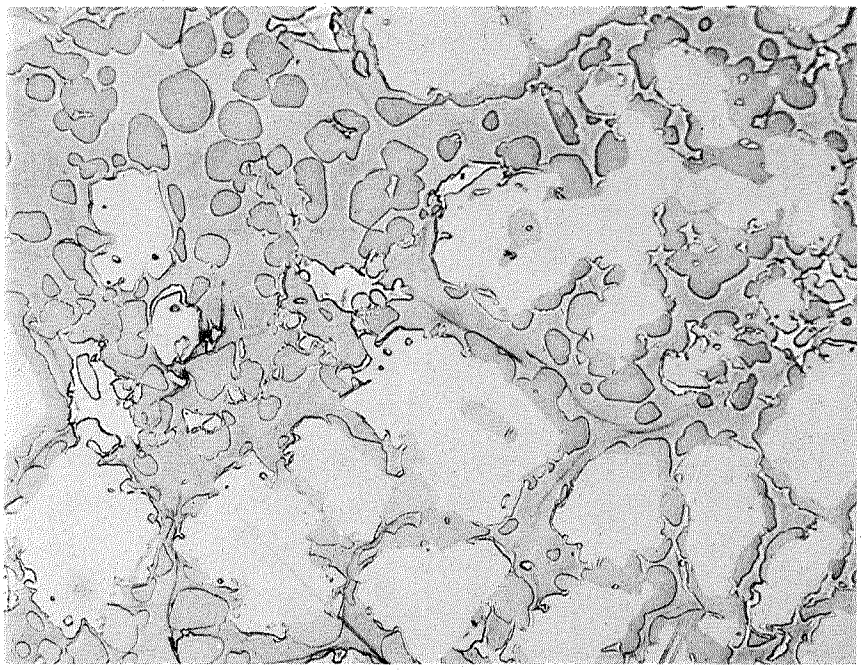

Fig. 25. 25($CoGe_2$) 75(CoSi); 760 °C; 2000 hr; 150X

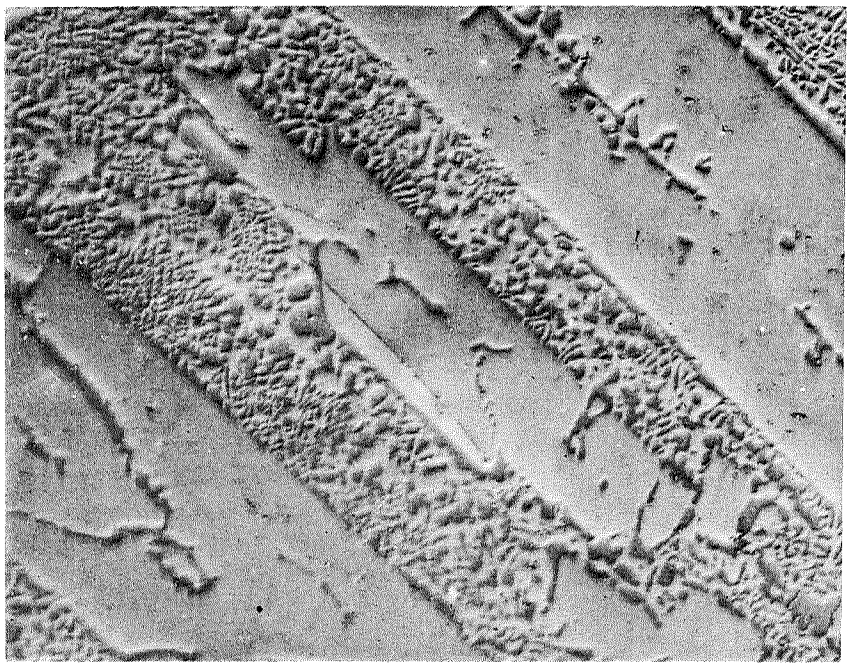

Fig. 26. 10Co20Ge70Si; 760 °C; 2000 hr (polarized light, oblique lighting)

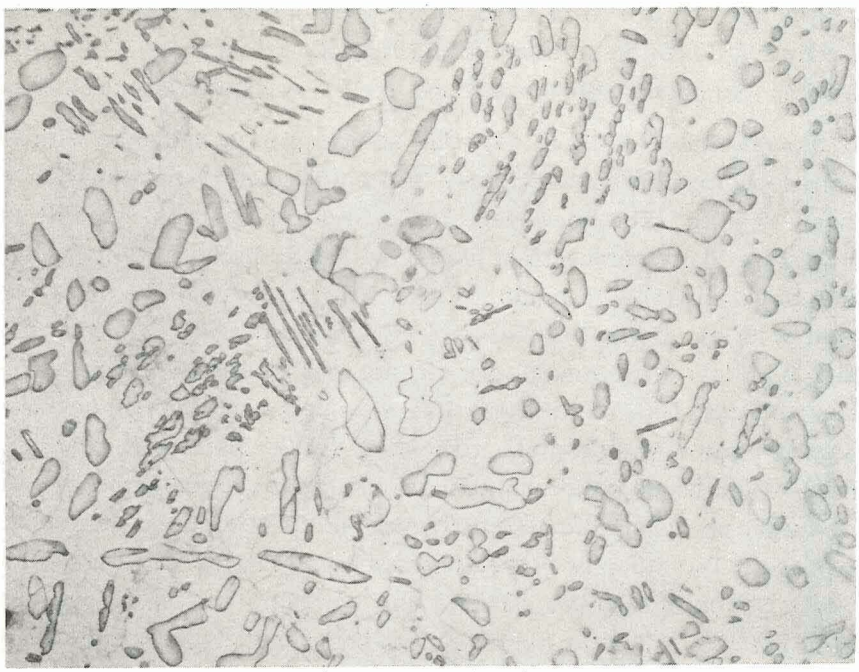

Fig. 27. 60Co20Si20Ge; 950 °C; 360 hr; 250X

Fig. 28. 75Co10Si15Ge; 950 °C; 360 hr; 250X

in solid solution (Fig. 29). Range XI is a two phase area in which Co_2Si with probably not much more than 5 mol % Co_2Ge in solid solution (Fig. 30) exists in equilibrium with Co_2Ge based solid solutions. No actual alloys are found here. The area exists of necessity.

Range XII is constituted of Co, Si, Ge solid solutions in equilibrium with $Co_2Si(Ge)$ (Fig. 31). The microphotograph shows clearly the complicated transformation structure which most probably resulted from the eutectoid Co_3Si decomposition, as well as white islands, which are most likely remnants of unreacted Co_2Si due to initially incomplete peritectic reaction of $Co_2Si(Ge)$ with liquid. Range XIII finally contains three phase equilibria of $Co_2(Ge, Si)$ solid solution, Co(Si, Ge) solid solution and $Co_2Si(Ge)$ (Fig. 32) and finally range XIV in which no alloys were made must consist of a two phase area where $Co_2Si(Ge)$ is in equilibrium with Co(Si, Ge). This leaves the area denoted U as an unknown in which no real assignment of phases was possible. The alloy $(CoGe_{.9})(CoSi_{.1})$ did not, as expected, contain CoGe and the CoSi based solid solution but instead it showed CoGe and a nonassignable set of lines which might perhaps indicate a deformation of CoGe due to the introduction of Si. The alloy is two phase. The other two three phase alloys (Fig. 33 and Fig. 34) both contained CoGe, and the Co(Si, Ge) solid solution. The latter, however, was of a CoGe content which was rather puzzling, if one considers their relative positions. Also, extra lines were found not conforming to the extra lines in the $(CoGe_{.9})(CoSi_{.1})$ alloy, but checking rather well in many instances with a pattern calcuable for Co_2Ge_3 from Schubert's structure data. Finally, DTA results on these alloys are rather complex showing four peaks (for the three phase alloys) in very close succession, i.e., (for $Co_{45}Si_{09}Ge_{46}$) 829 °C, 889 °C, 948 °C, 1070 °C. We believe at the present time that the appearance of Co_2Ge_3 or a similar alloy which is formed peritectoidally rather complicates this area too much to advance any interpretation of the phase relationships around the region of CoGe.

REFERENCES TO SECTION V

1. M. Hansen, Constitution of Binary Alloys, McGraw Hill, New York, 1958.
2. R.P. Elliot, Constitution of Binary Alloys, First Supplement, McGraw Hill, New York, 1965
3. F.A. Shunk, Constitution of Binary Alloys, Second Supplement, McGraw Hill, New York, 1969.
4. H.F. Goldschmidt, Interstitial Alloys, Plenium Press, New York, 1967.
5. G.V. Samsonov and V.N. Bondarev, Germanides, Consultants Bureau, Inc., New York, 1969.
6. H. Nowotny, F. Benesovsky and C. Brukl, Monatsh. Chem., 92, 365 (1961).
7. P. Stecher, F. Benosovsky and H. Nowotny, Monatsh. Chem., 94, 549 (1963).
8. H. Holleck, F. Benosovsky and H. Nowotny, Monatsh. Chem., 96, 570 (1965).
9. L.H. Brixner, J. Inorg. Nucl. Chem., 25, 783 (1963).
10. L.H. Brixner, J. Inorg. Nucl. Chem., 25, 257 (1963).

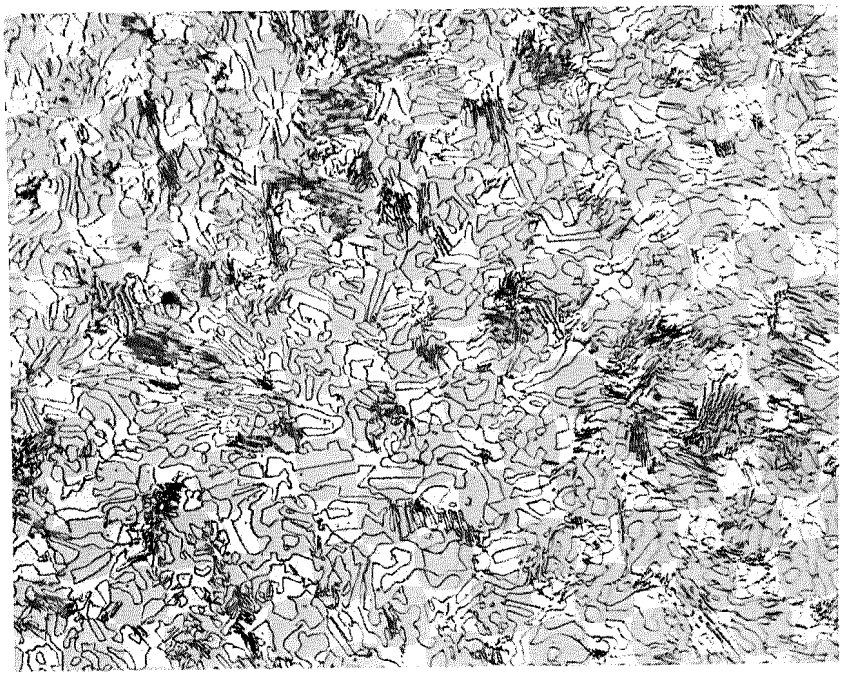

Fig. 29. 17Co13Si12Ge; 950 °C; 260 hr; 300X

Fig. 30. 5(Co_2Ge) 95(Co_2Si); 760 °C; 2000 hr

Fig. 31. $Co_{.75}Si_{.2}Ge_{.05}$, 760 °C, 2000 hr (primary phase is most likely undissolved α-Co_2Si; eutectoid is composed of α-Co_2Si + ϵ-Co; 300X)

Fig. 32. 58Co32Si10Ge; 950 °C; 360 hr; 250X

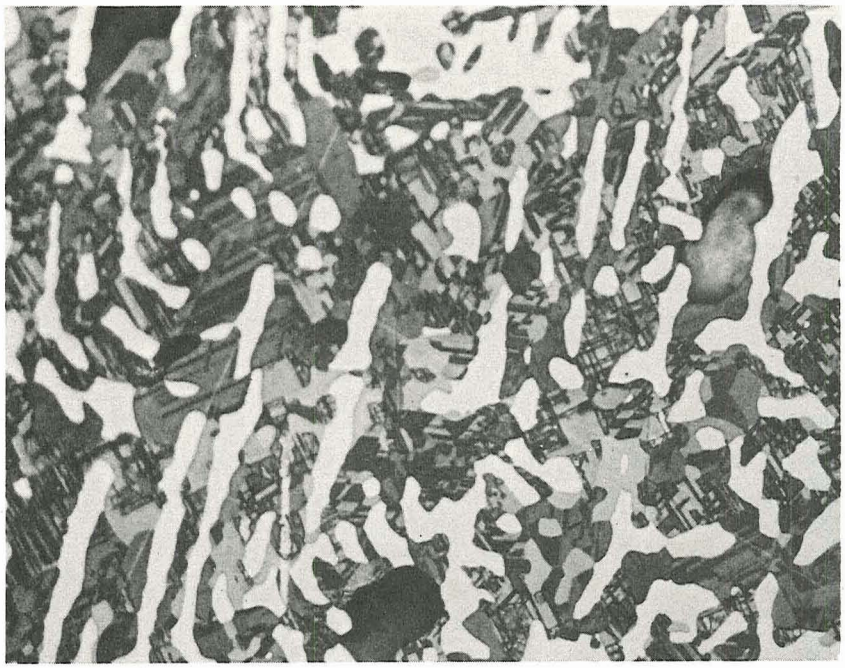

Fig. 33. 45Co9Si46Ge; 750 °C; 1000 hr; 650X (regular light)

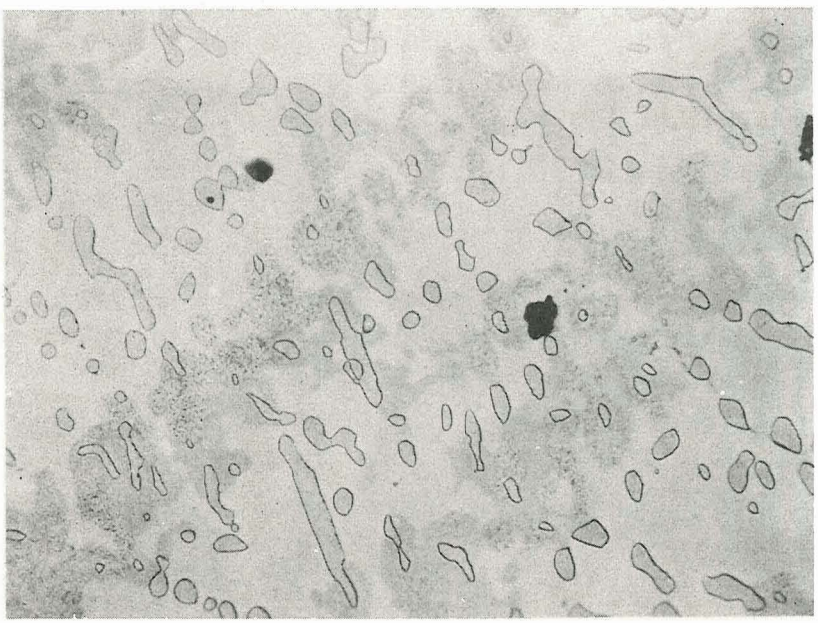

Fig. 34. $Co_{.4}Ge_{.55}Si_{.05}$, 760 °C, 2000 hr (matrix of $CoGe_2$; insulator type precipitate is probably CoSi s.s. plus unidentified third phase; 200X)

VI THE PALLADIUM GERMANIUM SYSTEM*

A. Introduction

U. S. Patent no. 3342646 (A.G.F. Dingwall to RCA, Sept. 1967) claims the use of noble metals, specifically palladium as a high temperature braze for Ge-Si alloys. Although, to the extent of the writer's knowledge, Pd was never used in the manufacture of thermoelectric devices in the U.S., it was found to be present in some Ge-Si couples of German manufacture.

Since we belived that, in accordance with the general alloy chemistry of the platinum metals with Si and Ge, very low melting eutectics could be expected in such a brazed joint, an investigation of the Pd-Ge-Si systems was started to demonstrate this fact and clarify just how low in temperature such eutectics would go. It became, however, soon apparent that the knowledge of the binary Pd-Ge system was so rudimentery as to not allow any meaningful investigation of the ternary Pd-Ge-Si system. The only definite piece of constitutional information to be gathered on that system was that the compounds Pd_2Si and Pd_2Ge form a continuous series of solid solutions. All other alloys made in the system were too difficult to interpret, although it did become clear immediately that melting points of the order of ~700 °C were not uncommon in the system. Hoping to clarify the ternary system later on, we concentrated on the binary Pd-Ge system for the time being.

B. Literature Survey

G. V. Samsonov and V. N. Bondarev reviewed the work on germanides recently.[1] Their review of the Pd-Ge system is based solely on the well known work by Schubert and his associates,[2,3,4,5] who made a tentative evaluation of the system mainly in terms of what compounds were present. No phase diagram was given, although low melting eutectics at ~700 °C were indicated.

Other pertinent systems in this context such as Pt-Ge, etc. can be found in reference 1 as well.

---

*F. Wald and S. J. Michalik

C. Experimental Methods

The materials used were obtained from the following sources. Palladium was the spectrographically standardized Pd sponge from Johnson Matthey and Co., London. The Ge used came from Sylvania Electric Products, Tonawanda, Pennsylvania. It was semiconductor grade zone refined ingot material (minimum resistivity at 27 °C = 40 Ω-cm).

Charges of ~5 g total were weighed to the nearest 0.1 mg on an analytical balance. The lower melting compositions were then melted in evacuated quartz ampoules. The higher melting ones were argon arc melted on a water cooled copper hearth. No weight losses or increases were found.

The following alloy compositions were prepared: Ge with 10, 20, 25, 30, 37, 40, 47.5, 50 (PdGe), 52.5, 60, 66 2/3 (Pd_2Ge), 69, 71.4 (Pd_5Ge_2), 75, 80, 83 1/3, 84, 85, 87.5, 90, 95, at. % Pd. All of them were viewed under the microscope after having been polished and etched with aqua regia using standard metallographic procedures.

2.5 g of material were used for differential thermal analysis which was carried out in a commercial unit.[6] DTA runs were repeated with alloys annealed for 2200 hr at 645-675 °C. X-ray powder photographs were taken with a Philips Debye Scherrer powder camera of 114.6-mm diameter. The readings were converted into d-spacings and evaluated as stated before. (Section on Co-Si-Ge).

D. Results

The phase diagram up to 75% at. % Pd as constructed from DTA results and supported by metallographic and X-ray results is shown in Fig. 35. The system is constituted of a regular eutectic at 32 ± 2 at. % Pd between Ge and PdGe at 735 ± 2 °C. The solubility of Pd in Ge is very small indeed. The lattice parameter for pure Ge $a_0 = 5.6576$ was the same within the limits of accuracy as that of 5.6571 ± 0.0012 computed for Ge in the 90% Ge 10% Pd alloy annealed at 675 °C.

Figs. 36 and 37 show alloys with hypo- and hypereutectic structures in this region. PdGe is formed by a peritectic reaction from the melt at 830 ± 5 °C. No maximum was found for the compound but the DTA peak found for the 50 at. % Pd, 50 at. % Ge composition was very sharp, both on heating and cooling. Thus, the compound is assumed to lie exactly at the intersection of the peritectic horizontal and the two respective liquidius lines. Nevertheless, some very low maximum cannot be entirely excluded. The next compound in the system is Pd_2Ge, which melts with a very sharp maximum at 1350 ± 10 °C. Figs. 38 to 40 show the single phased alloys at PdGe and Pd_2Ge together with a two phase structure at 40 at. % Ge, 60 at. % Pd. X-ray results on both these alloys confirm the structures described by Schubert, et al.[2,3] The d-spacings, however, differ slightly for the single phase alloys and for the respective two phase alloys. Thus, some phase lattitude for both compounds must be assumed. The next three alloys with 69 at. %, 71. 4 at. % (Pd_5Ge_2) and 75 at. % (Pd_3Ge) show clearly the peritectic formation of

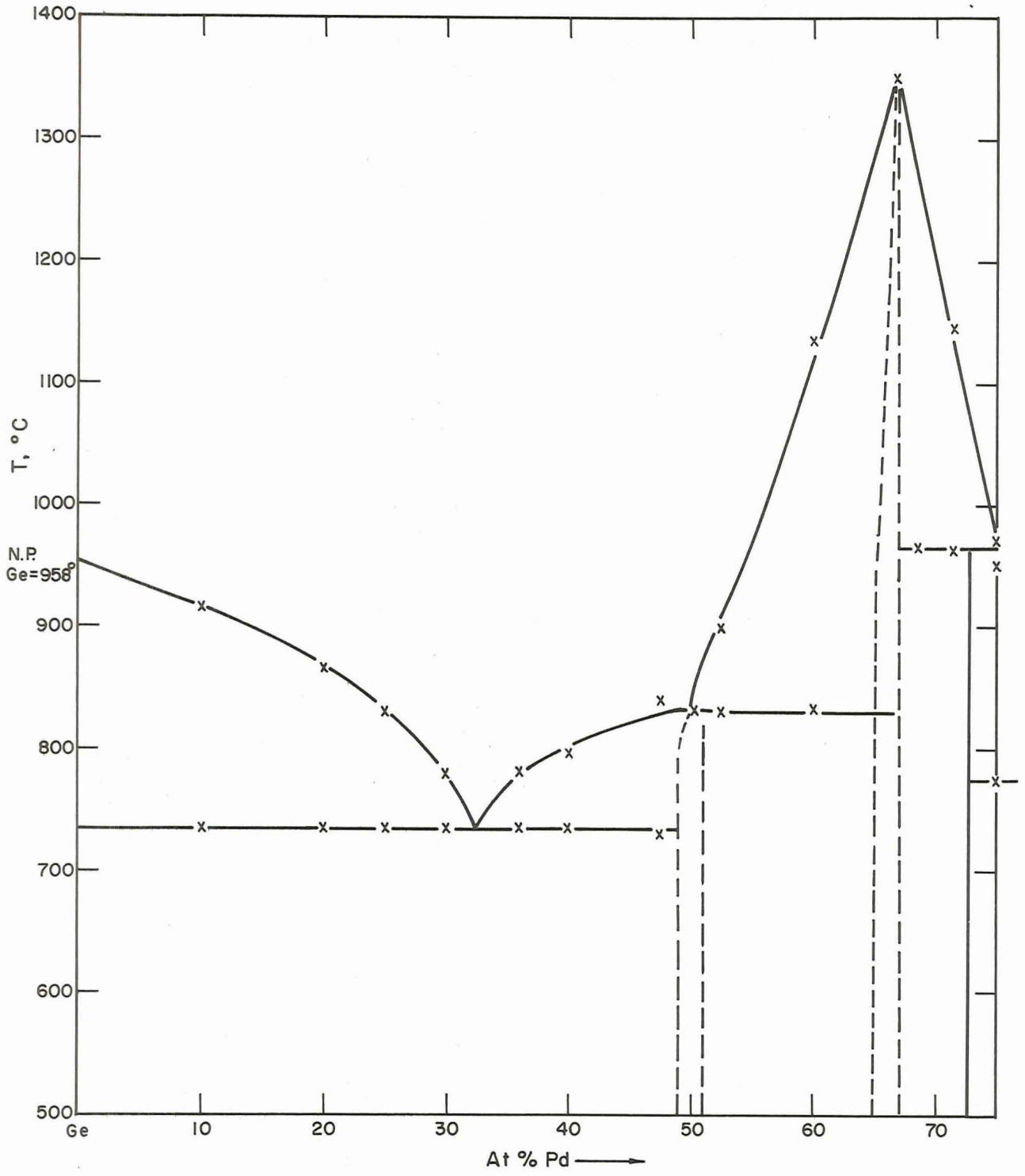

Fig. 35. Pd-Ge system (Pb concentrations up to 75 at. %)

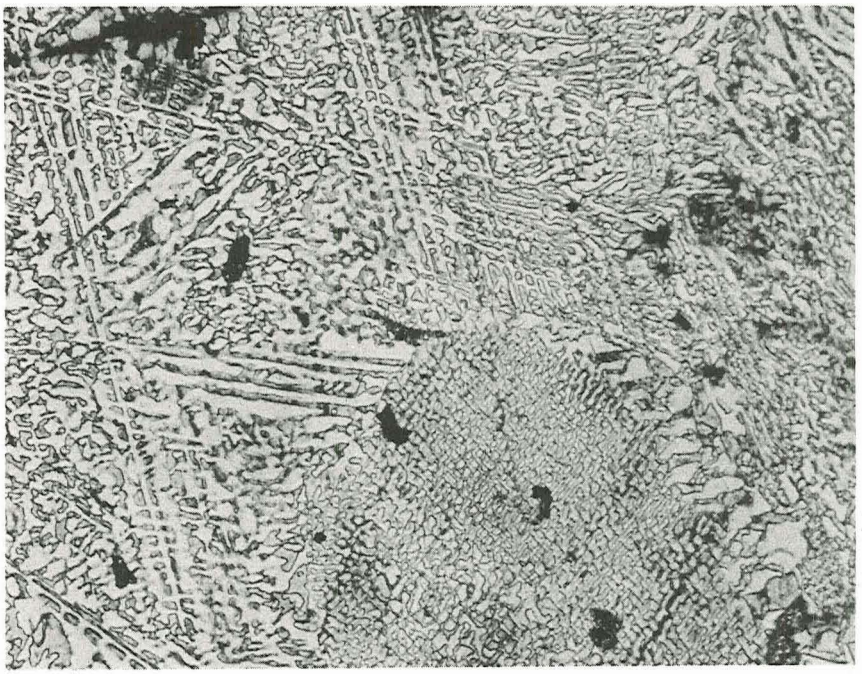

Fig. 36. As-cast 30Pd-70Ge (200 X)

Fig. 37. As-cast 37Pd-63Ge; polarized light (150X)

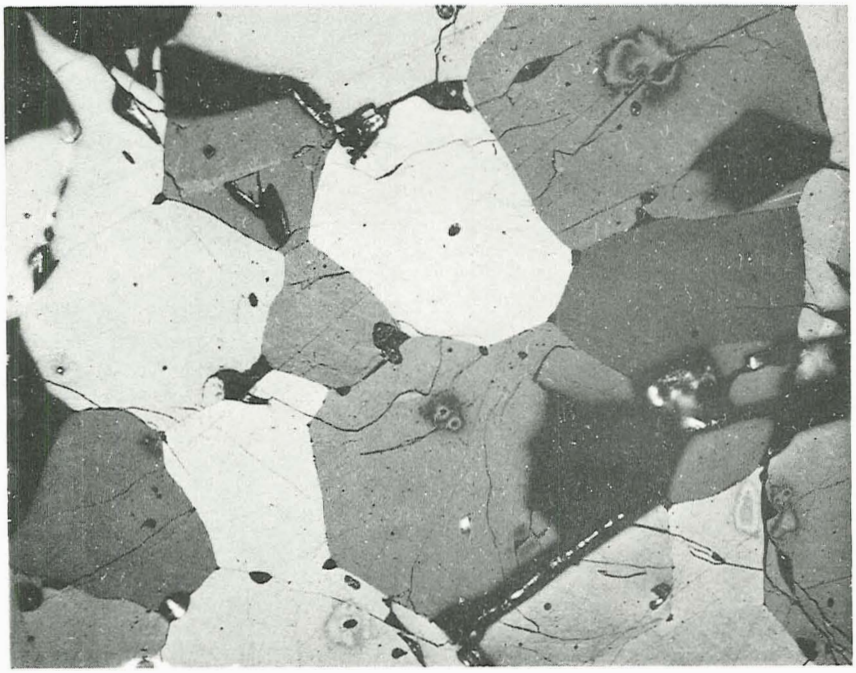

Fig. 38. PdGe; 675 °C; 2200 hr; polarized light (100X)

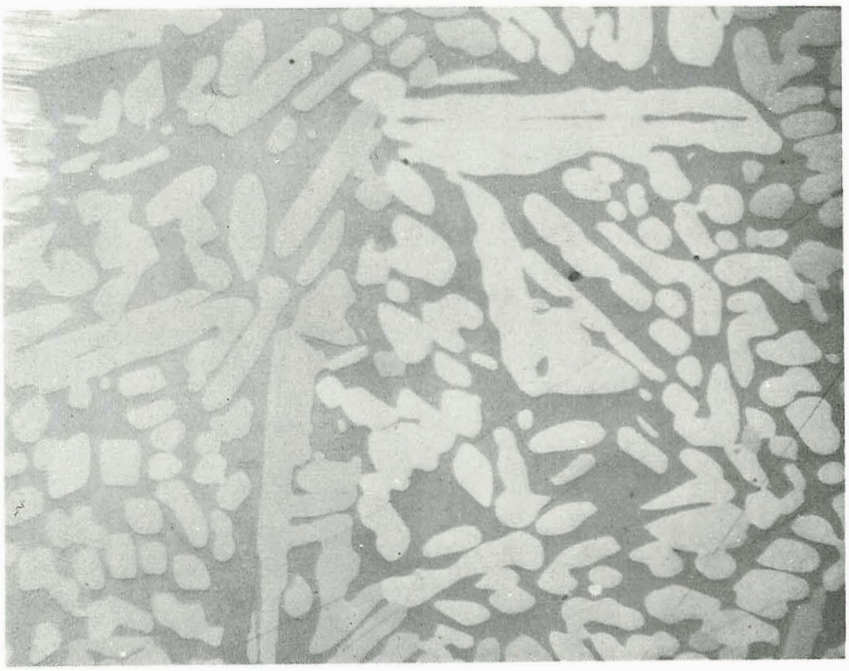

Fig. 39. 60Pd-40Ge; 675 °C; 2200 hr; polarized light (100X)

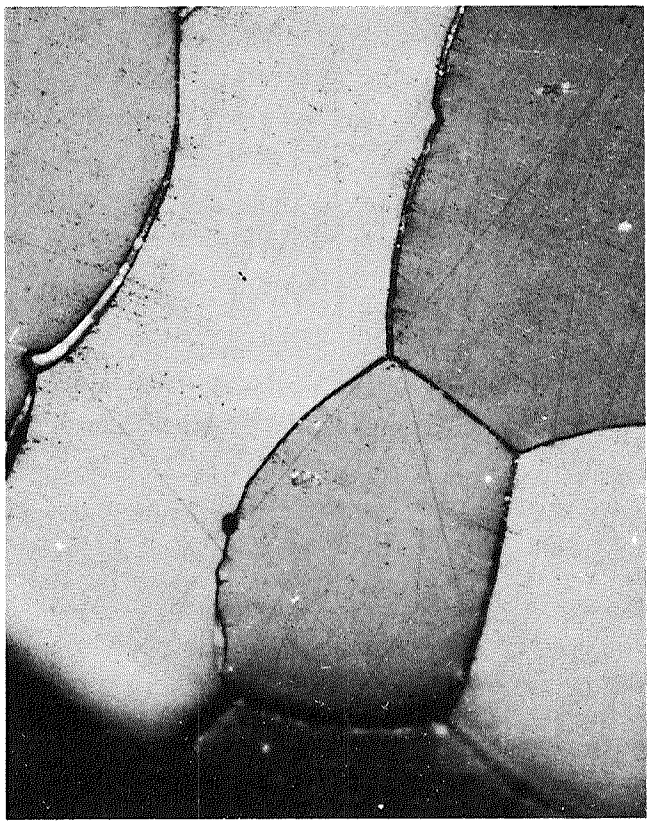

Fig. 40. Pd_2Ge; 675 °C; 2200 hr; polarized light (150X)

another compound at 965 ± 5 °C in this region. This compund is not Pd_5Ge_2 since this composition is clearly two phase even after annealing at 675 °C for 2200 hr (Fig. 41). X-ray results also show it as two phase consisting of Pd_2Ge and the $Pd_{3-x}Ge$ phase mentioned below. Also, the alloy with 75 at.% Pd is two phase (Fig. 42). Nevertheless, X-ray investigations demonstrate that the spectra in this region can be roughly indexed as cubic. We believe therefore that a compound similar to Pt_3Ge exists in this system. Pt_3Ge has a slightly distorted Cu_3Au type structure which would satisfy our rough indexing. Thus, because the phase is clearly deficient in Pd as demonstrated by the two phase nature of the 25 at.% Ge, 75 at.% Pd alloy (as-cast as well as annealed), we will assign the notation $Pd_{3-x}Ge$ here.

From here on until 100% Pd, no clear-cut phase assignments could be made. The system becomes exceedingly complex as is clearly demonstrated by the plot of DTA results shown in Fig. 43.

We believe that the existence of the eutectic between the $Pd_{3-x}Ge$ phase and the $Pd_{84}Ge_{16}$ phase is probably sufficiently supported both by DTA results as shown and by the fact that a eutectic structure is present in alloys with 75 at. % 80 at. % and 83 1/2 at.% Pd in the as-cast state (Fig. 44).

Also, we believe that $Pd_{84}Ge_{16}$ exists probably down to room temperature since the difference between the as-cast and the 675 °C annealed structure is rather striking (Figs. 45 and 46). One might assume that the twinned brass type structure is the β-tungsten type described by Schubert, et al.[5] The fact is that in many alloys in that region we did find X-ray lines which might indeed belong to such a structure but only in as-cast samples. In these samples, those lines were present together with lines of a Pd-Ge solid solution. Nevertheless, after annealing these lines disappeared, to be replaced by a set of many lines which was impossible to index. Thus, one might suggest that the 84 Pd - 16 Ge alloy instead of being not wholly homogenized is transforming, after the brass structure had been formed from the original alloy. This view might be supported by looking at the alloy with 83.33 at. % Pd which seems to be more fully transformed (Fig. 47). Even this tenuous assumption does not shed any notable amount of light on the problem of phase assignments in this region. Only further work will allow to unravel the complexities in this area and some further work on the system is planned before publication in the open literature.

REFERENCES TO SECTION VI

1. G. V. Samsonov and V. N. Bondarev, Germanides, Consultants Bureau, New York 1969.
2. H. Pfisterer and K. Schubert, Zeitsch. f. Metall Kunde, 41, 358 (1950).
3. K. Anderko and K. Schubert, Zeitsch. f. Metall Kunde, 44, 307 (1953).
4. K. Schubert and K. Anderko, Naturwiss. 39, 351 (1952).
5. K. Schubert, et al., Naturwiss. 50, 41 (1963).
6. T. + T. Controls Co., Media, Pennsylvania. U.S.A.

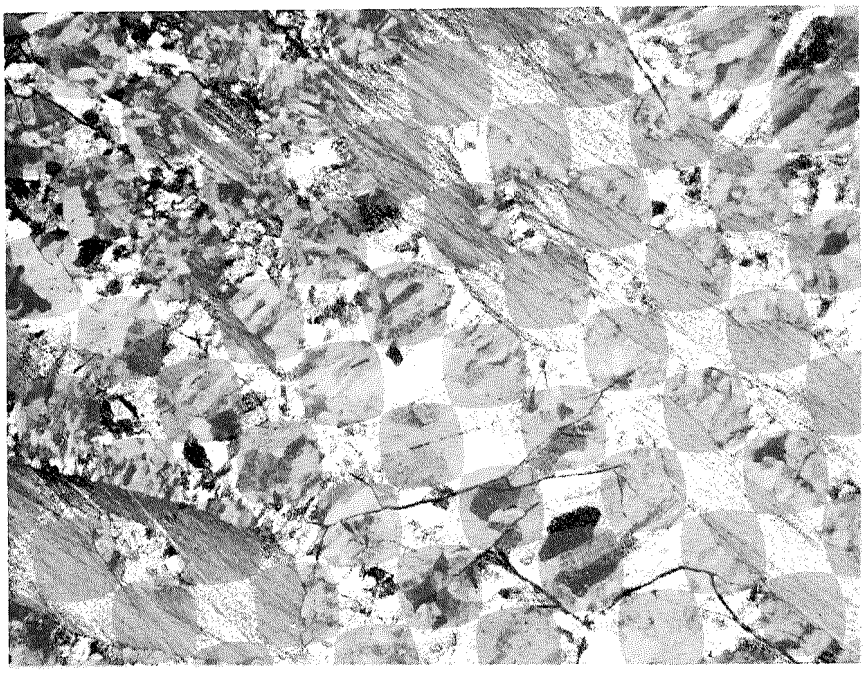

Fig. 41. Pd_2Ge; 675 °C; 2200 hr; polarized light (200X)

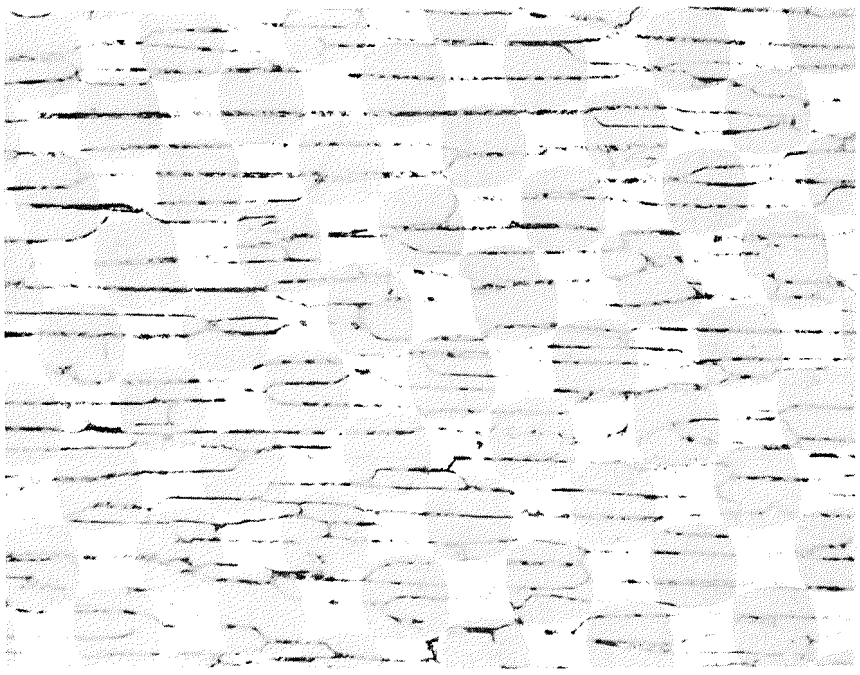

Fig. 42. 75Pd-25Ge; 675 °C; 2200 hr (125X)

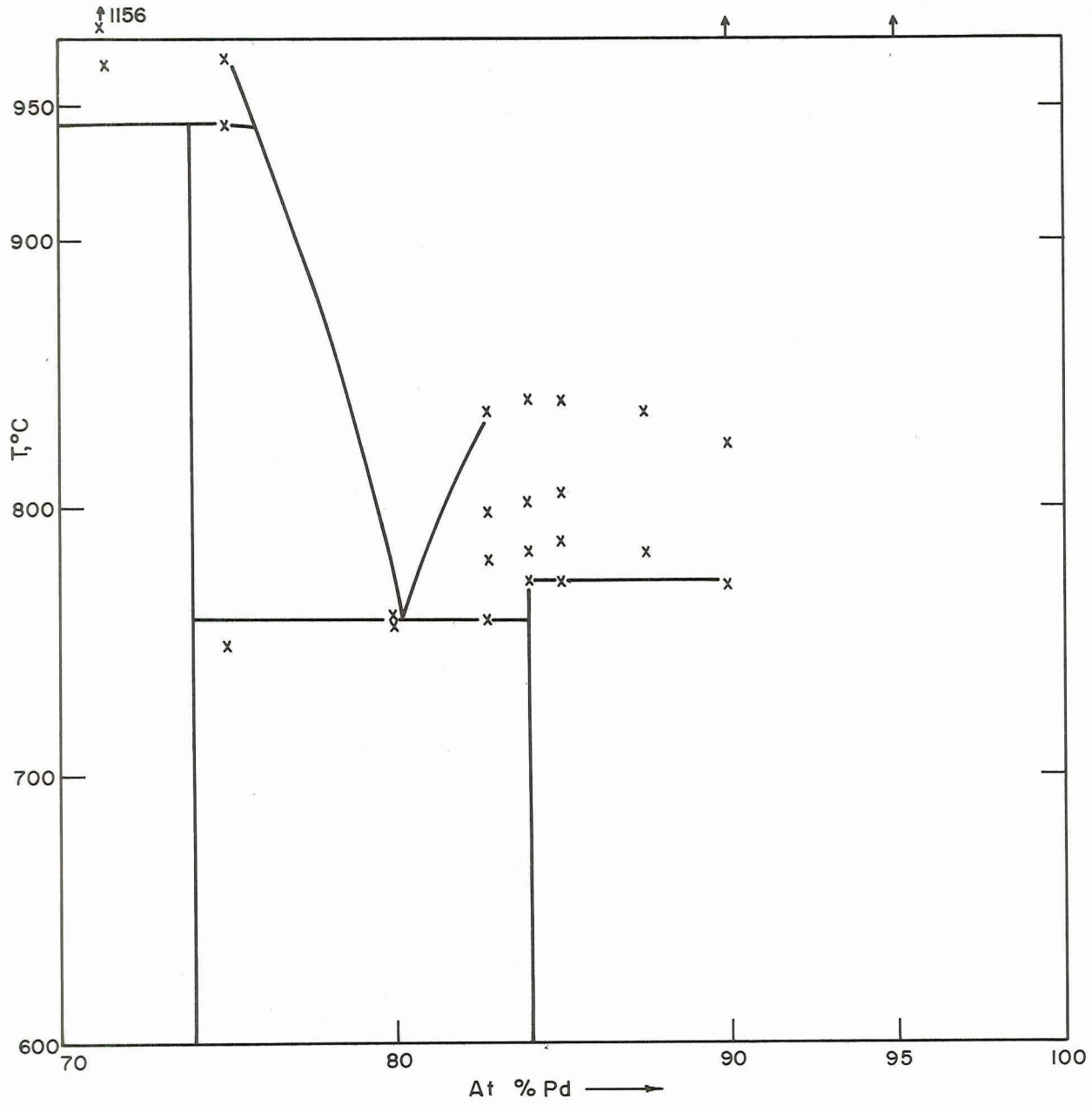

Fig. 43. DTA results in the Pd-Ge system with Pd concentrations over 75 at. %

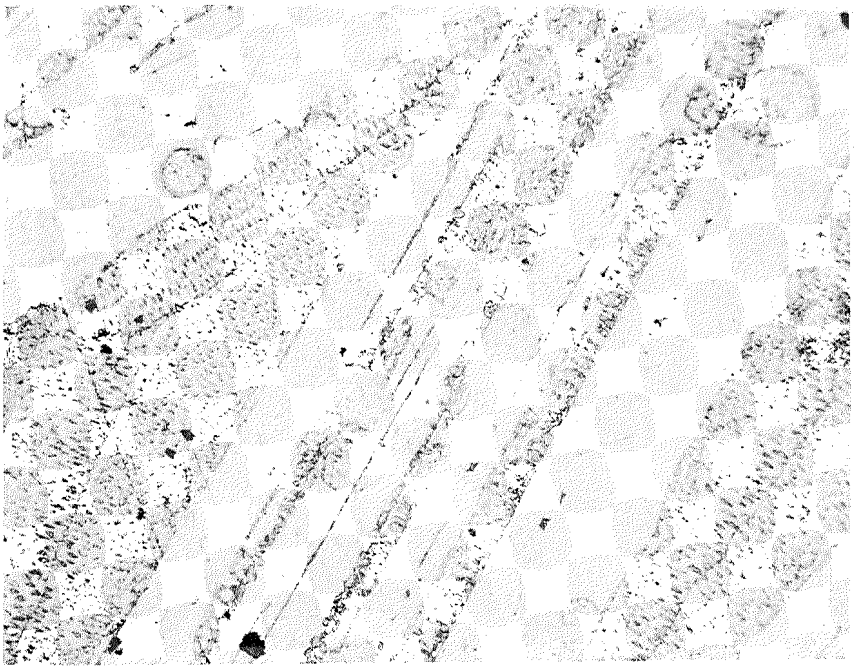

Fig. 44. As-cast 80Pd-20Ge (100X)

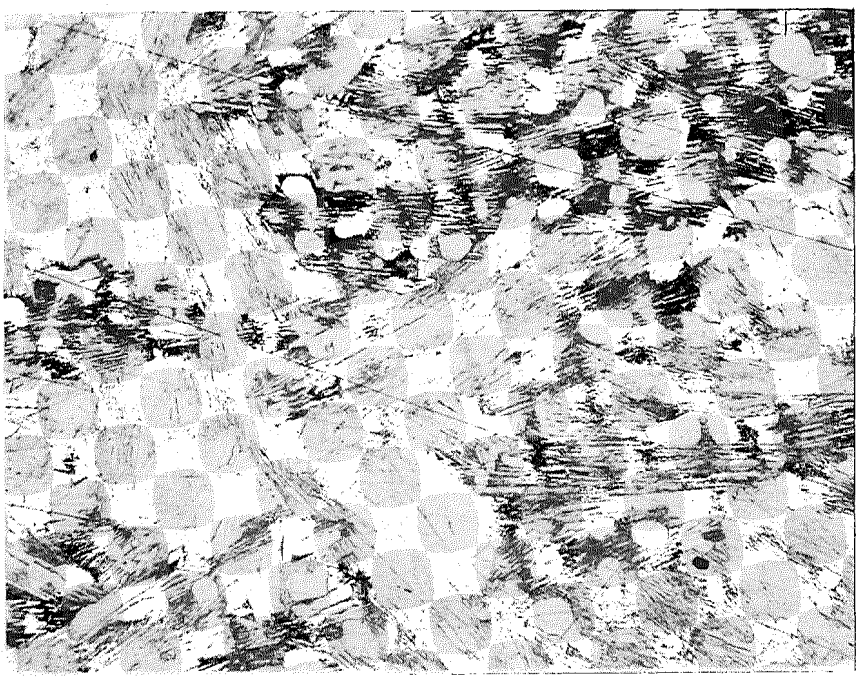

Fig. 45. As-cast 84Pd-16Ge (120X)

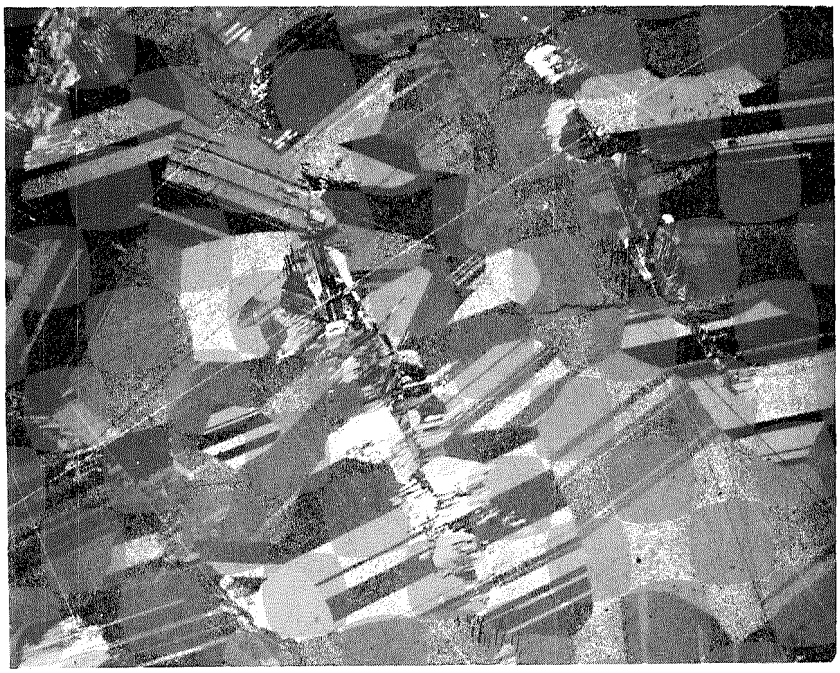

Fig. 46. 84Pd-16Ge; 645 °C; 2150 hr; polarized light (100X)

Fig. 47. 16 2/3Ge-83 1/3Pd; 645 °C; 2150 hr;; polarized light (125X)

Appendix A.*

SUMMARIES OF PREVIOUS REPORTS ON CONTRACT NAS5-9149

*This appendix contains a collection of all abstracts or summaries presented in the various reports on the contract.

I. QUARTERLY REPORTS

A. March 1 Through May 31, 1965

The purpose of this study is to define in fundamental terms the most appropriate system and process for the reproducible fabrication of low-resistance, high-strength bonds of nonmagnetic electrodes to PbTe and PbTe-SnTe thermoelectric alloys. Investigations during this period have covered the following areas: precision of thermoelectric property measurements has been evaluated; thermoelements have been studied physically and by chemical analyses; procedures have been refined for diffusion bonding of W to n-type PbTe and the effects of bonding on thermoelectric properties and effects of some process variables evaluated; the effect of temperature on the contact resistance of W on PbTe was studied; diffusion bonding and SnTe brazing of p-type PbTe-SnTe to W was studied; metallographic techniques were developed for examination of unbonded and bonded structures.

B. June 1 Through August 31, 1965

The purpose of this study is to define in fundamental terms the most appropriate system and process for the reproducible fabrication of low-resistance, high-strength bonds of nonmagnetic electrodes to PbTe and PbTe-SnTe thermoelectric alloys. During this period, SnTe braze-bonding of Ta and W electrodes to $Pb_{.5}Sn_{.5}Te$ thermoelements was studied, in addition to investigating diffusion bonding of W electrodes to $Pb_{.5}Sn_{.5}Te$. Some diffusion-bonded elements were examined by the electron beam microprobe technique. The designing of a sixteen-specimen, gradient life testing device was completed. Physical and chemical evaluation of commercially available thermoelements was continued.

C. September 1 Through November 30, 1965

The purpose of this study is to define the most appropriate system and process for the reproducible fabrication of low-resistance, high-strength bonds of nonmagnetic electrodes to PbTe and PbTe-SnTe thermoelectric alloys. During this period, study of diffusion-bonding of W electrodes to $Pb_{.5}Sn_{.5}Te$ thermoelements was continued. Experiments in bonding to dense PbTe and $Pb_{.7}Sn_{.3}Te$ with W electrodes were conducted. Reaction of W with PbTe was examined. Life testing and physical and chemical evaluation of thermoelements were continued.

D. December 1, 1965 Through February 28, 1966

The purposes of this study are: (1) to define the most appropriate system and process for the reproducible fabrication of low-resistance high-strength bonds of nonmagnetic electrodes to PbTe and PbTe-SnTe thermoelectric alloys, (2) to study degradation processes in these materials, and (3) to study the junctions of these materials with their electrodes. Equilibria between Ta, PbTe, and SnTe and between W and PbTe were investigated, along with diffusion bonding of W to powdered and sintered PbTe materials. The diffusion bonding process for 3N and 3P thermoelements was scaled up for increased production of bonded elements.

E. March 1 Through May 31, 1966

The purposes of this study are: (1) to define the most appropriate system and process for the reproducible fabrication of low-resistance, high-strength bonds of nonmagnetic electrodes to PbTe and PbTe-SnTe thermoelectric alloys, (2) to study degradation processes in these materials, and (3) to study the junctions of these materials with their electrodes. During the past quarter, bonding process variables were investigated, e.g., pressure, jig configurations, and oxygen concentration in the gas stream. Segmented elements of Si-Ge-PbTe were fabricated, and diffusion bonding of p-type PbTe to W was examined. Investigations of Phase equilibria were continued in the systems SnTe-Ta, W, Fe and PbTe-Ta, and Fe. Evaluation and testing of bonded and unbonded thermoelemts were continued.

F. November 1, 1966 Through January 31, 1967

The purposes of this study are: (1) to define an appropriate system and process for fabrication of low-resistance, high-strength bonds of nonmagnetic electrodes to PbTe and PbTe-SnTe thermoelectric alloys, (2) to study degradation processes in these materials and their junctions with nonmagnetic electrodes, and (3) to study the fundamental chemical behavior of PbTe and Si-Ge thermoelectric alloys with potential electrode materials.

During the past quarter, the effect of high quality contact surface finishes on bonding of W to $Pb_{.4}Sn_{.6}Te$ thermoelements was investigated. Optimized couples of PbTe and Si-Ge-PbTe segmented couples for life testing were designed, along with a sixteen-couple gradient life tester for PbTe couples. Life test results at 600 °C for 4700 hr on 3N-W and 3P-W junctions are reported. Phase diagrams for the systems Fe-PbTe and Fe-SnTe-PbTe, and results of investigations in the systems Ag-Pb-Te, Ag-Sn-Te, Ni-Pb-Te, and Co-PbTe and Co-SnTe are presented.

G. February 1 Through April 30, 1967

The purposes of this study are: (1) to define an appropriate system and process for fabrication of low-resistance, high-strength bonds of nonmagnetic electrodes to PbTe and PbTe-SnTe thermoelectric alloys, (2) to study degradation processes in these materials and their junctions with nonmagnetic electrodes, and (3) to study the fundamental chemical behavior of PbTe thermoelectric alloys with potential electrode materials.

During this quarter, work has been concerned with preparation of PbTe couples, construction of couple test devices, and life testing of bonded elements. Results are presented from an 800-hr gradient life-test of W-bonded n and p elements. Phase diagrams of the Ag_2Te-PbTe and Au-PbTe systems are presented, along with results of investigations in the Fe-PbTe, Au-SnTe and Co-SnTe systems.

II. INTERIM SUMMARY REPORTS

A. Period From February 26, 1965 Through October 30, 1966

1. Bonding studies

a. Ta-SnTe braze bonding and W-diffusion bonding have been evaluated in terms of chemical, electrical and mechanical stability.

b. Although the Ta-SnTe braze bonding procedure initially produced satisfactory electrical and mechanical structures, chemical incompatibilities (tantalum telluride formation) make Ta-SnTe brazed structures unsatisfactory.

c. W-diffusion bonding is accomplished at 830 to 840 °C for 15 to 20 min with a deadweight load of 30 g/cm^2.

d. The W-diffusion process reproducibly yields room temperature bond contact resistivities of less than 10 $\mu\Omega\text{-cm}^2$ for n-type and less than 30 $\mu\Omega\text{-cm}^2$ for p-type SnTe-PbTe.

e. The contact resistance has been determined as a function of temperature for n-type PbTe. The resistivity follows the relationship $\rho_c \propto T^{2.9}$.

f. Bonding has little effect on the Seebeck voltage of either n- or p-type thermoelements.

g. The tensile strengths of the W-diffusion bond have been measured in excess of 2500 psi. Failure in tension and shear generally occurs in the bulk thermoelement.

h. The mechanism of W-diffusion bonding is still unknown; however, the bonding appears to be associated with oxygen and/or small concentrations of impurities.

2. Compatibility of lead and tin telluride with metals

The chemical reaction behavior of 17 metallic elements towards lead telluride and of 10 towards tin telluride was surveyed.

The following findings were made:

a. The reaction $xPbTe + yM \rightarrow M_yTe_x + xPb$ was found to go from left to right for the following elements: Ti, V, Cr, Mn, Zn, Ga, Zr, Nb, Cd, In and Ta. It was found to go from right to left for Fe and W. Complicated reactions were found for Mo, Ni, Cu, Ag, Ga, and In.

b. The reaction $xSnTe + yM \rightarrow M_yTe_x + xSn$ was found to go from left to right for the following elements: Mn, Zn, Cd; and from right to left for Fe and W. Complicated reaction behavior was found for Mo, Ni, Cu, Ag, Ga, and In.

c. The findings were systematized with respect to the position of all elements in the periodic table. It can be shown that the question of whether elements react or not can be answered using heats of formations of tellurides calculated from electronegativity values presented in Table III-V according to:

$$\Delta H = 23.07 \times z(X_a - X_b)^2/N$$

where

x = number of bonds broken,

X_a and X_b = electronegativities according to Table III-Vm

N = number of atoms,

H = heat of formation per g/atom.

To determine the number of bonds broken, the valency of Te is assigned constant at -2. Entropy contributions are generally shown to be negligible. Application of this rule is limited to elements which follow the straight reaction equations cited in 1 and 3. Similar considerations can be applied to the reaction behavior of alloys and intermetallic compounds.

3. Thermoelement evaluation

a. The major and minor impurities of 3N, 3P, and 2P elements have been identified by chemical analyses.

b. The oxygen contents of 3N, 3P, and 2P elements have been established by vacuum fusion analysis. The average levels in parts-per-million are 70, 420, and 70, respectively.

c. Densities of the pressed and sintered thermoelements have been measured and found to be 8.06, 6.65, and 7.6 gm/cm^2 for 3N, 3P, and 2P, respectively.

d. The average sizes and distributions of pores in the pressed and sintered materials were measured.

e. Various mechanical properties of the three materials have been measured including microhardness, tensile, compressive, and shear strength.

4. Life testing

a. Tungsten-bonded elements life-tested isothermally at 600 °C for as long as 2600 hr have shown no degradation effects associated with the tungsten electrode. Contact resistances have shown a gradually decreasing rate of increase with time at temperature. This behavior appears to level off at an average room temperature resistance of approximately 100 $\mu\Omega$.

b. Results from a 500 hr system test of the gradient life-test module show encouraging stable behavior of n- and p-bonded elements operating between approximately 500 and 30 °C.

5. Life test station

A sixteen element compact-fully automated life test station has been designed, constructed and placed into operation.

6. Si-Ge-PbTe segmented elements

a. Si-Ge-PbTe segmented elements have been prepared using a W diffusion-bonded intermediate.

b. Calculations on an optimized couple design utilizing Si-Ge-PbTe legs indicate that substantial gains in power output and power densities may be realized.

B. Period From November 1, 1966 Through July 31, 1967

1. Constitutional investigations

The basic constitutional principles of the systems Co-PbTe, Co-Sn-Te, Re-PbTe and Re-SnTe are presented. This concludes the basic investigations of the chemical compatibility between lead and tin telluride and elemental metals. The information gained is summarized from a fundamental viewpoint, and a method of estimating the reactivity of alloys is suggested.

2. Bonding studies

a. High quality surface finishes on W and 3P contact surfaces do not significantly improve initial contact resistances; however, close dimentional control is necessary.

b. Hydrogen annealing at 820 °C improves the bonding performance of 3P to tungsten; treatment below 600 ° was not found to affect the oxygen content of 3P elements.

3. Couple design, preparation, and testing

a. PbTe couples (3N and 3P) have been successfully prepared for life testing by simultaneous bonding to a common W shoe.

b. Segmented Si-Ge-PbTe couples were designed and prepared; preliminary measurements of efficiency were made. At a hot junction temperature of approximately 800 °C, the maximum efficiency achieved has been approximately 7.6%, and the maximum power output, 2.10 watts per couple.

4. Couple test devices

a. A sixteen-station life test device for testing PbTe couples under operational conditions of gradient and load has been designed and constructed.

b. A test device for measurements of efficiency and electrical characteristics of segmented couples has also been constructed.

5. Life testing

a. Results of an 800-hr gradient life test of W-bonded 3N and 3P elements indicate the main source of degradation to be an increase in the resistance of the p elements and a decrease in their Seebeck voltage. Decreases in the Seebeck voltage of both legs contribute most heavily to the initial degradation of power; however, the rate of degradation had decreased sharply by the 800-hr point.

b. A second gradient life test during this period of bonded and unbonded 3P elements has reached 2600 hr. The presence of water vapor in the system has caused substantial increases in the contact resistance of most of the bonded elements. Decreasing Seebeck voltage remains the main source of degradation of the unbonded elements and those bonded elements which have remained low in resistance.

c. Isothermal life tests of bonded 3P elements at 525 °C for 1000, 2000 and 3000 hr have revealed substantial increases in element resitance. These tests also indicated that initial contact resistance is not a reliable indicator of the performance of the contact during testing and that differences between batches of 3P material can substantially affect the life of the elements and contacts.

d. Life testing of W-bonded 3N and 3P elements showed minor changes in 3N bonded elements at 600 °C for 4700 hr, but 3P elements decreased in resistance and most electrodes were oxidized to the point of destruction of the bond.

III. SEMIANNUAL PHASE REPORTS

A. August 1, 1967 Through January 31, 1968

1. Constitutional studies

Tin-Telluride-Metal System: Accurate lattice constant determinations on SnTe as incorporated in SnTe-Metal alloys revealed changes in the original lattice constant of the starting $Sn_{.492}Te_{.508}$ composition.

From these findings, it has to be concluded that PbTe-SnTe thermoelectric alloys in contact with metals might change their composition and therefore their electrical properties over long periods of time.

Since such conditions could be important for the mechanism of aging of tungsten contacts to 3P material, a more thorough investigation of similar changes in the W-PbTe-SnTe system is indicated.

Silicon-Germanium-Metal-Alloys: Investigations of the interaction of Si-Ge solid solution alloys with Ti, Zr, V, Nb, Ta, Cr, Mo, W, Mn, Re and Co have revealed two basic types of constitution. The first is one in which equilibria between Si-Ge solid solutions and solid solutions of metal silicides and germanides exist. The elements Ti, Zr, Ta, and Co apparently belong to this category. The second type of system produces a metal silicide in equilibrium with either pure Ge or with the Si Ge solid solution. Elements behaving in this fashion are W, V, Nb, Cr, Mo, Mn, and Re. It was also found that phosphorous present as a dopant in n-type Si-Ge was concentrated in the $MoSi_2$ formed by addition of Mo. This is taken to indicate that metal phosphides (and presumably borides in the p-type material) can form and apparently dissolve in the metal silicide.

2. Segmented Si-Ge-PbTe thermocouples

Measurements of the efficiency of segmented couples have shown efficiencies of approximately 9% at hot junction temperatures of 800 ° and above, and power outputs of 2.25 to 2.8 watts per couple.

3. Pore migration

Quantitative metallography has shown evidence for fairly extensive migration of pores in pressed and sintered $Pb_{.4}Sn_{.6}Te$ thermoelements after operation for 3800 hr in a temperature gradient from 510 to 50 °C.

4. Life testing

Isothermal Testing: Tungsten bonds to 3P elements have been tested to 6000 hr at 525 °C. One half of the bonds remained intact; those measured showed an increase to 95 $\mu\Omega$ - cm^2 contact resistivity from an initial value of 16 $\mu\Omega$ - cm^2.

Gradient-Testing of W-Bonded 3N-3P Couples: Six of fourteen bonded couples tested to 800 hr at a hot junction temperature of approximately 520 °C survived approximately 35 unscheduled thermal cycles with unchanged total resistance.

Gradient-Testing of W-Bonded 3P Elements: Post-test analysis of gradient tested elements showed decreased resistivity and Seebeck voltage at hot ends of elements and precipitation of extensive amounts of an unidentified phase at intermediate and high temperatures.

B. February 1, 1968 Through July 31, 1968

This report presents constitutional results on the Co-Si-Ge system and the PbTe-MnTe system. In substantial detail, life testing of elements and couples is discussed, and data for couples tested over 2900 hr under gradient conditions are shown.

C. August 1, 1968 Through January 31, 1969

Information contained in the present report may be placed in three major categories:

1. Constitutional studies

Metal-Silicon-Germanium Systems: Data on the Pd-Si-Ge system are presented. In particular, a suggestion of a phase diagram for the binary germanium palladium system is made. Also, certain thoughts on the alloy chemistry of group VIII silicides and germanides are outlined.

Lead Telluride Containing Systems: A correction on the PbTe-MnTe system shown in the last semiannual report is given.

2. Testing of tungsten diffusion bonded lead telluride

Isothermal tests are discussed, but no coherent interpretation of all these tests has been made. The most significant result here is that in a number of isolated cases p-type junctions are still intact after 10,000 hr of testing. In fact, one junction tested increased from 75 $\mu\Omega$ to only 240 $\mu\Omega$ after 10,000 hr of total testing. It will be attempted to arrive at a coherent interpretation of all life test results, isothermal and gradient, for the next report.

3. Engineering design studies

a. A design philosphy and drawings for a high temperature cesium vapor heater using alumina tubes is presented.

b. A concept and a design philosophy for a modular segmented thermoelectric package using Ge-Si/PbTe is shown. Detailed drawings are enclosed and certain design studies are reported.

D. February 1, 1969 Through July 31, 1969

The metallurgical section of this report discusses studies of the Co-Si-Ge gystem in some detail and also presents results on the Pd-Ge system. Furthermore, a summary of all life test results on tungsten diffusion bonded lead-telluride is given together with an explanation of the bonding process and a detailed description of the bonding cycle.

Progress in the construction of cesium plasma lamps as high temperature heaters is reviewed. The present status of this part of the project is that all parts are available now, but have not been assembled and tested. Finally, a major part of this report deals with the progress achieved in the design and construction of the segmented submodules already described in previous reports.

E. August 1, 1969 Through January 31, 1970

Metallurgical investigations during the present reporting period centered around the high Co-end of the Co-Ge-Si system, where we hope to find a eutectic suitable for brazing $MoSi_2$ to Si-Ge thermoelectric material. Since phase relationships in all other parts of the Co-Ge-Si diagram are relatively favorable, success in locating a eutectic with a suitable melting point would immediately make bonding studies feasible.

The second part of this report describes bonding of the segmented Si-Ge/PbTe couples which are to be used in the submodules. Furthermore, preliminary mechanical and thermal tests on submodule components are described, and the module assembly procedures are outlined.

Finally, redesign and rework required on the thermoelectric test fixture for submodule testing are described. The Appendix presents a literature study of binary systems which might be pertinent for Si-Ge hot shoe brazing.

Appendix B*

PUBLICATIONS IN THE OPEN LITERATURE RESULTING
FROM WORK UNDER CONTRACT NO. NAS 5-9149, SO FAR

* The journal or book reference and the abstract of the publications are given in each case.

I. IEEE-AIAA Proceedings of Thermoelectric Specialist Conference

In May 1966, the IEEE held jointly with the AIAA a Thermoelectric Specialists Conference. Three papers were published in the proceedings of that conference which are available from IEEE headquarters, 345 East 47th Street, New York, New York 10017.

1. Evaporation Rates of PbTe and $Pb_{.5}Sn_{.5}Te$ Pressed and Sintered Thermoelements by H. E. Bates and Martin Weinstein: The evaporation rates of pressed- and sintered-PbTe and $Pb_{.5}Sn_{.5}Te$ thermoelements were measured over the temperature range 400 - 600 °C. Rates for PbTe varied from 2×10^{-2} to 175 mg/cm^2/hr, and for $Pb_{.5}Sn_{.5}Te$ from 4×10^{-1} at 450 °C to 45 mg/cm^2/hr at 600 °C, respectively. Calculated values of the vapor pressures of PbTe from these data are in good agreement with previous investigations.

2. The Preparation and Properties of Segmented Lead Telluride-Silicon-Germanium Thermoelements by H. E. Bates and Martin Weinstein: The W-diffusion bonding approach for lead telluride has been utilized in the preparation of silicon-germanium-lead telluride thermoelements. This approach has been found to produce bonds to the PbTe base thermoelements with room temperature contact resistivities of 20 $\mu\ \Omega$-cm^2 for n-type PbTe and 30 $\mu\ \Omega$-cm^2 for p-type PbTe-SnTe. N-type segmented elements produce an electrical power output of 1.38 watts with a hot junction temperature of 800 °C and a cold junction temperature of 115 °C. P-type segmented elements with a hot junction temperature of 800 °C and a cold junction temperature of 145 °C produced an electrical power output of 1.20 watts. The average overall segmented couple efficiency is calculated to be 11.2%.

3. The Bonding of Lead Telluride With Non-Magnetic Electrodes by H. E. Bates, F. Wald, and Martin Weinstein: A W-diffusion bonding technique has been developed which produced metallurgically sound, low resistance bonds to p- and n-type pressed and sintered PbTe base thermoelements. Electron microprobe analyses and PbTe equilibria studies have shown W and PbTe to be chemically compatible at 600 °C. The W-diffusion process reproducibly yields room temperature bond contact resistivities of less than 5 $\mu\ \Omega$-cm^2 for n-type PbTe and less than 30 $\mu\ \Omega$-cm^2 for p-type SnTe-PbTe. The W-n-type PbTe contact resistivity has been shown to follow the relationship $\rho_c \propto T^{2.9}$. Bond strengths in excess of 2500 psi have been obtained.

The requirements of metallurgical bonds are critically reviewed along with techniques for evaluation of long term electrical, mechanical, and chemical stability.

II. Advanced Energy Conversion, Vol. 6, pp. 177-180 (1966), Sublimation Rates in Vacuo of PbTe and $Pb_{0.5}Sn_{0.5}Te$ Thermoelements by H. E. Bates and Martin Weinstein.

Abstract — The sublimation rates of pressed- and sintered-PbTe and $Pb_{0.5}Sn_{0.5}Te$ thermoelements were measured over the temperature range 400-600 °C. Rates for PbTe varied from 2×10^{-2} to 175 mg/cm^2/hr, and for $Pb_{0.5}Sn_{0.5}Te$ from 4×10^{-1} at 450 °C to 45 mg/cm^2/hr at 600 °C, respectively. Calculated values of the vapor pressures of PbTe from these data are in good agreement with previous investigations.

III. Journal of Less Common Metals, Vol. 13, pp. 579-590 (1967), Constitutional Investigations in the Silver-Lead-Tellurium System by F. Wald.

The phase diagram of the pseudobinary section Ag_2Te-PbTe has been determined. A large eutectoidal region was found on the Ag_2Te side stabilizing the high temperature b.c.c. form of Ag_2Te at temperatures as low as 475 °C. Surveys in other areas of the system revealed only one other pseudobinary section at lower temperatures between Ag_5Te_3 and PbTe.

Electrical measurements showed that alloys of PbTe containing 3-4 mol % of "AgTe" were p-type; along the Ag_2Te-PbTe and Ag_5Te_3-PbTe sections, alloys with similar concentrations of these silver compounds were n-type. Some of the alloys show reasonable thermoelectric properties.

IV. Transactions, TMS-AIME, Vol. 242 (1968):

1. On the Constitution of the Pseudobinary Section Lead Telluride-Iron by F. Wald and R. W. Stormont, pp. 72-75: The phase diagram of the pseudobinary section PbTe-Fe was determined. It was found to contain a monotectic and a eutectic reaction, the latter one taking place at 14 at. % Fe and 875 ± 5 °C. The solid solubility of iron in PbTe was found to be 0.3 at. % by electronmicroprobe analysis. No solubility of PbTe was detected in iron. Slight deviations from true pseudobinary behavior were found to occur in the range of 5 to 10 at. % Fe.

2. The Pseudobinary Section of PbTe and Gold by D. J. Mottern and F. Wald, pp. 150-151.

3. On the Constitution of the System Cobalt-Lead Telluride by F. Wald and R. W. Stormont, pp. 747-749.

V. Advanced Energy Conversion, Vol. 7, pp. 275-287 (1968), The Compatibility of Lead and Tin Telluride with Metals by H. E. Bates, F. Wald, and M. Weinstein.

Abstract — For the design of efficient joining methods and the evaluation of the long term stability of thermoelectric junctions, a basic knowledge of the appropriate phase equilibria is desirable. The chemical reaction behavior of lead- and tin-telluride with a number of metals was therefore surveyed.

Guertler's "Klar-Kreuz" method has been used to establish the direction of the reactions:

$$xPbTe + yM \rightleftharpoons M_yTe_x + xPb$$

or the corresponding reactions with SnTe.

For the metals investigated with PbTe it was found that in the case of Ti, V, Cr, Mn, Zn, Ga, Zr, Nb, Cd, In, and Ta the reaction goes from left to right. For Fe and W it proceeds from right to left. In the cases of Ni, Cu, Ag, and Mo the equilibria are more complex and cannot be described by the cited equation. Reactions of SnTe with metals were quite similar. Again, Mn, Zn, Cd, and Ta were found to react from left to right, Fe and W from right to left. Here, too, Ni, Cu, Ag, and Mo followed more complex equilibria.

VI. Energy Conversion, Vol. 8, pp. 135-140 (1968), Estimation of the Chemical Compatibility of Alloys with Lead Telluride and Tin Telluride Thermoelectric Materials by F. Wald.

Summary — A method is presented which allows an estimation of whether a thermoelectric material based on lead- or tin-telluride will chemically react with a given metallic alloy. This method involves a comparison of the heats of formation of a mixture of tellurides which would be formed by the alloy upon reaction, relative to the heats of formation of lead- or tin-telluride. The heats of formation are evaluated from electronegativity differences based on experimentally determined reactions of lead and tin telluride with elemental metals. Such estimation of heats of formation obviously contain large absolute errors. It can, however, be shown that for the nine alloys investigated good agreement between the prediction of reaction and the behavior found experimentally indeed exists.

VII. SAMPE Journal, October/November 1968, Materials Research Problems in the Direct Conversion of Thermal Radiative and Chemical Energy into Electricity by F. Wald and Martin Weinstein.

Abstract — Direct energy conversion methods such as thermoelectricity, solar-cells, thermionics, and fuel cells are presently in a state of development where their practical and commercial use for the solution of various specialized power supply systems is possible.

A number of problem areas, particularly in materials, are however still hindering the most effective use of such devices. The present paper discusses the general mechanisms of electrical energy production in the four direct energy conversion methods mentioned above and points out some of the materials limitations currently encountered in the use of devices based on these methods.

VIII. Intersociety Energy Conversion Engineering Conference Record, pp. 229-231 (1968), On the Efficiency of Segmented Si-Ge-PbTe Thermocouples by H. E. Bates and Martin Weinstein.

High efficiency thermoelectric devices are desirable for reduction of fuel costs in RTG's and increased power-to-weight ratio for space applications.

The best known thermoelectric power generation materials, PbTe and SiGe, have optimum temperature ranges which complement each other for operation over a temperature interval of 800° - 1000°C to 200° - 50 °C. Devices utilizing these materials over such a temperature interval should exhibit higher conversion efficiency than either material alone.

Segmented couples have been prepared with SiGe and PbTe (3N and 3P) as the hot and cold segments, respectively. The two materials are joined by bonding to a common tungsten intermediate.

Results are presented of efficiency measurements on segmented couples of SiGe-PbTe optimized for operation between 800° and 50 °C. The efficiency was determined by measuring the heat flux from the cold sides of the thermocouple legs. Conversion efficiencies in excess of 9% have been measured with power outputs of 2.25 watts per couple at 0.15 volts and 15 amperes when the couples were operated between 800° and 55 °C.

IX. Intersociety Energy Conversion Engineering Conference Record (1970), The Design and Testing of Segmented Thermocouple Modules by S. Mermelstein.

X. Future Publications

Two further papers are planned for publication, both by F. Wald and S. J. Michalik dealing with the palladium-germanium system and the cobalt-silicon-germanium system.

Appendix C

PATENTS

This appendix contains titles and numbers of the two patents issued based on work under Contract No. NAS 5-9149. Both patents were filed by NASA under provisions of Section 305 of the National Aeronautics and Space Act of 1958, and all rights to these patents thus rest with NASA.

1. U. S. Patent No. 3447233 Issued on June 3, 1969. Title: Bonding Thermoelectric Elements to Nonmagnetic Refractory Metal Electrodes. The invention was filed September 30, 1966 based on work by M. Weinstein and E. J. Sherwin.

2. U. S. Patent No. 3452423 Issued on July 1, 1969. Title: Segmenting Lead Telluride-Silicon-Germanium Thermoelements. The invention was filed September 30, 1966 based on work by M. Weinstein, H. E. Bates, and J. Epstein.